The Astrophysical Journal Supplement Series, 140:407–456, 2002 June

SPACE TELESCOPE IMAGING SPECTROGRAPH OBSERVATIONS OF HIGH-VELOCITY INTERSTELLAR ABSORPTION-LINE PROFILES IN THE CARINA NEBULA[1]

Nolan R. Walborn
Space Telescope Science Institute, 3700 San Martin Drive, Baltimore, MD 21218; walborn@stsci.edu

Anthony C. Danks
Emergent-IT, 1801 McCormick Drive, Suite 280, Largo, MD 20774; Anthony.Danks@emergent-IT.com

Gladys Vieira
Science Systems and Applications, Inc., Code 681, NASA Goddard Space Flight Center, Greenbelt, MD 20771; gvieira@hunin.gsfc.nasa.gov

and

Wayne B. Landsman
Science Systems and Applications, Inc., Code 681, NASA Goddard Space Flight Center, Greenbelt, MD 20771; landsman@mpb.gsfc.nasa.gov
Received 2001 October 3; accepted 2001 December 28

ABSTRACT

An atlas of ultraviolet interstellar absorption-line profiles toward four stars in the Carina Nebula is presented. The observations have been made with the Space Telescope Imaging Spectrograph on the *Hubble Space Telescope*, with a resolving power of 114,000. Low-ionization, high-ionization, and excited-state lines from a wide array of chemical species are included. Extensive measurements of radial velocities, velocity dispersions, and column densities of individual components in these profiles are also given. The unprecedented capabilities of STIS reveal many more velocity components than previously known; most of the high-velocity components in previous observations with the *International Ultraviolet Explorer* are now resolved into multiple subcomponents, and even higher velocities are seen. The great range of line strengths available permits the detection of the low-velocity components in the weakest lines, and progressively higher velocities in stronger lines (in which the low-velocity components become completely blended). The weak and high-ionization lines trace global structure in the H II region, while the strong low-ionization lines show intricate high-velocity structure that likely originates relatively near to the O stars observed. The extreme velocities found in the low-ionization lines toward these four stars are −388 and +127 km s^{-1}, with 23–26 resolved components in each. Some components in different stars may be related, but many are different in each line of sight. A remarkably well-defined Routly-Spitzer effect is found in this region. Temporal variations toward one star observed twice have already been reported. These measurements will be used in subsequent astrophysical analyses to further constrain the origins of the phenomena.

Subject headings: ISM: abundances — ISM: individual (Carina Nebula) — ISM: kinematics and dynamics — ISM: lines and bands — ISM: structure — ultraviolet: ISM

On-line material: machine-readable tables

1. INTRODUCTION

The interstellar absorption lines toward the O stars ionizing the Carina Nebula (NGC 3372) have been known for some time to display some of the most extreme velocity profiles in the Galaxy. A complete survey of previous work and a description of the intricate interstellar phenomenology in this region were given recently by Danks et al. (2001), so they need not be repeated here. In this paper we present an extensive atlas and measurements of interstellar-line profiles in our Space Telescope Imaging Spectrograph (STIS) observations of four Carina Nebula O stars. The high resolution and signal-to-noise of these data substantially extend previous knowledge of the phenomenon, revealing even higher velocities and finer component substructure. These results provide further evidence of the extreme spatial variations in the interstellar profiles over small angular distances, and they have revealed large temporal variations in one line of sight over 22 months (Danks et al. 2001). They also yield further information about the qualitatively different behavior in the low-ionization lines (e.g., C II, Mg II, Fe II) on the one hand, and the high-ionization (C IV, Si IV, Al III) and excited-state lines on the other. These data and measurements should enable significant progress toward a physical understanding of the extremely structured interstellar medium in the Carina Nebula.

2. OBSERVATIONS

The STIS observations of the four targets in our *Hubble Space Telescope* (*HST*) General Observer (GO) program No. 7301 were made between 1998 March and 1999 April, as detailed in Table 1. The prior "early-release" observations (ERO) of CPD −59°2603, which permitted the detection of temporal variations in its interstellar profiles by comparison with the later data, were obtained by program No. 7137 in 1997 June (Walborn et al. 1998; Danks et al.

[1] Based on observations with the NASA/ESA *Hubble Space Telescope* obtained at the Space Telescope Science Institute, which is operated by the Association of Universities for Research in Astronomy, Inc., under NASA contract NAS5-26555.

TABLE 1
STELLAR AND EXPOSURE DATA

Star	R.A. (J 2000) Decl. (J 2000)	Spectral Type	V $B-V$	Date	Echelle	Central Wavelength (Å)	Exposure Time (s)	Flux (ergs cm^{-2} s^{-1} Å^{-1})
CPD −59°2603	10 44 47.42	O7 V((f))	8.77	1997 June 6	E140H	1416	1730	7E−12
	−59 43 53.6		0.14		E230H	2762	1250	3E−12
				1999 Apr 19	E140H	1234	5160	7E−12
						1416	3180	7E−12
						1598	4800	7E−12
					E230H	2513	2820	3E−12
						2762	2340	3E−12
HD 93205	10 44 33.82	O3.5 V((f+))	7.75	1999 Apr 20	E140H	1234	1200	5E−11
	−59 44 15.3	+ O8 V	0.05			1416	780	4E−11
						1598	1380	4E−11
					E230H	1763	2220	3E−11
						2513	780	1E−11
						2762	720	1E−11
HDE 303308	10 45 05.96	O4 V((f+))	8.17	1998 Mar 19	E140H	1234	1680	2E−11
	−59 40 06.4		0.13			1416	1140	2E−11
						1598	2460	2E−11
				1998 Mar 20	E230H	1763	4080	1E−11
						2513	1080	6E−12
						2762	1020	6E−12
HD 93222	10 44 36.33	O7 III((f))	8.11	1998 Dec 28	E140H	1234	2220	3E−11
	−60 05 28.8		0.05			1416	1560	3E−11
						1598	2400	3E−11
					E230H	1763	4020	2E−11
						2513	1380	9E−12
						2762	1140	8E−12

2001). Three of these O stars (HD 93205, HDE 303308, and CPD −59°2603) are located relatively near one another in the northern part of the Carina Nebula and near η Carinae, while the fourth (HD 93222) is situated in the southern part of the nebula (see the maps and figure shown by Walborn 1982, 1995, respectively). This circumstance is relevant to the comparisons among their interstellar profiles below.[2]

The data were acquired with the STIS high-resolution echelles E140H in the far-UV (FUV) and E230H in the near-UV (NUV), and the respective multianode microchannel plate array (MAMA) detector for each of the two wavelength regions (Woodgate et al. 1998). Only one exposure in each configuration was obtained in the ERO program, as detailed in the earlier papers, but in the GO program three echelle settings, covering 200–300 Å each, were obtained in each wavelength regime for all targets except the faintest, CPD −59° 2603, for which the longest NUV exposure had to be omitted. These settings provide complete coverage of the FUV region, 1150–1700 Å, and (with three settings) half of the NUV, 1600–3150 Å, the latter being selected to cover the greatest number of interesting interstellar lines. The exposure details are given in Table 1; the last column lists the stellar continuum flux at the central wavelength.

The entrance apertures were $0\farcs2 \times 0\farcs09$ in the FUV and $0\farcs1 \times 0\farcs09$ in the NUV. The nominal 2 pixel resolving power of these STIS configurations is 114,000 (2.6 km s^{-1}). The ERO observations were obtained in the STIS Time-Tag mode, in which the 125 μs samples are combined and Doppler compensation for the spacecraft motion is applied in the postobservation data processing; while the GO observations were performed in the Accum mode, with automated on-board Doppler compensation in effect. The Doppler correction is made in integer pixels (1.3 km s^{-1}). The telluric excited-state O I lines (Spitzer & Fitzpatrick 1993) shown in Figure 15 are probably resolved due to atmospheric motions (Jenkins & Tripp 2001); our Gaussian fits to these features yielded FWHM values from 2.9 to 6.6 km s^{-1}, in agreement with their results. The typical signal-to-noise in these data is 40.

3. MEASUREMENTS

Following routine technical processing of the MAMA frames, the first step of the scientific data reduction is the removal of the scattered light present in the echelle images, which becomes progressively stronger toward shorter wavelengths. If not corrected, the scattered light causes an oversubtraction of the background, driving saturated lines negative. All of the images have been corrected for scattered light with an optical model of STIS developed by D. Lindler.[3] The detector background is subtracted separately from the scattered-light correction. A standard one-dimensional spectral extraction is per-

[2] The distance to the Carina Nebula adopted here is 2500 pc ($1' = 0.73$ pc in projection). A thorough discussion of the distance problem is given by Walborn (1995). The principal uncertainty is the value of the ratio of total-to-selective extinction, R, which may vary from star to star. The adopted distance is an average of spectroscopic determinations from the O stars corresponding to R values of 3 and 4, which is the likely range.

[3] CALSTIS Reference Guide (Version 5.1), http://hires.gsfc.nasa.gov/stis/software/software.html.

formed, with a slit height of 7 pixels for both FUV and NUV data. Next the continuum on each side of a line is defined by selecting smooth regions and fitting them with a polynomial usually of order two. The profiles are then normalized and a check on the scattered-light removal is made by verifying that the central, saturated part of each line is zero. Finally, overlapping wavelength coverages from adjacent echelle orders are weighted by the square of their inverse errors and summed.

A line-fitting program is used to arrive at cloud model parameters, namely a heliocentric radial velocity, velocity dispersion,[4] and saturation-corrected column density for each of the components. The line-spread function used by the program is the model one given in the STScI STIS Instrument Handbook, which has a narrow (1.6 km s^{-1}) core, but wings due to the telescope point-spread function that degrade the spectral resolution. The program utilizes a "Levenberg-Marquardt algorithm" to create the optimal fit, and it generates an error estimate as well as a difference fit for the spectral range. Fits were performed starting with the weaker lines such as Mg II 1239, 1240 Å and Mn II 2576, 2594, 2606 Å in which the lowest velocity components are resolved, and then progressing through more saturated lines such as Mg I 2852 Å and Fe II 1608, 2382, 2586, 2600 Å. The velocity solutions for these weaker lines were used as inputs to fit the saturated portions of the stronger lines Al II 1670, Si II 1526, and O I 1302 Å. In this manner, velocity structure for the fits to the saturated portions of the strongest low-ionization lines, Mg II 2796, 2803 Å and C II, C II* 1334, 1335 Å was built up with confidence. Whenever possible, the high-ionization lines were fitted independently, but in some severely blended cases velocities derived from low-ionization components had to be adopted. In general, radial velocities adopted from other line fits can be recognized by their zero decimals. In order to prevent divergence of the fits in the most blended and saturated portions of the profiles, upper limits to the allowed velocity dispersions were fixed at 10 km s^{-1} for the low-ionization lines, and 12 km s^{-1} for the high-ionization lines. In a few cases for which it appeared to be appropriate, lower velocity dispersions were fixed to prevent the program from defaulting to the upper limits in blended regions; these cases are also generally distinguished by their zero decimals. Examples of fits to a low-ionization and a high-ionization profile are shown in Figures 1*a* and 1*b*, respectively.

Radial velocities of unblended components are accurate to $\sim$1 km s^{-1}, the limiting factors being the thermal stability of STIS, wavelength zero points, and the dispersion solutions. Unsaturated column densities have typical accuracies of 10%; those judged to be more uncertain than twice that amount are flagged with colons in the data tables. No measurements are reported in cases of blends between two different species, or when there were four or more adjacent velocity components within a completely black trough.

4. RESULTS

The intricate interstellar profiles revealed by STIS toward these Carina Nebula O stars are presented here in an atlas format, while extensive measurements of individual velocity components are given in the accompanying tables. The atlas is arranged as follows. Two figures for each star (Figs. 2–9) present the low-ionization lines, ordered by increasing line strength; the first figure in a consecutive pair has four parts, each of which is a montage of five line profiles, while the second figure of the pair shows the highly complex, overlapping C II, C II* profiles separately. Then an additional figure for each star (Figs. 10–13) displays the high-ionization doublets as montages of six lines. Finally, two more figures (Figs. 14 and 15) are montages of two complex but interesting wavelength regions containing partially overlapping excited-state lines, with all four stars shown together in each case. Tables 2, 3, 4, and 5 provide measurements of heliocentric radial velocities, velocity dispersions, and column densities ordered by increasing radial velocity for each star. For a given velocity component, the chemical species are listed alphabetically, and multiple lines from the same species are in order of increasing wavelength. Similar (but often not identical) low- and high-ionization component velocities are listed together, with a blank line separating the latter from the former. The tables include measurements of additional lines not shown in the figures. Vacuum wavelengths are used throughout this paper.

4.1. *CPD −59° 2603*

This star was observed with STIS in both 1997 and 1999; partial analyses of the results, including large temporal variations in the profiles between the two epochs, have been presented by Walborn et al. (1998) and Danks et al. (2001). In Figures 2*a*–2*d*, the subset of profiles observed in 1997 are superposed with dashed lines, while the C II, C II* profiles at the two epochs are shown displaced in Figure 3. Entries in Table 2 for the same velocity component at the two epochs are distinguished by footnotes; of course, the majority were observed only in 1999 because of the limited wavelength coverage in 1997. In the case of the "69/72 km s^{-1}" components, measurements are given for only the first velocity in 1997 and the second in 1999, since the stronger feature at the lower velocity disappeared between the two epochs, and the weaker, higher velocity one was severely blended at the earlier epoch. The high-ionization interstellar lines in this spectrum are shown in Figure 10, and some further excited-state profiles in Figures 14 and 15. The Si IV doublet is shown for both epochs in Figure 10, but the Al III is missing because the grating setting that covers it had to be omitted from the program.

The prior ground-based (Walborn 1982) and *IUE* (Walborn & Hesser 1982) observations had revealed a total of nine low-ionization interstellar velocity components in this line of sight, including four with very high velocities. The more sensitive STIS data resolve multiple substructure in most of these components and detect many new ones, with a total of 25 components between −233 and +127 km s^{-1}.

Considering first the weaker lines (Fe II through Mn II in Figs. 2*a*–2*b*), one sees four dominant components at −38, −19, −3, and +8 km s^{-1}, in excellent agreement with measurements of the optical Ca II and Na I profiles (Walborn 1982). This structure will be seen to be quite similar toward all three stars in the northern part of the Carina Nebula, but very different toward the star in the southern part. The two

[4] The velocity dispersion b is related to the gas temperature T by $b^2 = (2kT/m) + \xi^2$, where ξ is the most probable speed of the turbulent motions and m is the atomic mass.

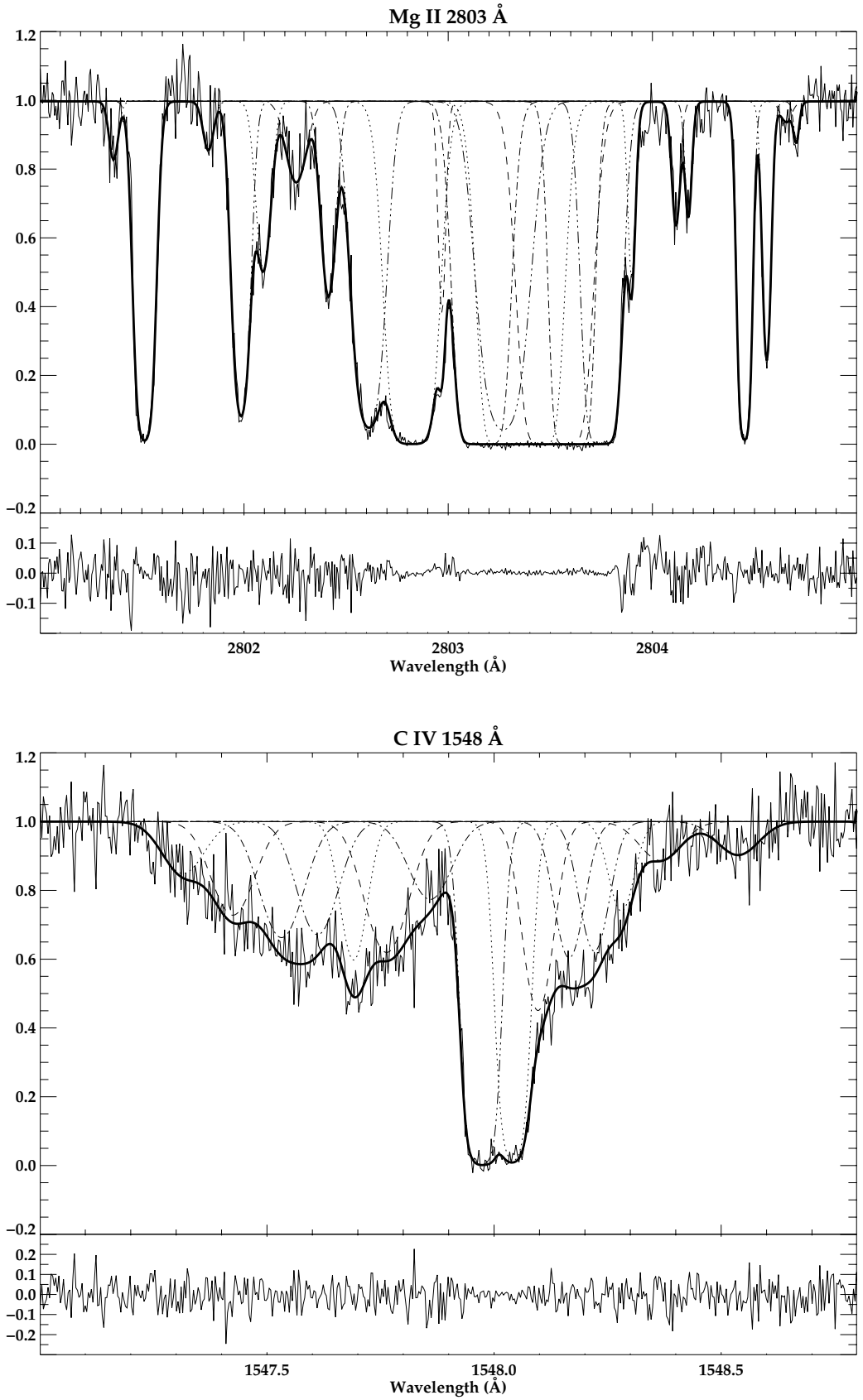

FIG. 1.—(*a*) Illustration of the profile fitting for the low-ionization line Mg II 2803 Å toward CPD −59°2603 in 1997. The lower panel shows the residuals. (*b*) Same for the high-ionization line C IV 1548 Å toward CPD −59°2603 (in 1999).

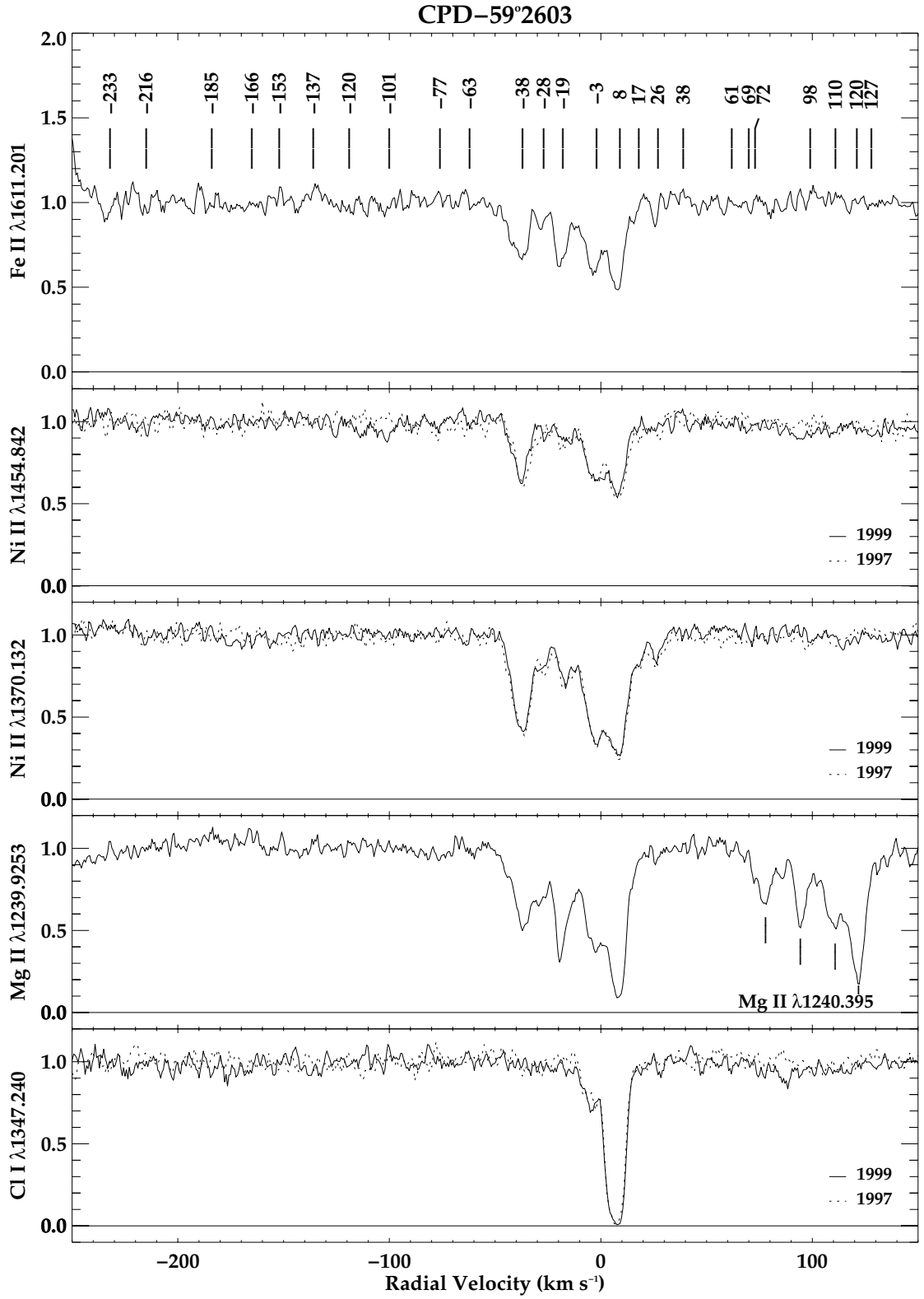

FIG. 2*a*

FIG. 2.—(*a*) Sequence of rectified, low-ionization interstellar-line profiles toward CPD −59°2603, ordered by increasing strength. In this and all subsequent plots, the data have been smoothed by 3 pixels. The heliocentric radial velocities (km s^{-1}) of all discrete components measured in the low-ionization lines are marked at the top. For lines observed at both epochs, the 1997 profiles are superposed with dashed lines. Other species present in a given panel are identified. The sequence continues in (*b*)–(*d*).

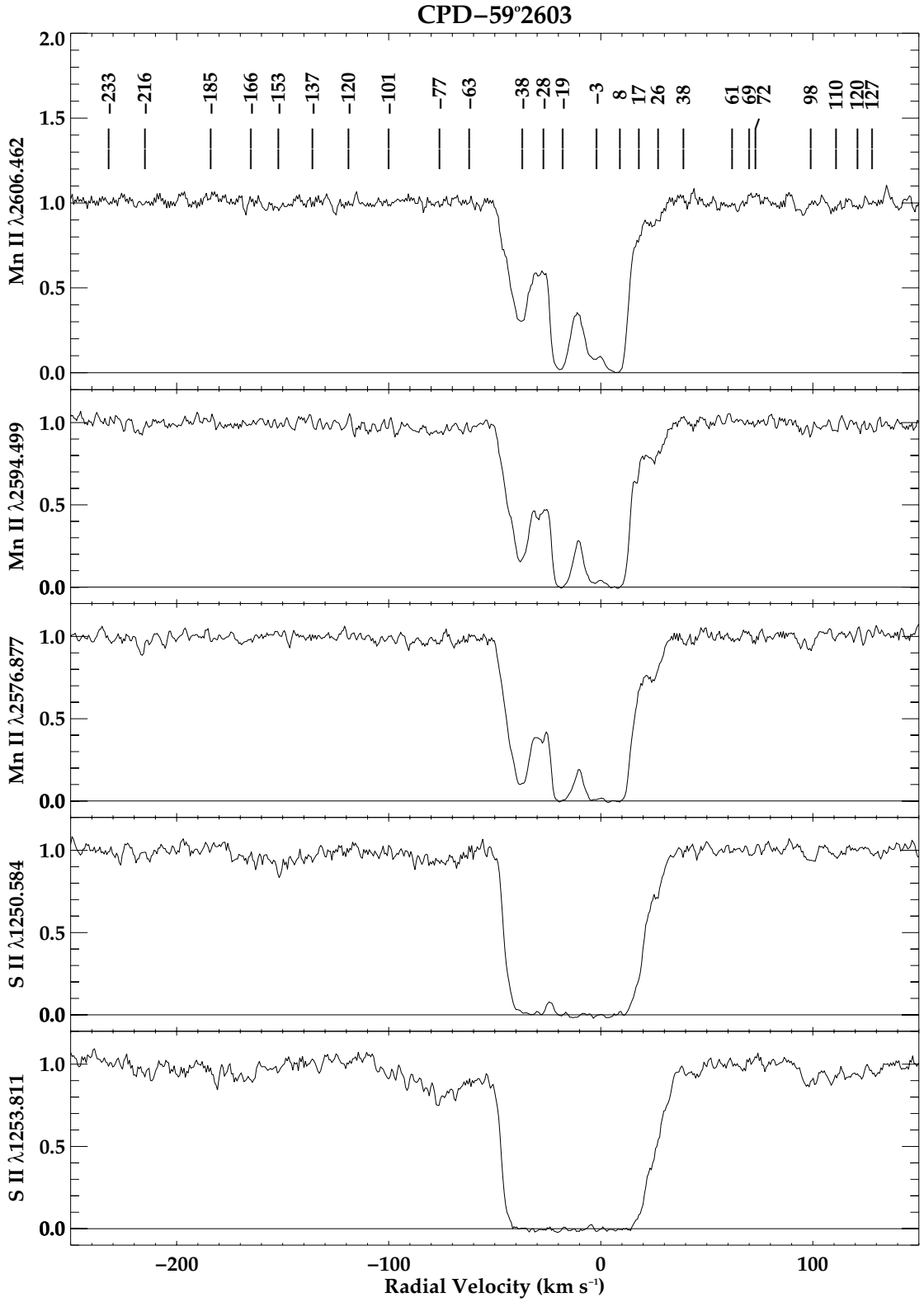
CPD−59°2603
−233
−216
−185
−166
−153
−137
−120
−101
−77
−63
−38
−28
−19
−3
8
17
26
38
61
69
72
98
110
120
127
Mn II λ2606.462
Mn II λ2594.499
Mn II λ2576.877
S II λ1250.584
S II λ1253.811
2.0
1.5
1.0
0.5
0.0
−200
−100
0
100
Radial Velocity (km s⁻¹)

FIG. 2*b*

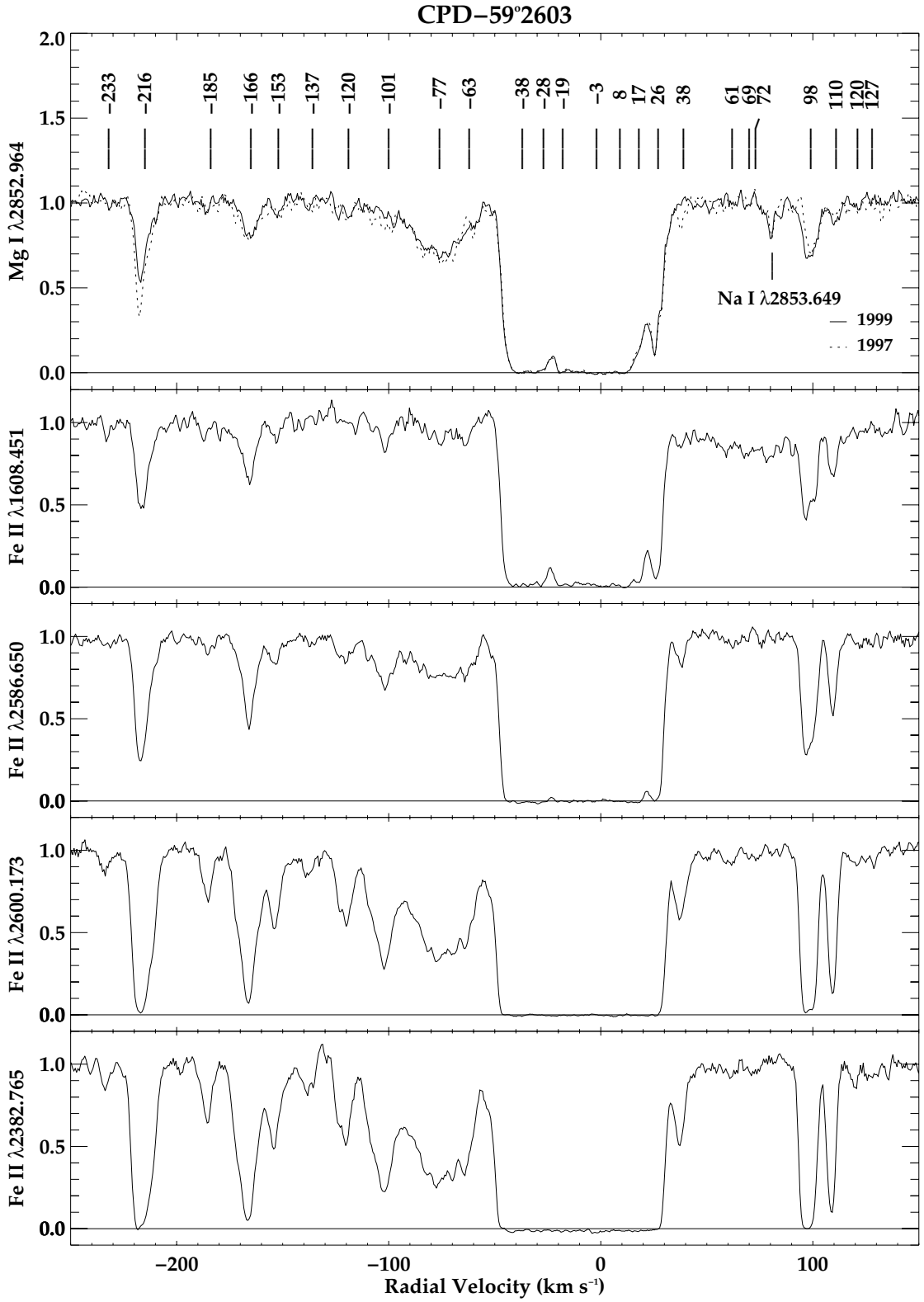
CPD−59°2603
Mg I λ2852.964
Fe II λ1608.451
Fe II λ2586.650
Fe II λ2600.173
Fe II λ2382.765
−233
−216
−185
−166
−153
−137
−120
−101
−77
−63
−38
−28
−19
−3
8
17
26
38
61
69
72
98
110
120
127
Na I λ2853.649
1999
1997
Radial Velocity (km s⁻¹)

FIG. 2*c*

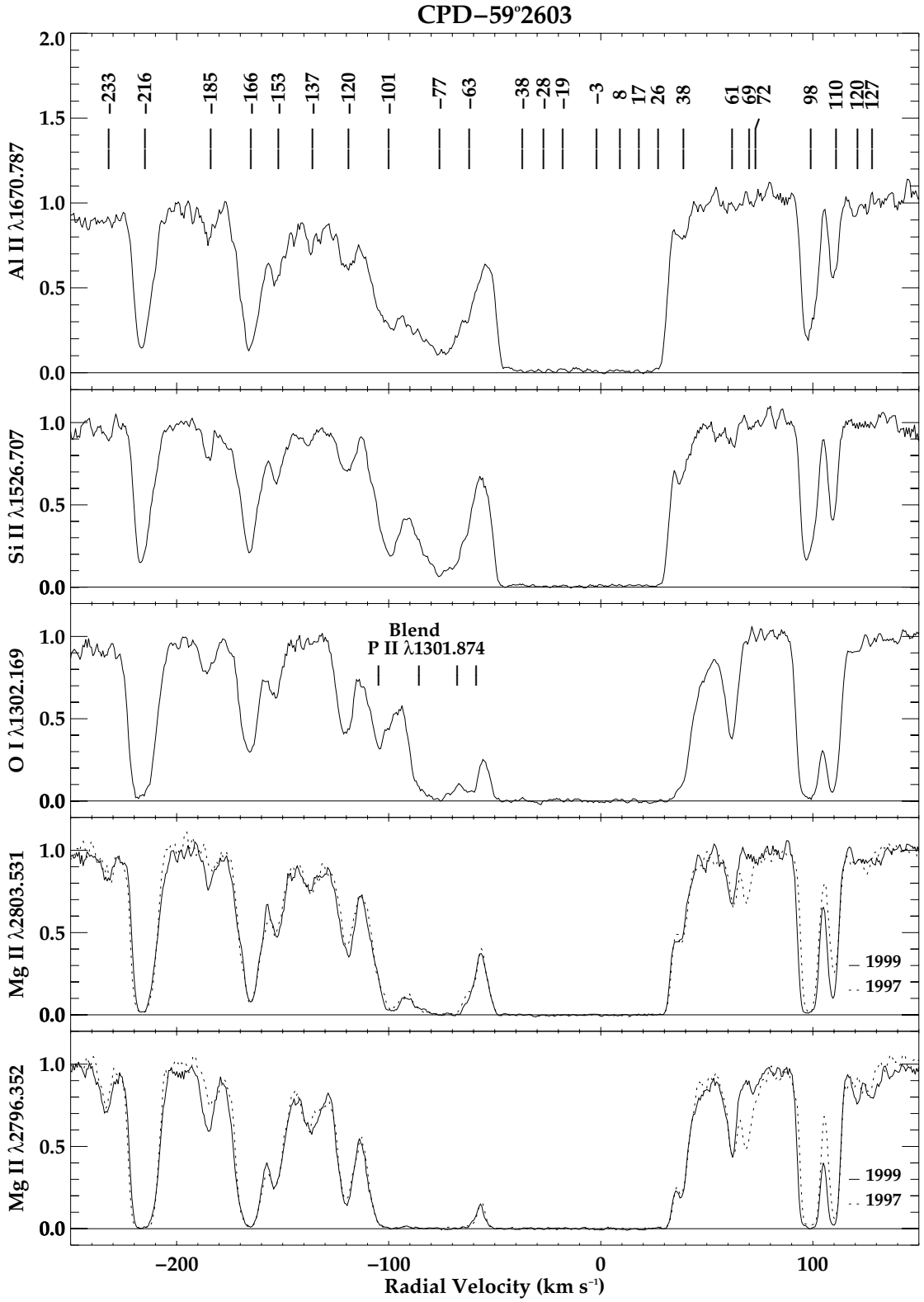
CPD−59°2603
Al II λ1670.787
Si II λ1526.707
O I λ1302.169
Blend
P II λ1301.874
Mg II λ2803.531
Mg II λ2796.352
1999
1997
1999
1997
−233
−216
−185
−166
−153
−137
−120
−101
−77
−63
−38
−28
−19
−3
8
17
26
38
61
69
72
98
110
120
127
2.0
1.5
1.0
0.5
0.0
−200
−100
0
100
Radial Velocity (km s⁻¹)

FIG. 2*d*

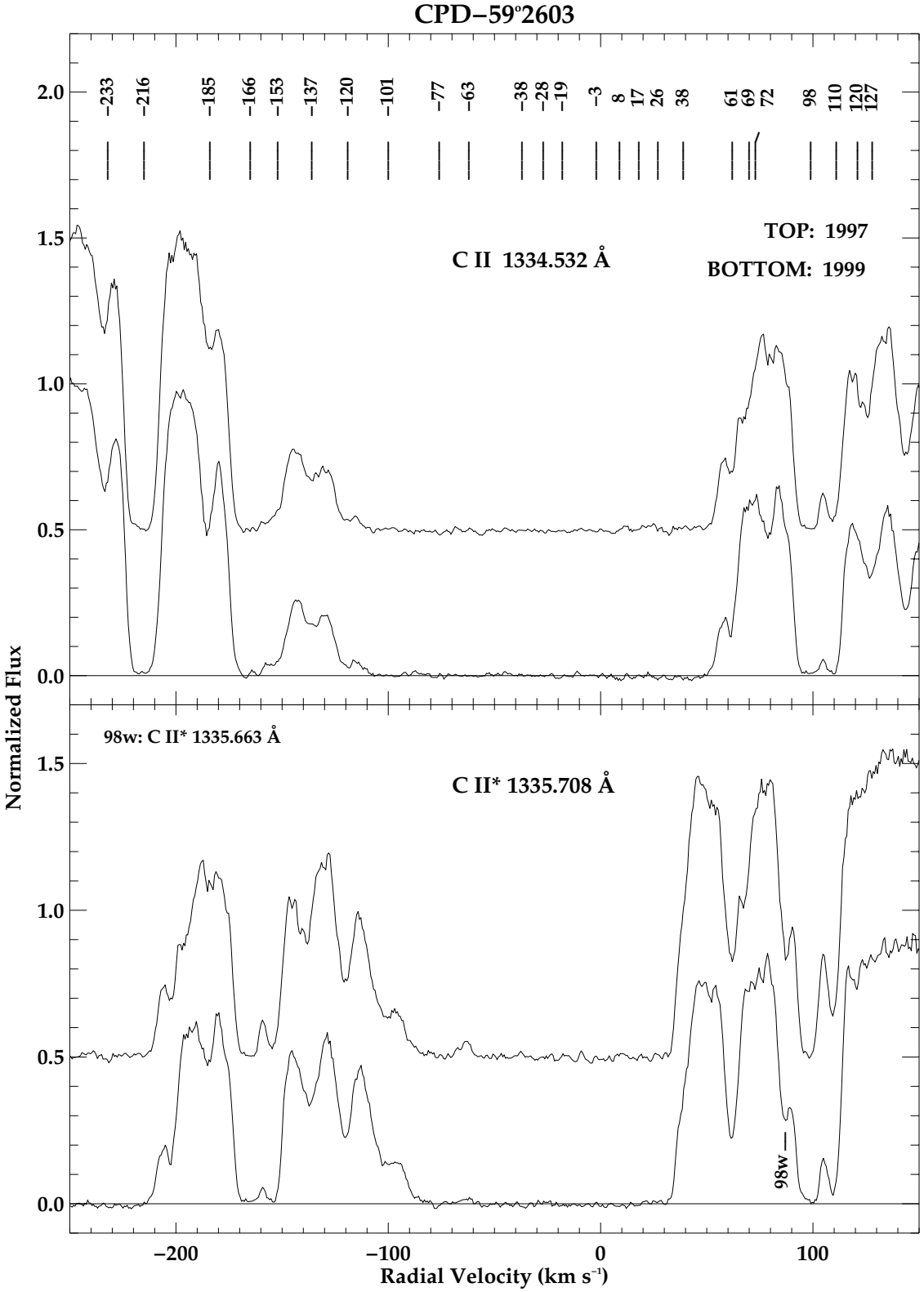

FIG. 3.—Rectified profiles of the very strong, partially overlapped interstellar C II, C II* lines toward CPD −59°2603 at both epochs, which are displaced by 0.5 continuum units. Note the disappearance of the +69 km s^{-1} component between the two epochs, and the resolution of the weaker of the two C II* lines at +98 km s^{-1} (denoted as "98w").

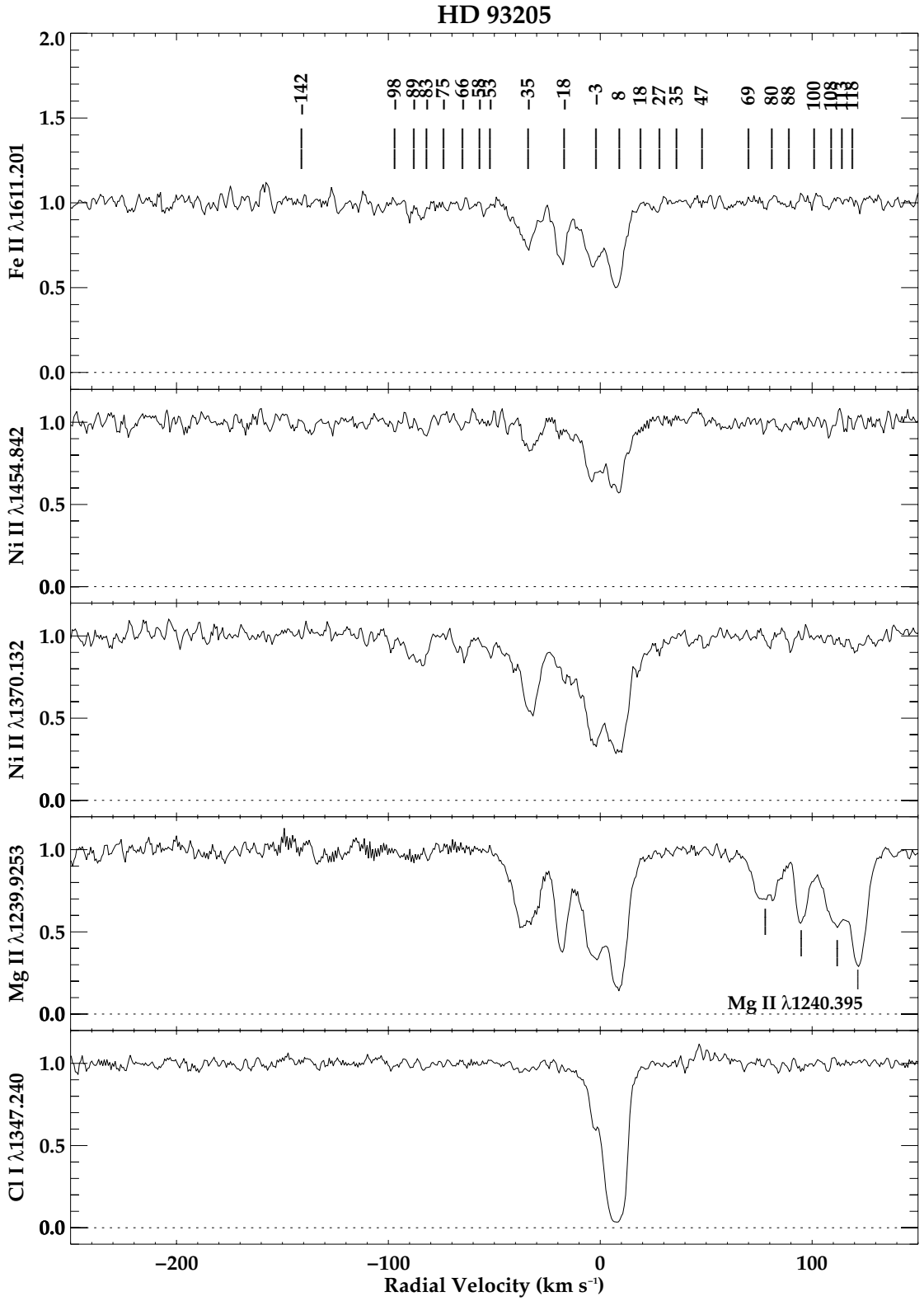

FIG. 4*a*

FIG. 4.—(*a*) Sequence of low-ionization interstellar-line profiles toward HD 93205. The sequence continues in (*b*)–(*d*).

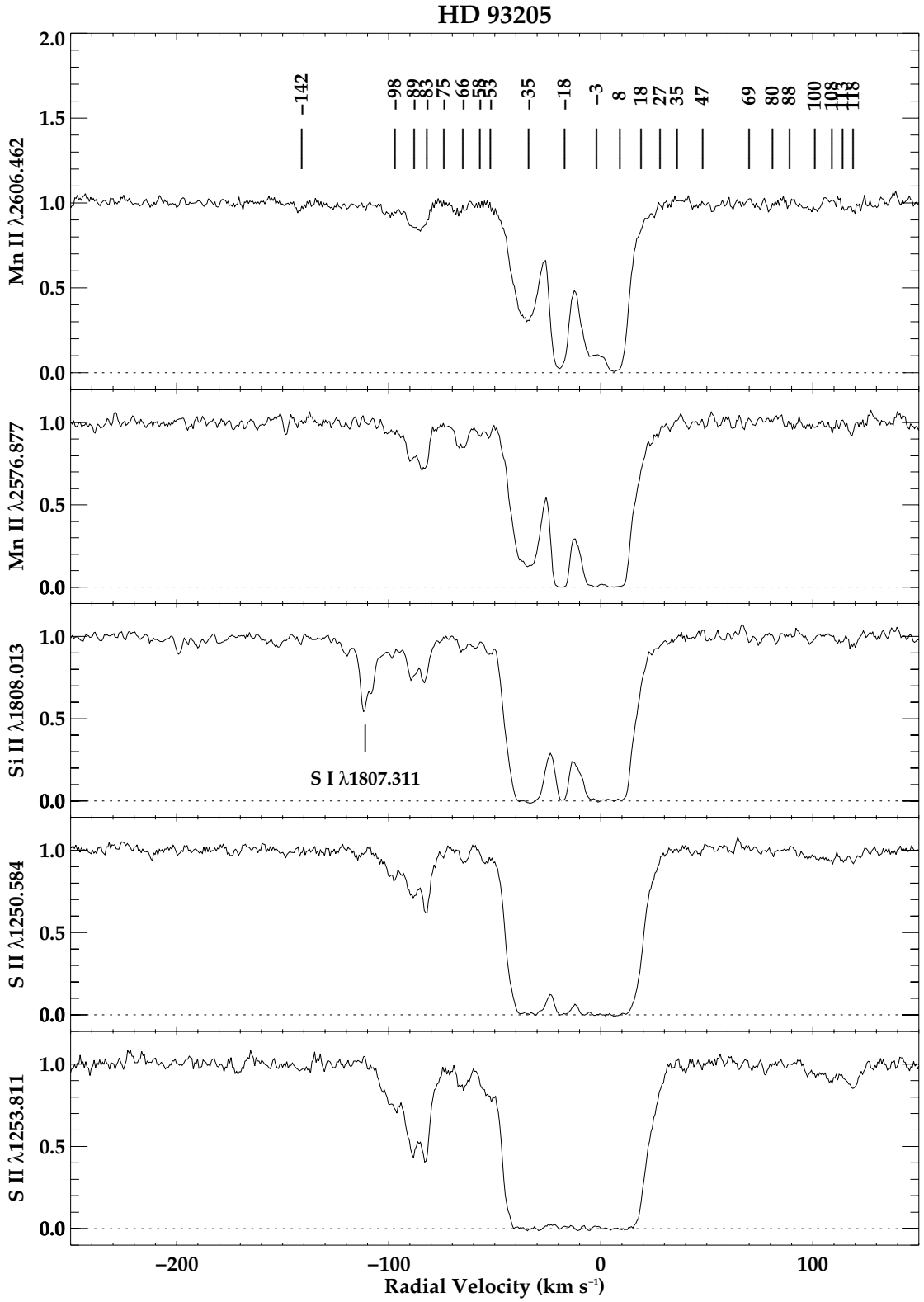
HD 93205
Mn II λ2606.462
Mn II λ2576.877
Si II λ1808.013
S I λ1807.311
S II λ1250.584
S II λ1253.811
−142
−98
−89
−83
−75
−66
−58
−53
−35
−18
−3
8
18
27
35
47
69
80
88
100
108
113
118
2.0
1.5
1.0
0.5
0.0
−200
−100
0
100
Radial Velocity (km s⁻¹)

FIG. 4*b*

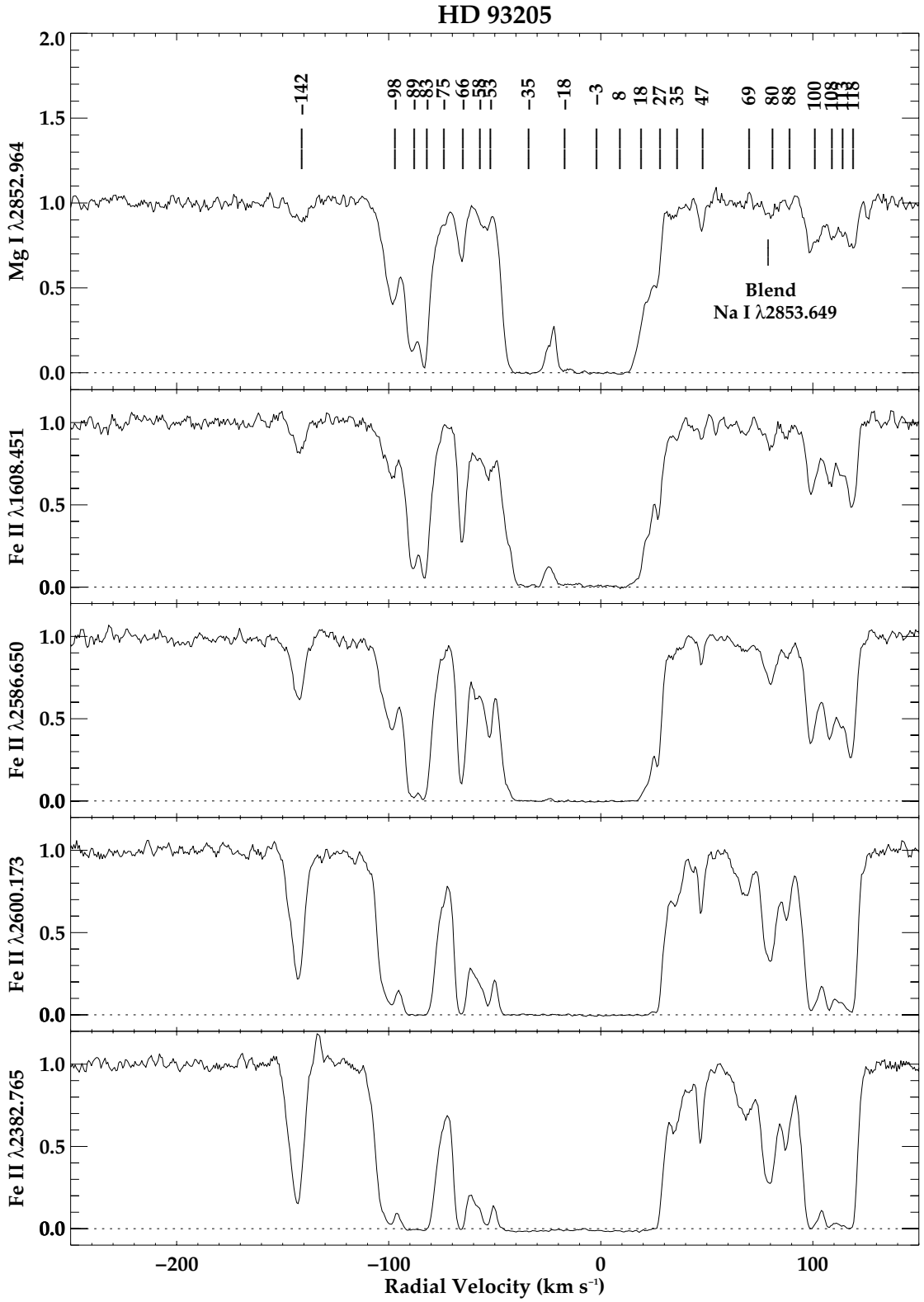
HD 93205
Mg I λ2852.964
Fe II λ1608.451
Fe II λ2586.650
Fe II λ2600.173
Fe II λ2382.765
−142
−98
−89
−83
−75
−66
−58
−53
−35
−18
−3
8
18
27
35
47
69
80
88
100
108
113
118
Blend
Na I λ2853.649
2.0
1.5
1.0
0.5
0.0
−200
−100
0
100
Radial Velocity (km s⁻¹)

FIG. 4*c*

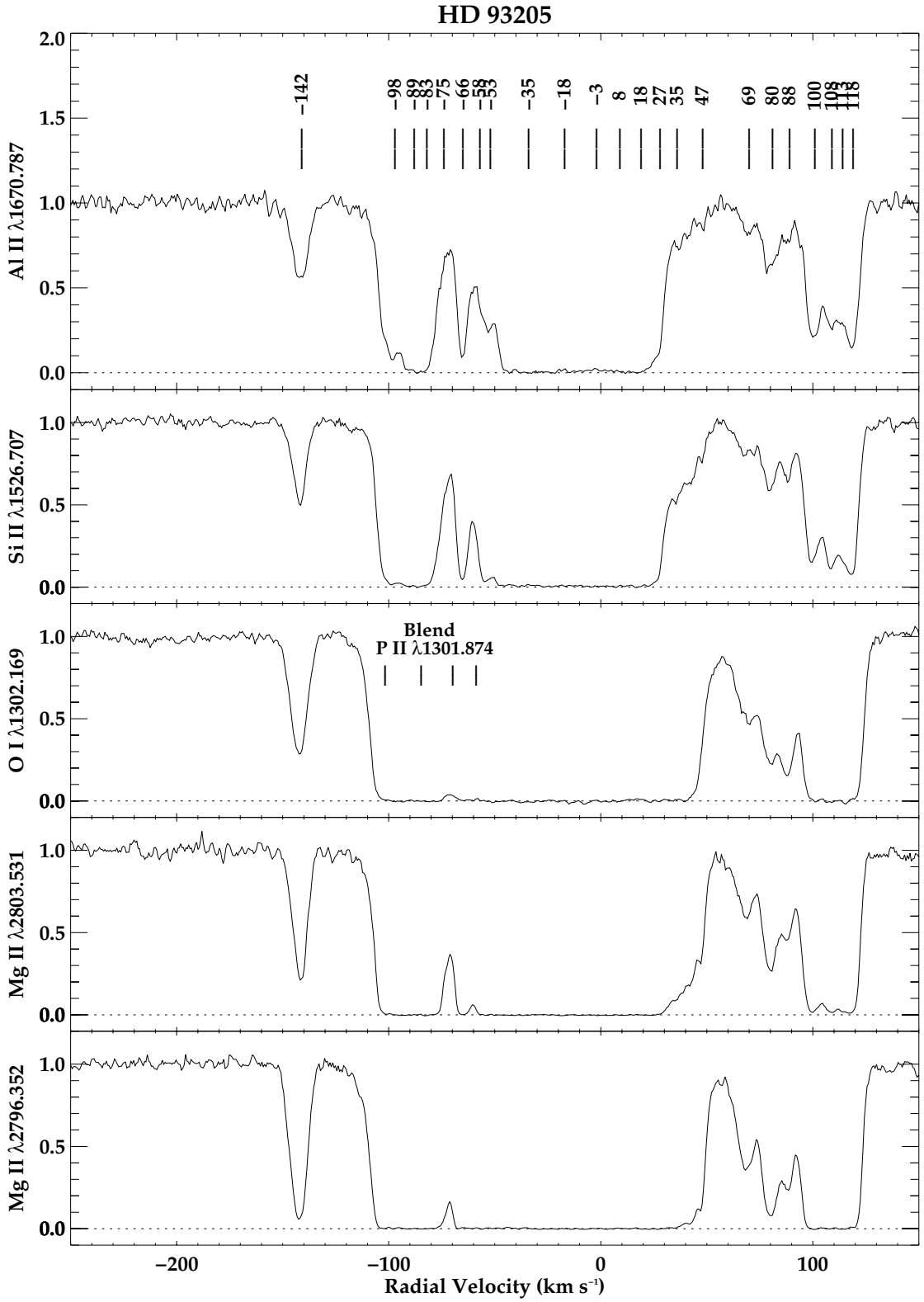
HD 93205
Al II λ1670.787
Si II λ1526.707
O I λ1302.169
Blend
P II λ1301.874
Mg II λ2803.531
Mg II λ2796.352
−142
−98
−89
−83
−75
−66
−58
−53
−35
−18
−3
8
18
27
35
47
69
80
88
100
108
113
118
2.0
1.5
1.0
0.5
0.0
−200
−100
0
100
Radial Velocity (km s⁻¹)

FIG. 4*d*

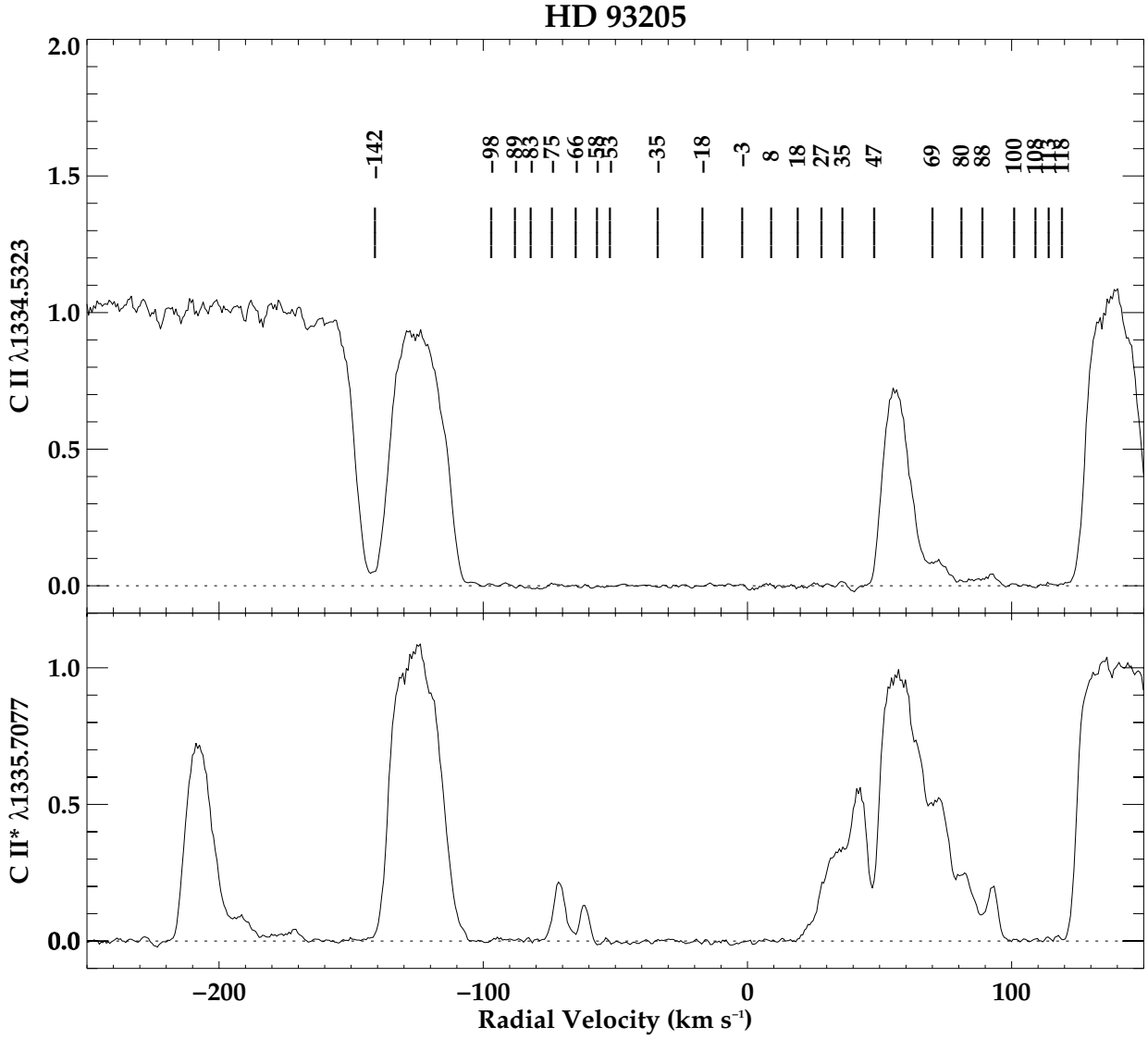

FIG. 5.—C II, C II* interstellar lines toward HD 93205

lower velocity components likely arise along the ~2500 pc line of sight[5] to the complex, but the −38 km s^{-1} and possibly the −19 km s^{-1} components are related to the global expansion of the H II region, as inferred from comparisons with the double nebular emission lines (Walborn & Hesser 1975) and the high-ionization absorption lines (Walborn, Heckathorn, & Hesser 1984, and below). Despite the overall similarities, marked differences occur in the relative strengths of these four velocity components among the different species, e.g., the much greater strength of the −19 km s^{-1} in the Mg II and Mn II lines, and of the +8 km s^{-1} in Cl I. When analyzed quantitatively, these differences will provide valuable diagnostics of the relative ionizations, abundances, and depletions in the material giving rise to the various components, and ultimately clues to their sites of origin.

The S II lines (Fig. 2*b*) are the most "useless," since the low- and intermediate-velocity components have become completely blended, while the high-velocity ones are not yet well detected. The latter appear clearly in Mg I (Fig. 2*c*) and strengthen to their maximum intensities in Mg II (Fig. 2*d*) and C II (Fig. 3). Again, despite the similarities in the profiles of the strong lines, significant differences can be seen in the relative strengths of certain components among the different species, e.g., the weaker −166 km s^{-1} and stronger +61 km s^{-1} in O I compared to adjacent profiles. As before, quantitative analyses of these effects will provide physical insights into the formation and origins of the different components. The C II, C II* profiles offer additional interesting information, namely the disappearance of the +69 km s^{-1} component and changes in the strengths of other components between the two epochs, confirming the Mg II variations reported by Danks et al. (2001); and the resolution of the weaker C II* 1335.663 Å line at +98 km s^{-1}. Both C II* lines are entered in Table 2 at the latter velocity to record

[5] No high-velocity interstellar lines due to galactic structure and differential rotation are expected in this direction (Rickard 1974). It is likely that at least some of the interstellar velocity components within about ±10 km s^{-1} arise along the general line of sight. Astrophysical analysis of some weak, low-velocity, heavy-element lines in Walborn et al. (1998) indicates that they may arise in diffuse clouds near the Sun.

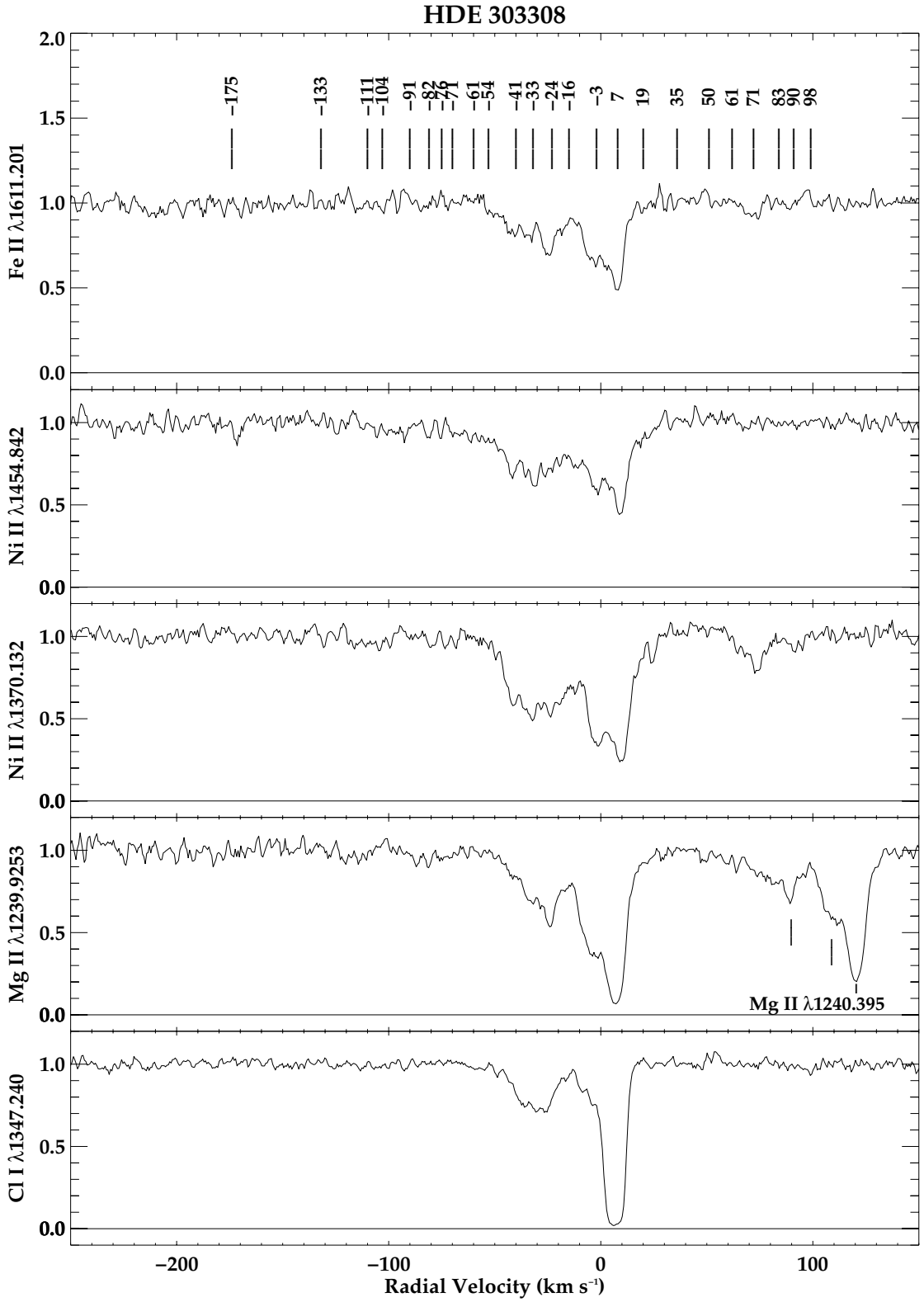

FIG. 6*a*

FIG. 6.—(*a*) Sequence of low-ionization interstellar-line profiles toward HDE 303308. The sequence continues in (*b*)–(*d*).

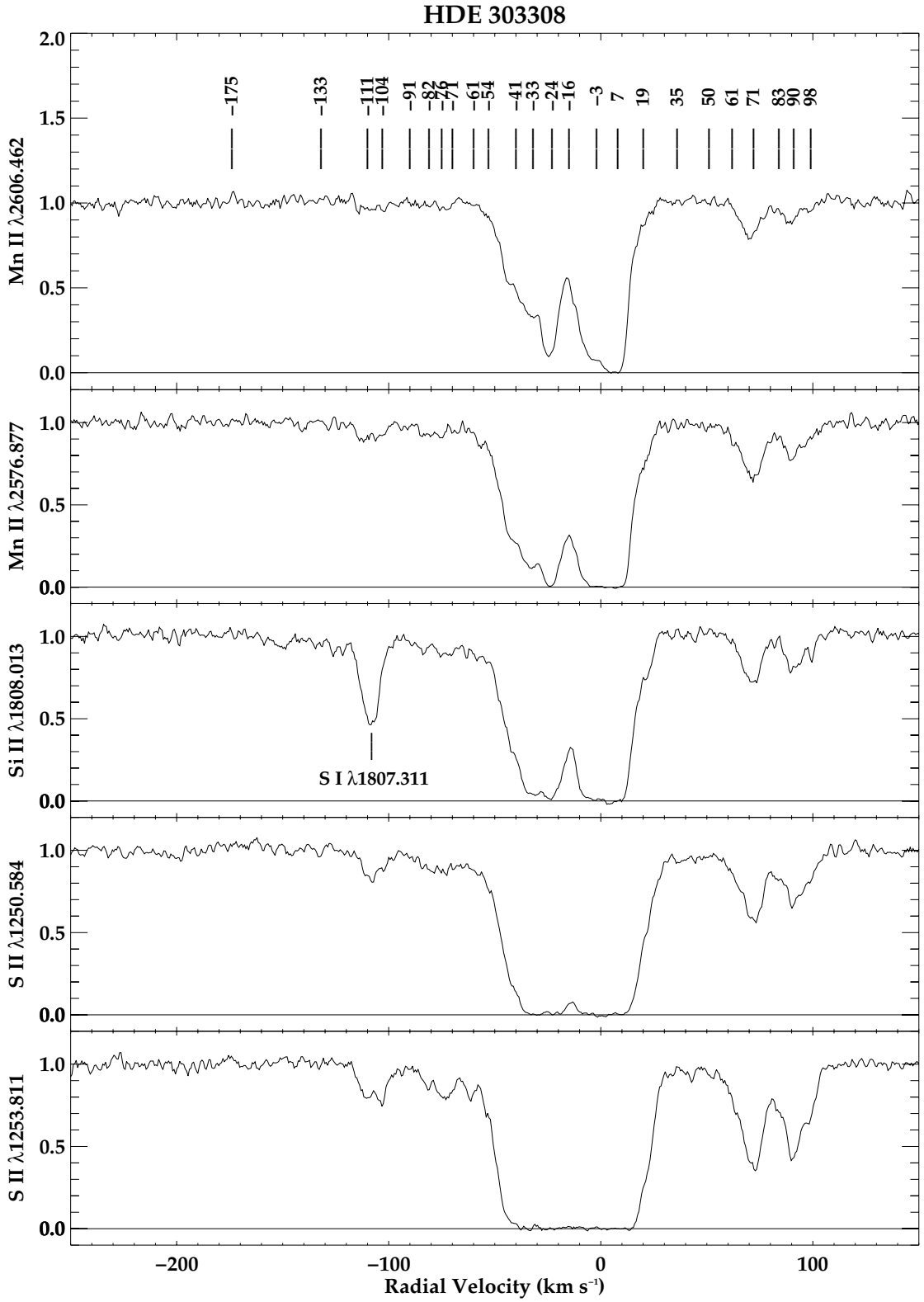
HDE 303308
Mn II λ2606.462
Mn II λ2576.877
Si II λ1808.013
S I λ1807.311
S II λ1250.584
S II λ1253.811
−175
−133
−111
−104
−91
−82
−76
−71
−61
−54
−41
−33
−24
−16
−3
7
19
35
50
61
71
83
90
98
2.0
1.5
1.0
0.5
0.0
−200
−100
0
100
Radial Velocity (km s⁻¹)

FIG. 6*b*

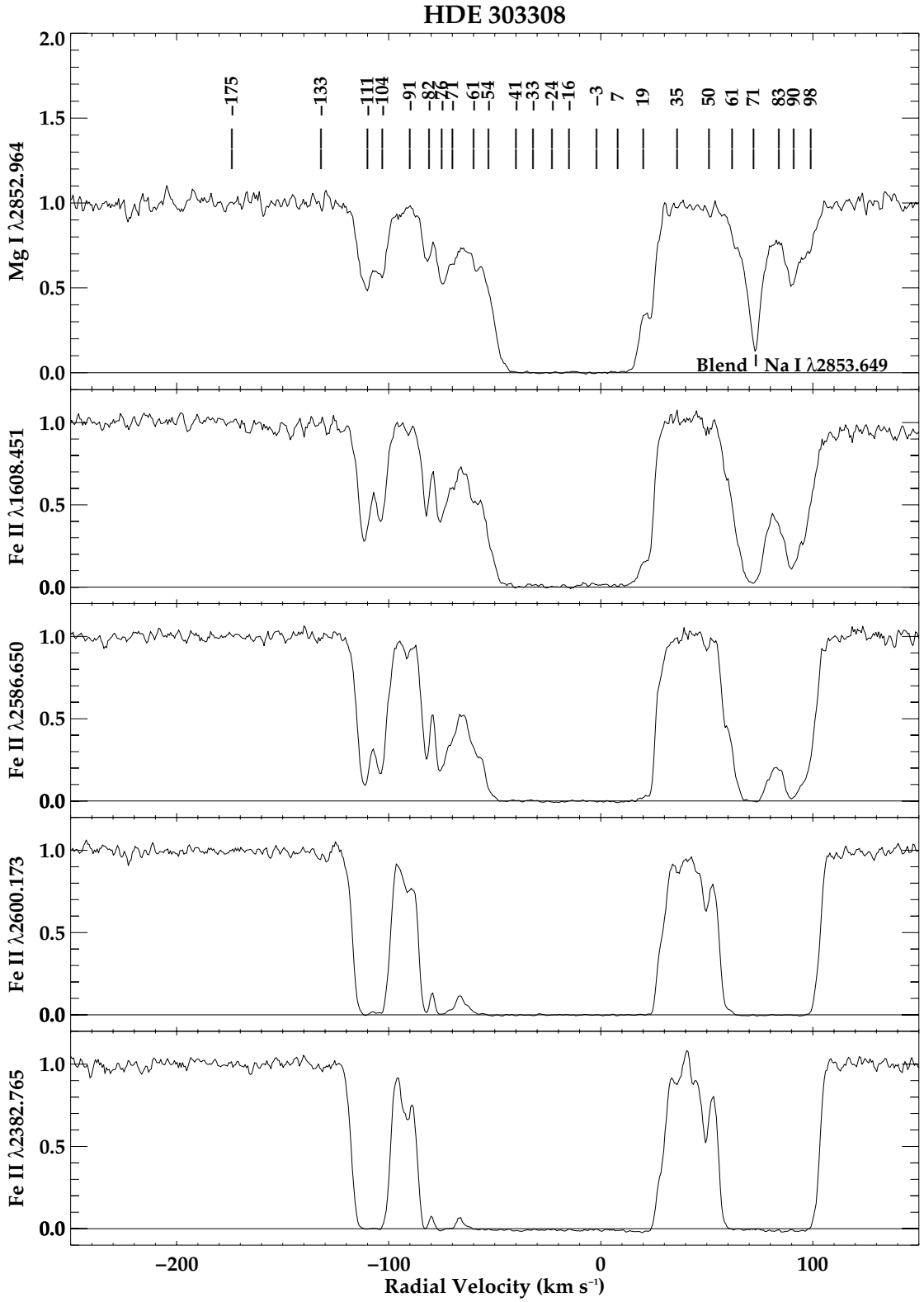
HDE 303308
Mg I λ2852.964
Fe II λ1608.451
Fe II λ2586.650
Fe II λ2600.173
Fe II λ2382.765
−175
−133
−111
−104
−91
−82
−76
−71
−61
−54
−41
−33
−24
−16
−3
7
19
35
50
61
71
83
90
98
Blend
Na I λ2853.649
2.0
1.5
1.0
0.5
0.0
−200
−100
0
100
Radial Velocity (km s⁻¹)

FIG. 6*c*

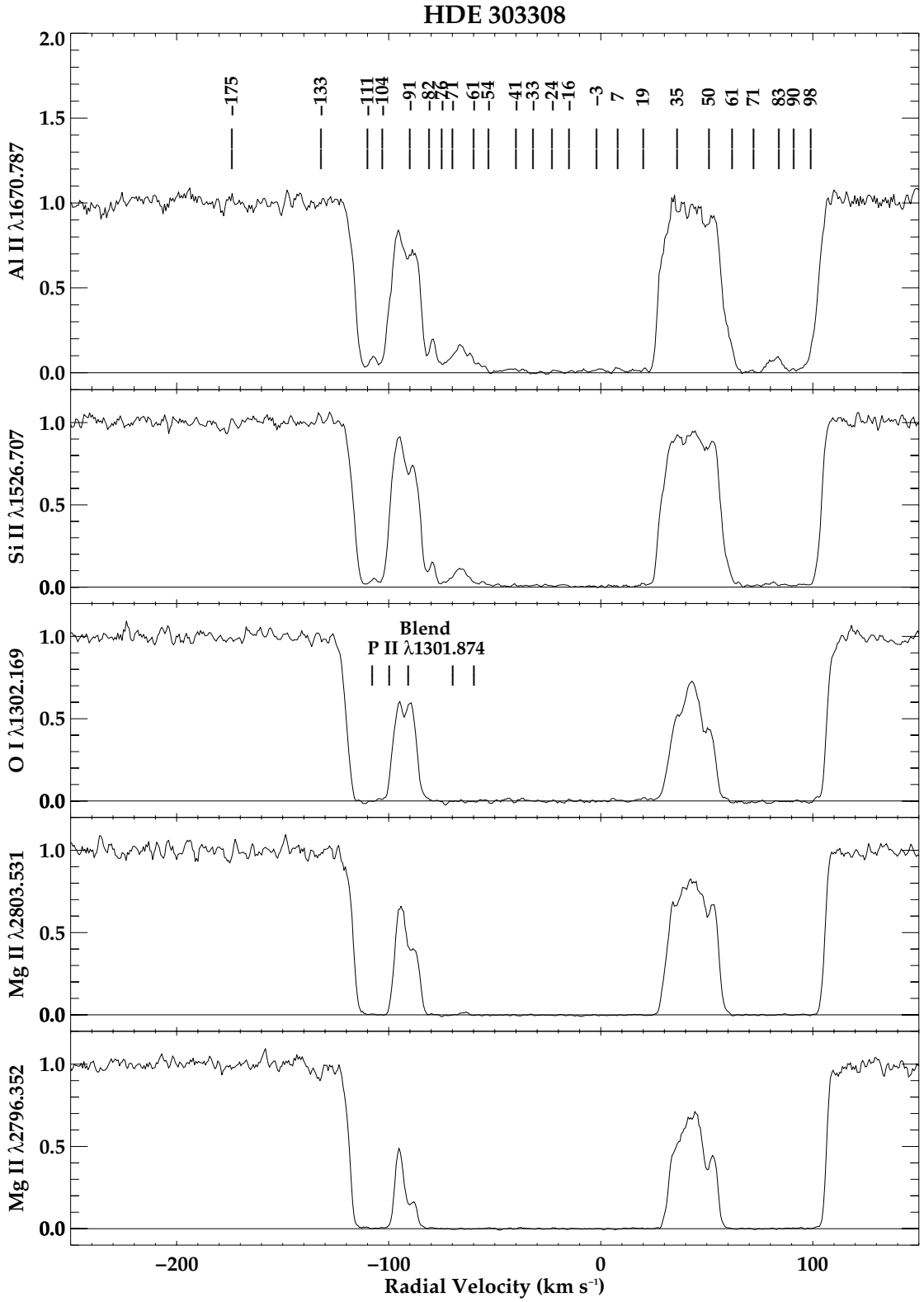
HDE 303308
Al II λ1670.787
Si II λ1526.707
O I λ1302.169
Mg II λ2803.531
Mg II λ2796.352
Blend
P II λ1301.874
−175
−133
−111
−104
−91
−82
−76
−71
−61
−54
−41
−33
−24
−16
−3
7
19
35
50
61
71
83
90
98
2.0
1.5
1.0
0.5
0.0
−200
−100
0
100
Radial Velocity (km s⁻¹)

FIG. 6*d*

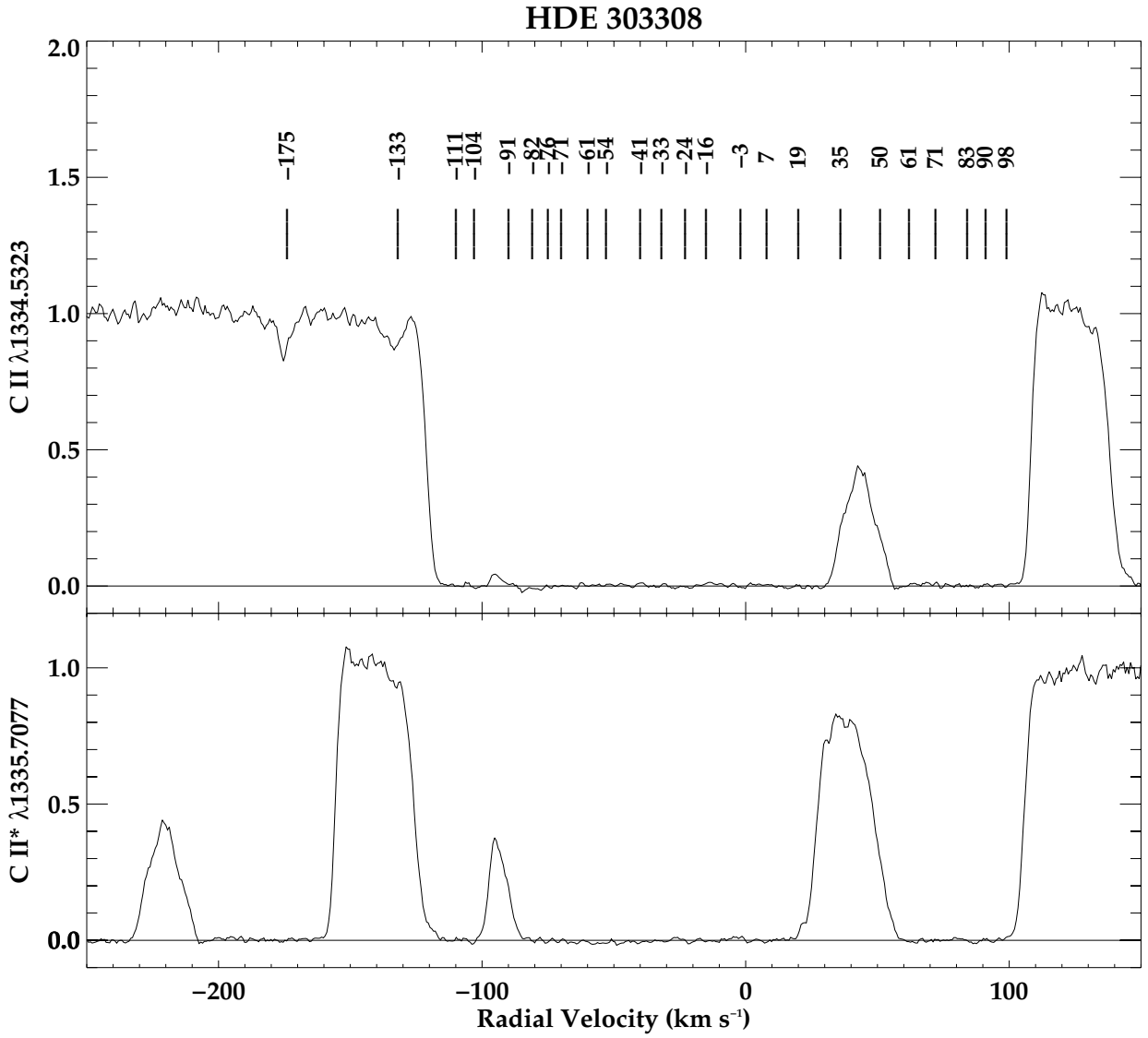

FIG. 7.—C II, C II* interstellar lines toward HDE 303308

their presence, although the fitting program assumes identical parameters for them.

As known from previous work, the dominant components of the high-ionization lines (Fig. 10) are at intermediate negative velocities, corresponding to the global expansion of the H II region (Walborn et al. 1984). Two principal components at −44 and −30 km s^{-1} have been fitted to the CPD −59°2603 profiles, based on the appearance of the C IV lines; the average of those velocities is similar to a dominant component resolved in the weak low-ionization lines, which is likely related. The features near zero velocity may provide a rare opportunity to investigate high-ionization lines along the general Galactic-disk line of sight, far from the hot stars against which they are observed, since H II region material at those velocities should be mostly behind the stars. There is clearly high-velocity structure in the high-ionization lines, but it is weaker and less well defined than in the low-ionization lines. The fitted high-ionization velocities tend to be similar to or more negative than those of the most similar low-ionization components (Table 2), which may or may not be significant at this early stage of the analysis. Although the very strong excited-state line of Si II* 1264.7 Å (Fig. 14) has well-marked high-velocity features, all of the excited-state lines (see Fig. 15 as well) share the property of the high-ionization lines that their dominant components are at the intermediate negative velocities. Note the strong telluric components of O I* and O I** in Figure 15 (Spitzer & Fitzpatrick 1993; Jenkins & Tripp 2001).

4.2. *HD 93205*

The low-ionization interstellar profiles toward this star are displayed in Figures 4*a*–4*d* and 5, the high-ionization lines in Figure 11, and some further excited-state lines in Figures 14 and 15. The corresponding measurements are listed in Table 3. In this and the subsequent data tables, measurements of the same lines from different (overlapping) images are specified by the central wavelengths of the latter in footnotes.

A total of six low-ionization velocity components, including two with very high velocities, were detected in the prior

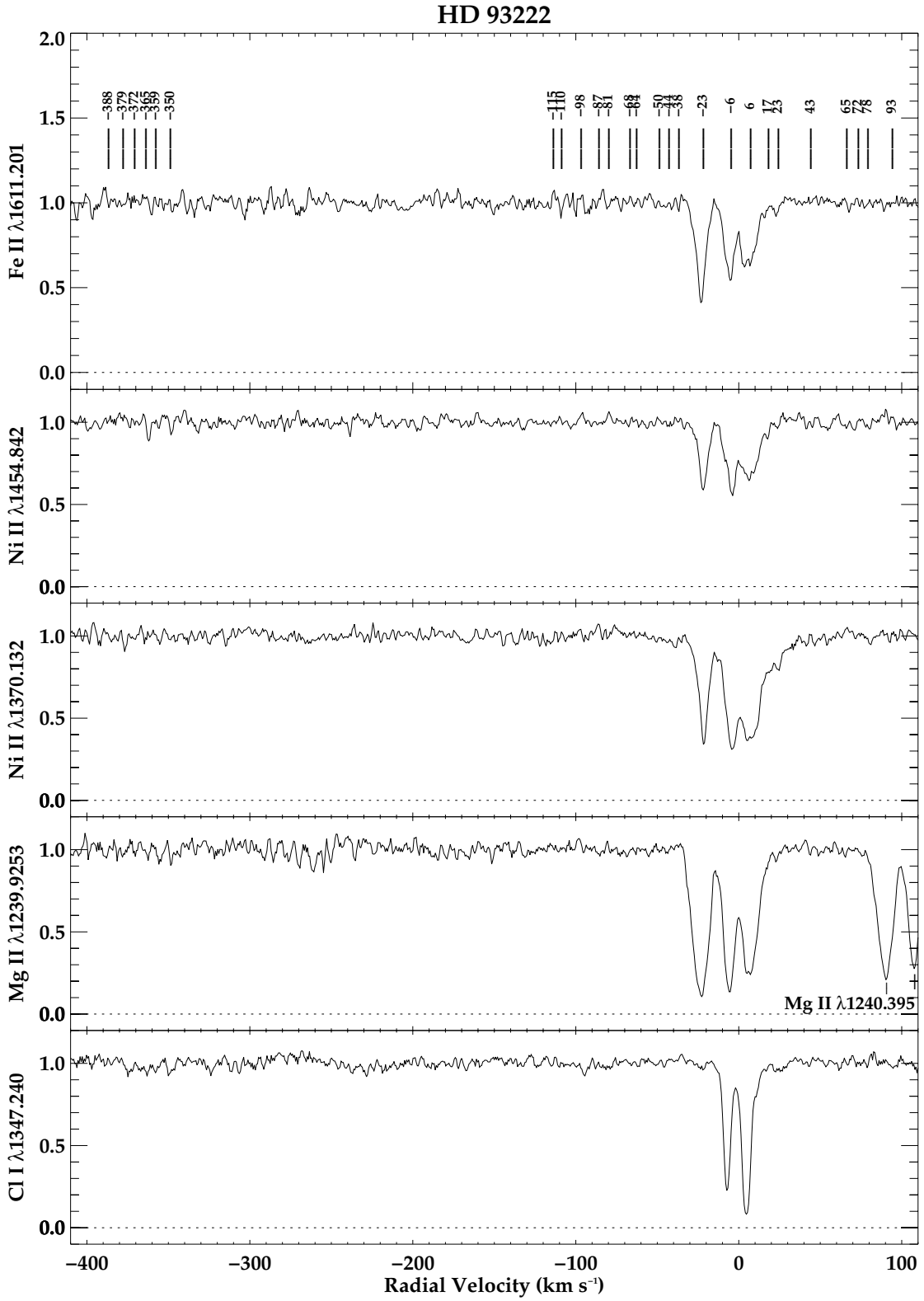

FIG. 8*a*

FIG. 8.—(*a*) Sequence of low-ionization interstellar-line profiles toward HD 93222. The sequence continues in (*b*)–(*d*).

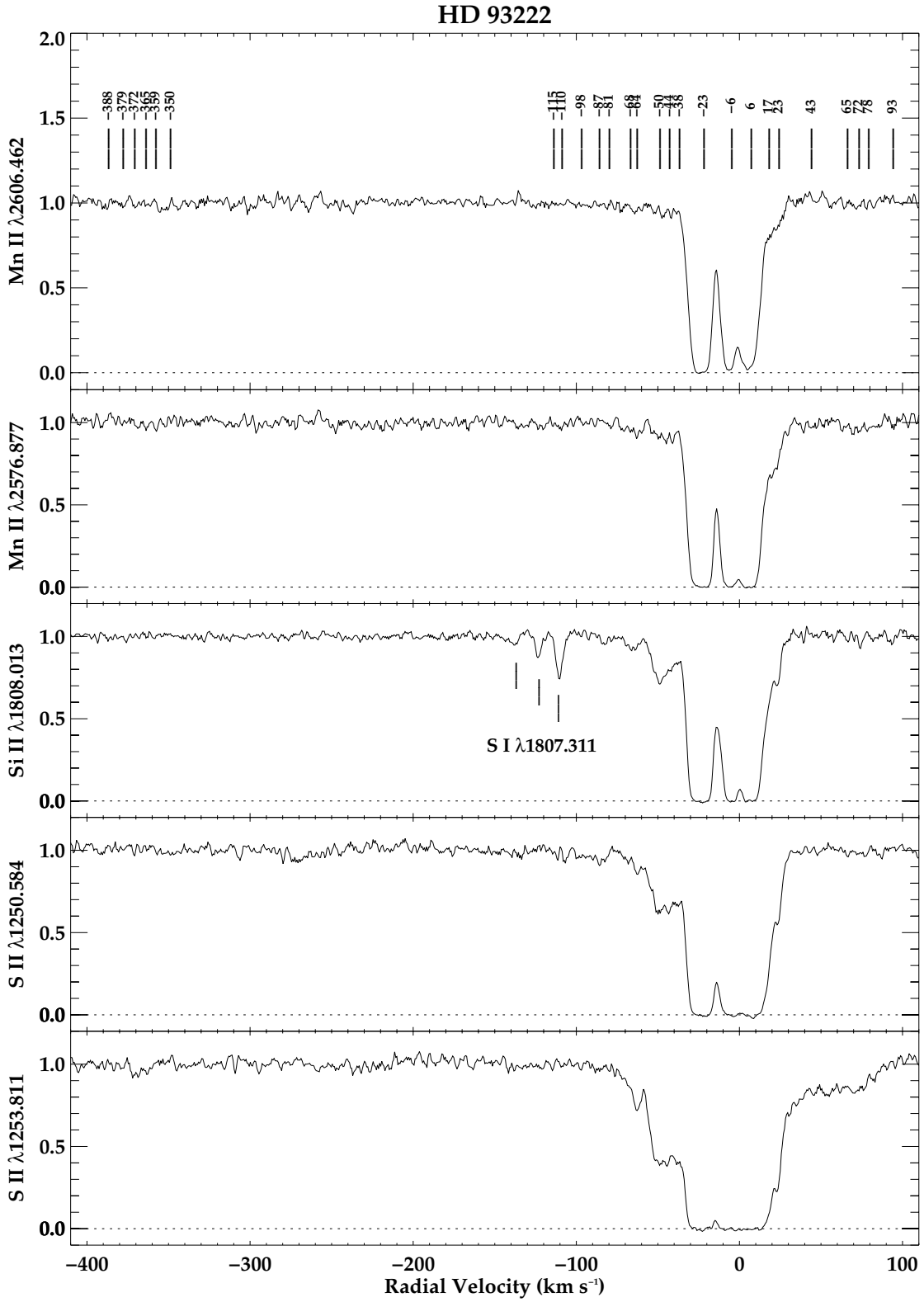
HD 93222
Mn II λ2606.462
Mn II λ2576.877
Si II λ1808.013
S I λ1807.311
S II λ1250.584
S II λ1253.811
Radial Velocity (km s⁻¹)

FIG. 8*b*

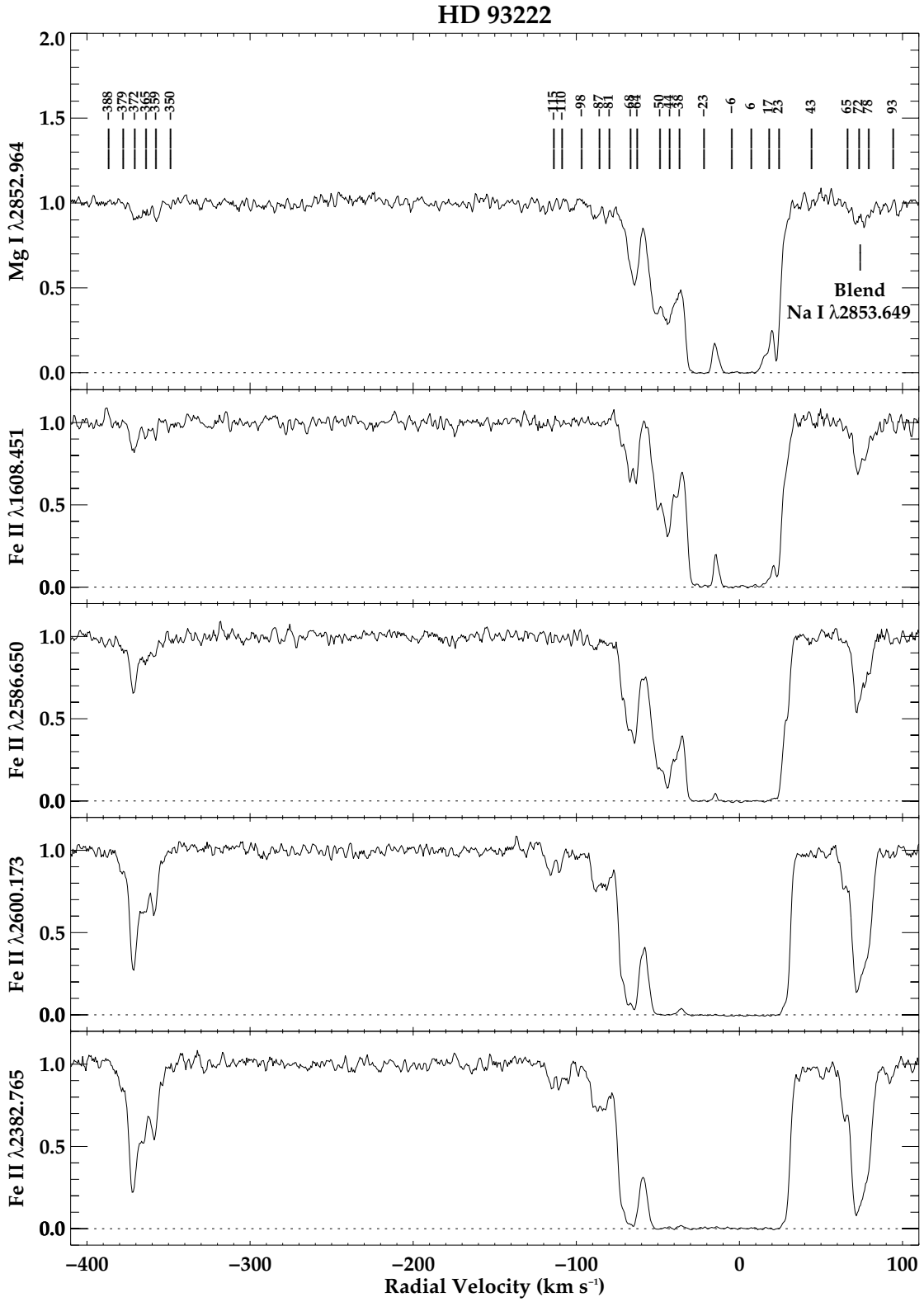
HD 93222
Mg I λ2852.964
Fe II λ1608.451
Fe II λ2586.650
Fe II λ2600.173
Fe II λ2382.765
Blend
Na I λ2853.649
Radial Velocity (km s⁻¹)

FIG. 8*c*

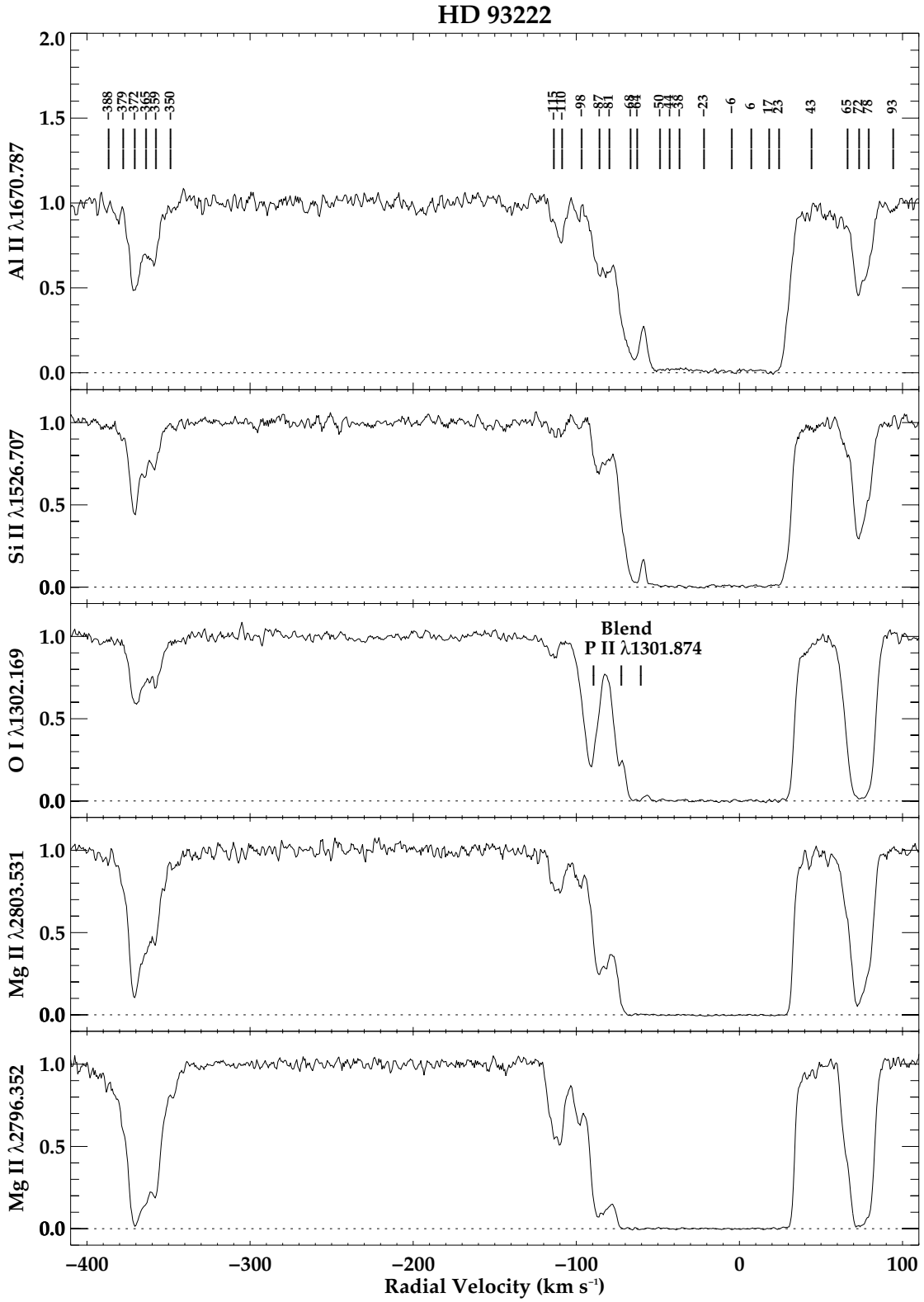
HD 93222
Al II λ1670.787
Si II λ1526.707
O I λ1302.169
Blend
P II λ1301.874
Mg II λ2803.531
Mg II λ2796.352
−388
−379
−372
−365
−358
−350
−115
−110
−98
−87
−81
−68
−64
−50
−44
−38
−23
−6
6
17
23
43
65
72
78
93
2.0
1.5
1.0
0.5
0.0
−400
−300
−200
−100
0
100
Radial Velocity (km s⁻¹)

FIG. 8*d*

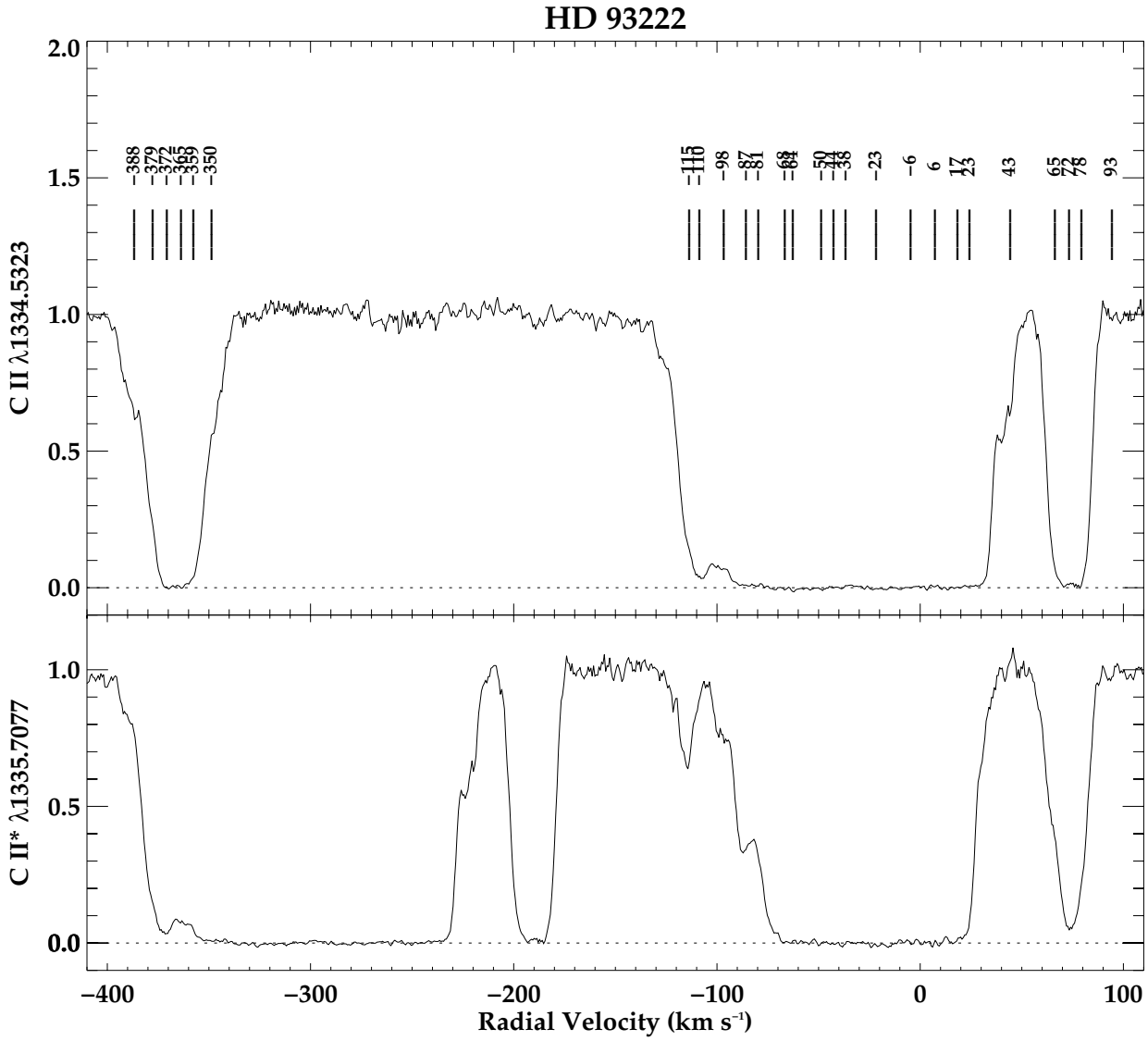

FIG. 9.—C II, C II* interstellar lines toward HD 93222. Note that the C II* features at −350 to −388 km s^{-1} are blended at the shortward edge of the black trough in C II.

ground-based and *IUE* studies. The STIS data reveal 23 low-ionization components ranging in velocity from −142 to +118 km s^{-1}. Particularly noteworthy are the extreme negative velocity, which corresponds to a quite strong component in the more intense lines that was not detected in the earlier work, and the resolution of the former −89 km s^{-1} feature into three strong subcomponents (Figs. 4*c*–4*d*).

The velocity structure in the weak lines at low and intermediate velocities (Figs. 4*a*–4*b*) is virtually identical to that in CPD −59°2603, demonstrating that it corresponds to global structure in the H II region, as well as the Galactic-disk line of sight. Unlike CPD −59°2603, however, HD 93205 has some high-velocity components already well detected in Mn II and S II (Fig. 4*b*), showing that they are intrinsically stronger than those toward the other star.

As in all cases, the strongest high-ionization (Fig. 11) and excited-state (Figs. 14 and 15) components are at an intermediate negative velocity, −35 km s^{-1} toward HD 93205, corresponding to the blueshifted near side of the expanding H II region. There is a major low-ionization component at an identical velocity, which likely has the same origin. The behavior of the other principal components in the high-ionization lines is interesting: the one at −61 km s^{-1} is proportional to the degree of ionization (strongest in C IV), while the blend of the −3 and +8 km s^{-1} components is inversely proportional (strongest in Al III). This behavior is consistent with an origin of the high negative-velocity feature within the H II region, but the low-velocity features along the Galactic-disk line of sight as predicted on morphological grounds above.

4.3. *HDE 303308*

This star, located 1′ north of η Carinae, has the most heavily blended interstellar profiles in the present sample. The low-ionization lines are shown in Figures 6*a*–6*d* and 7, the high-ionization lines in Figure 12, and further excited-state lines in Figures 14 and 15. The measurements are given in Table 4.

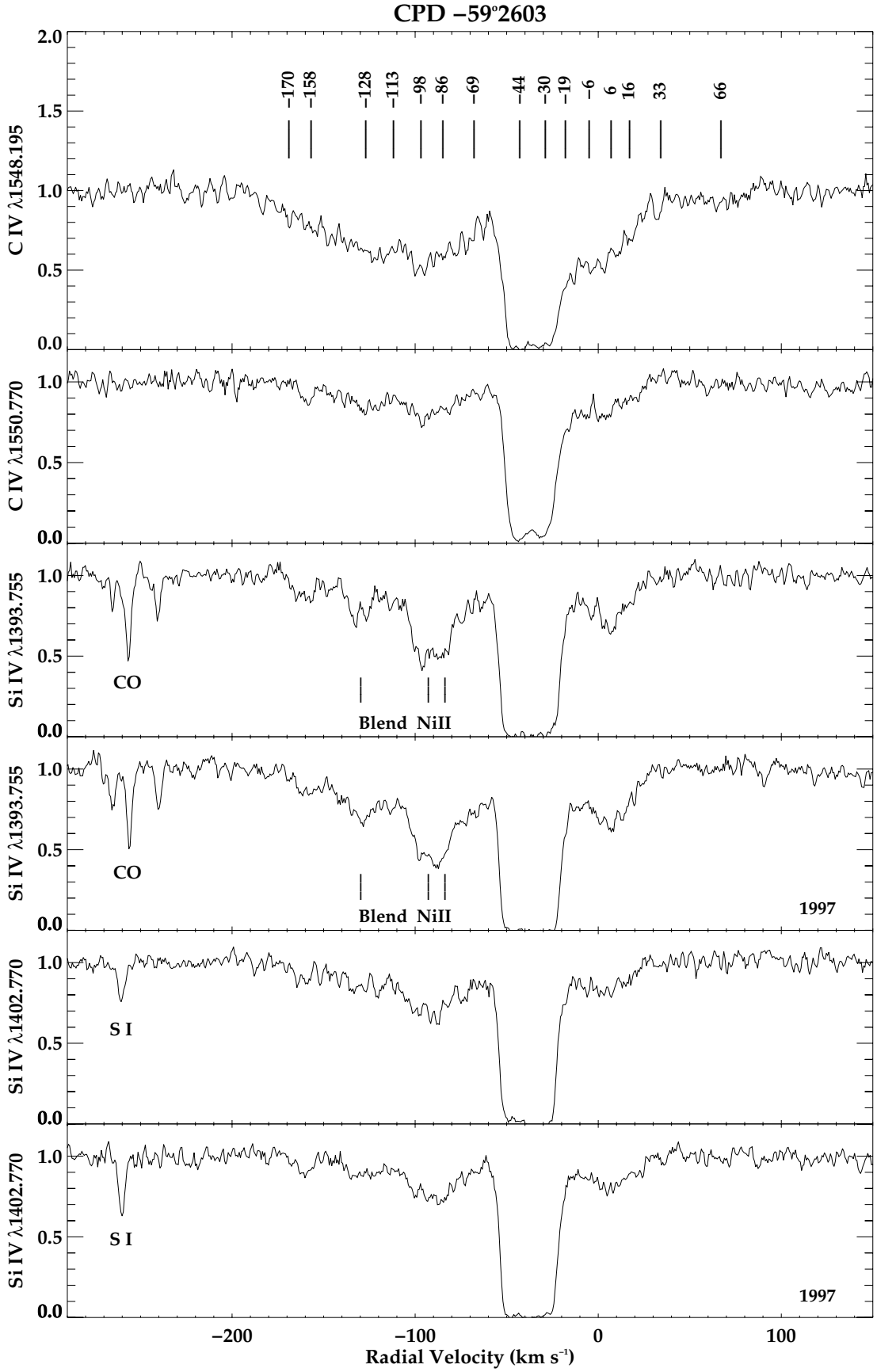

FIG. 10.—Rectified, high-ionization interstellar-line profiles toward CPD −59°2603. The heliocentric radial velocities (km s^{-1}) of the fitted components are marked at the top, and extraneous species in a given panel are identified. The Si IV lines were covered at both epochs; the 1997 data are so marked. (The Al III lines were not observed in this line of sight.)

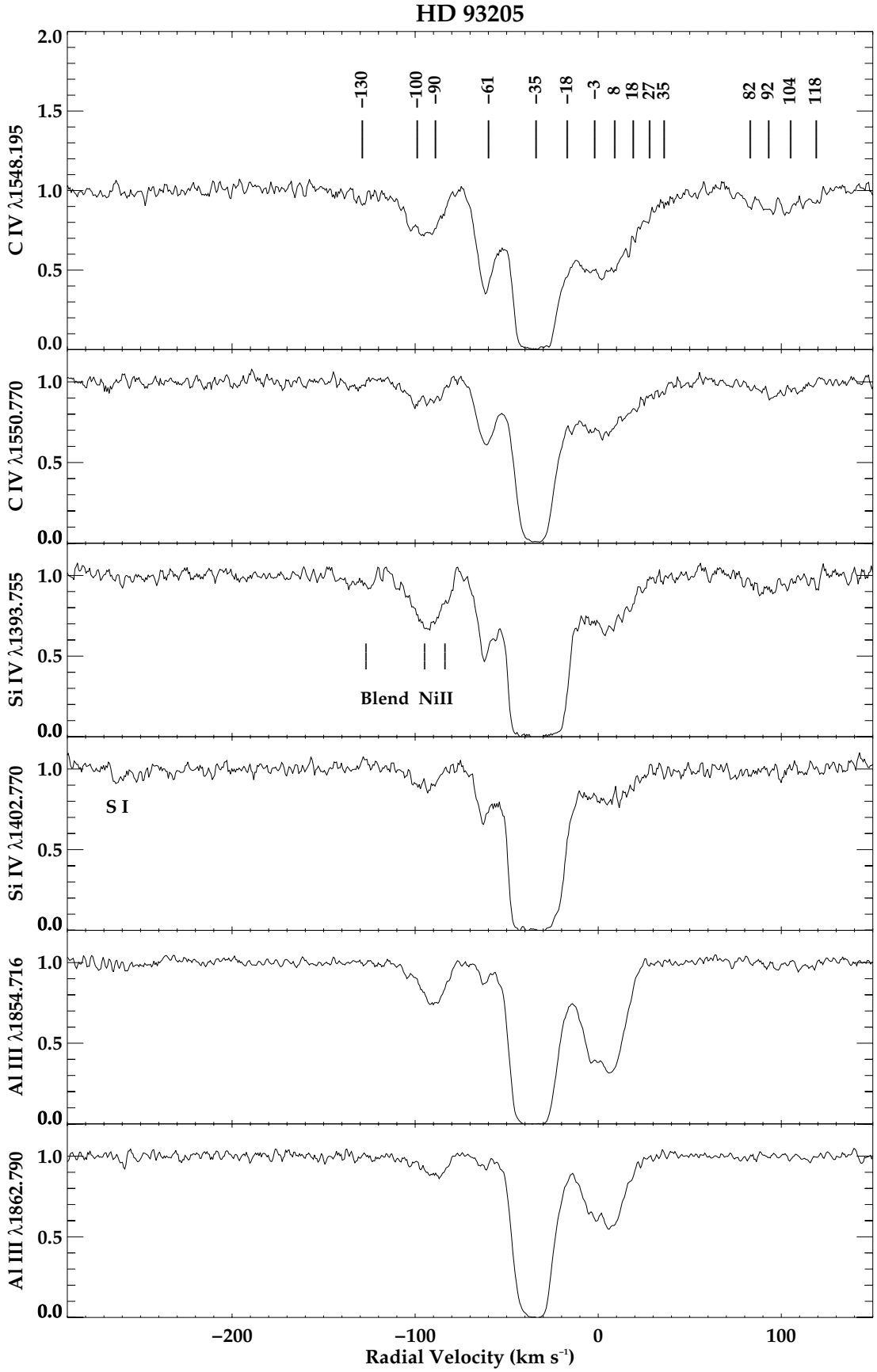

FIG. 11.—High-ionization interstellar-line profiles toward HD 93205

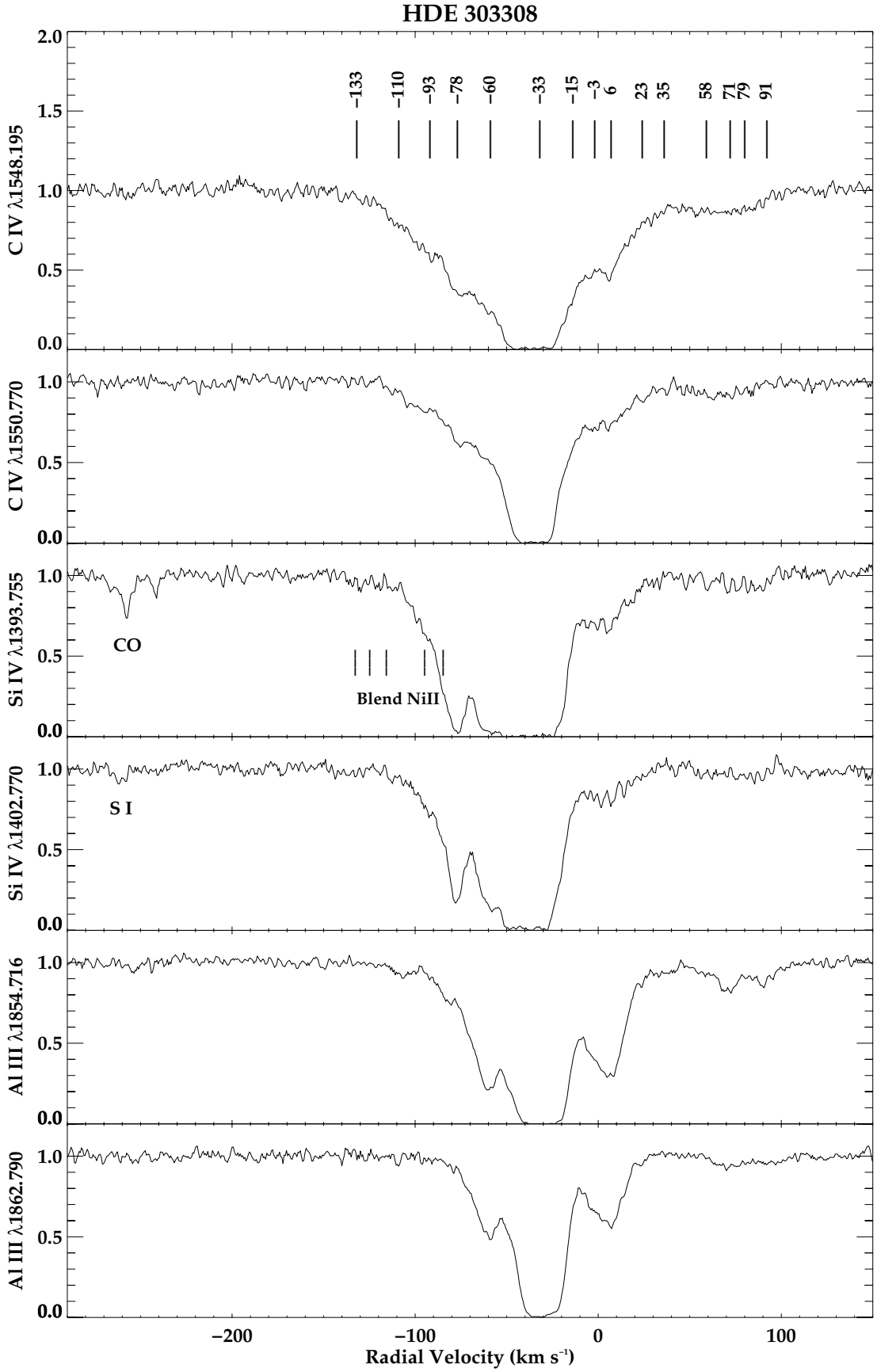

FIG. 12.—High-ionization interstellar-line profiles toward HDE 303308

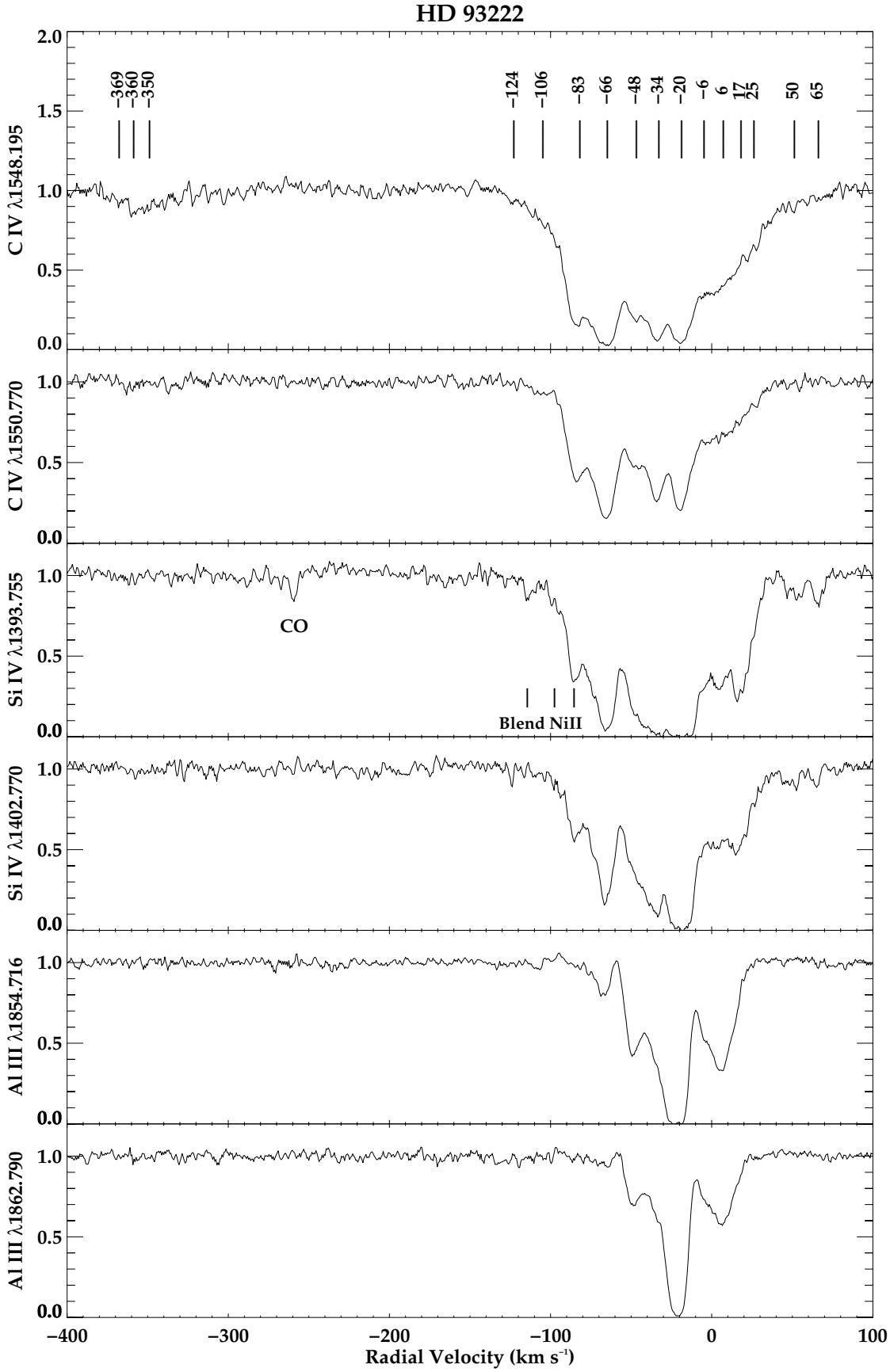

FIG. 13.—High-ionization interstellar-line profiles toward HD 93222

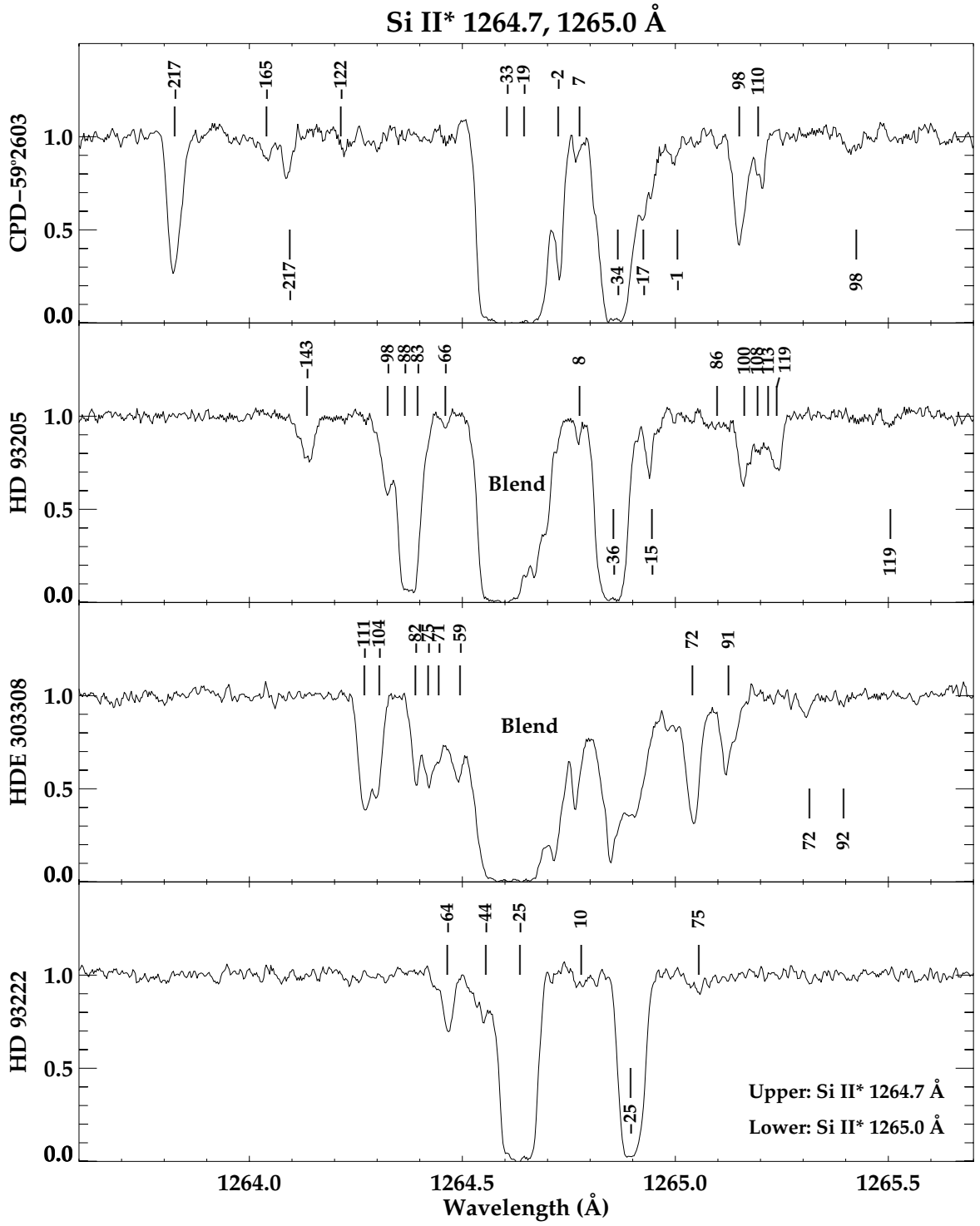

FIG. 14.—Overlapping Si II* 1264.7, 1265.0 Å interstellar-line profiles toward all four stars. Where unconfused, the heliocentric radial velocities (km s^{-1}) of discrete components are marked, for the 1264.7 Å line at the top of each panel, and for 1265.0 Å at the bottom.

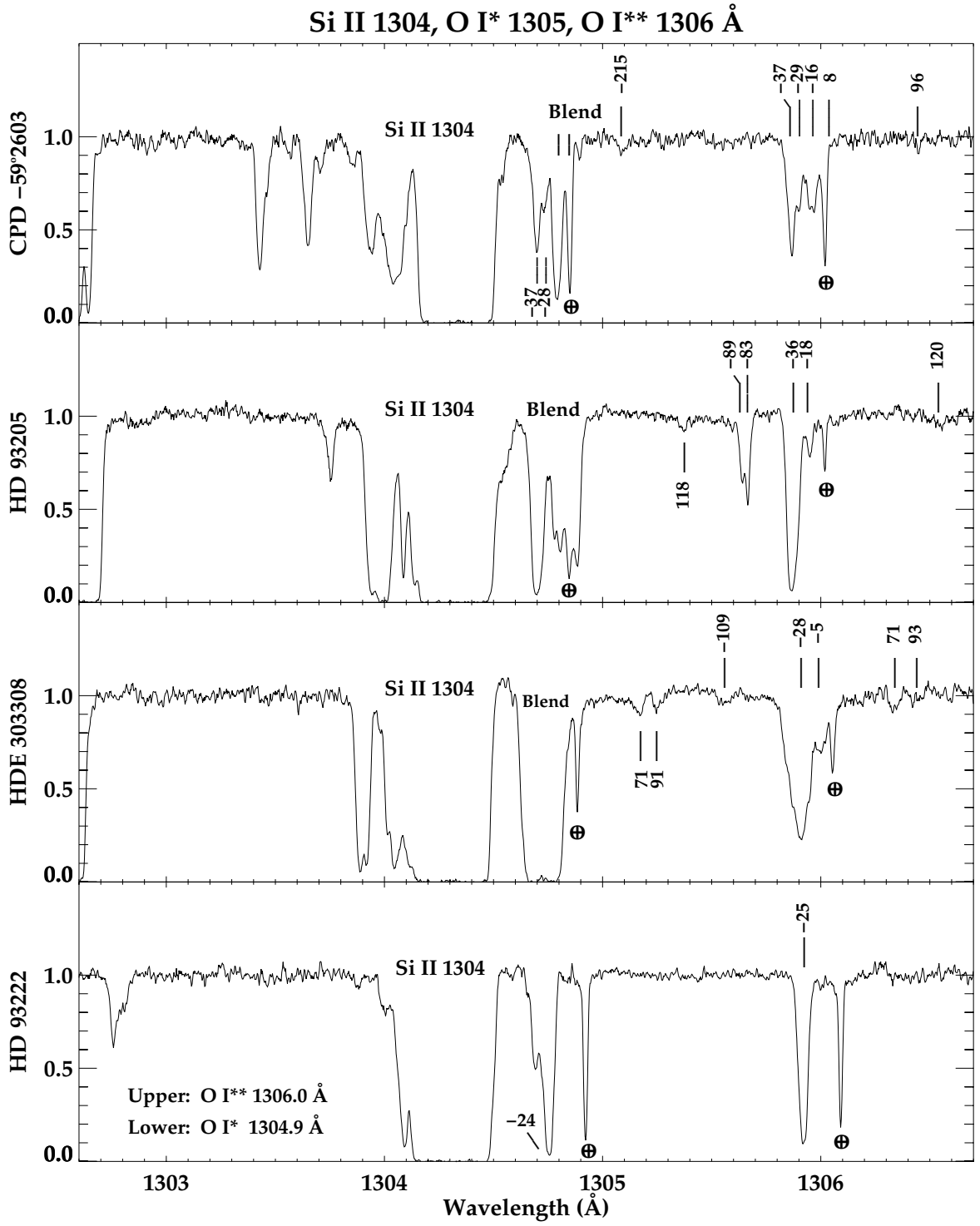

FIG. 15.—Partially overlapping interstellar-line profiles of Si II 1304, O I* 1305, and O I** 1306 Å toward all four stars. Where unconfused, the heliocentric radial velocities (km s^{-1}) of discrete components are marked, for the O I** line at the top of each panel, and for the O I* at the bottom. The telluric components of the O I*, O I** are marked with Earth symbols.

TABLE 2

CPD −59°2603

Ion	λ	v	b	log N
		−233 km s^{-1} Component		
Al II.....	1670.787	−233.00	7.48	11.08
C II.....	1334.532[a]	−232.65	3.81	12.83
	1334.532[b]	−234.01	4.14	12.91
Fe II.....	1608.451	−232.96	1.50	12.06:
	2382.765	−233.63	1.57	11.52
	2586.650	−232.44	3.42	11.98
	2600.173	−233.78	2.55	11.68
Mg II	2796.352[a]	−233.45	1.89	11.49
	2796.352[b]	−233.41	3.36	11.68
	2803.531[a]	−232.07	2.92	11.69
	2803.531[b]	−232.58	3.16	11.73
O I.....	1302.169	−235.01	5.31	12.76
Si II.....	1304.370	−231.04	2.43	11.85
	1526.707	−232.39	1.56	11.95
		−216 km s^{-1} Component		
Al II.....	1670.787	−216.09	3.96	12.29
C II.....	1334.532[a]	−214.71	5.13	14.45:
	1334.532[b]	−215.72	5.37	14.35:
Fe II.....	1608.451	−216.41	3.09	13.33
	2382.765	−216.26	3.60	13.45:
	2586.650	−216.55	3.40	13.34
	2600.173	−216.29	4.00	13.33
Mg I	2852.964[a]	−217.12	2.74	11.61
	2852.964[b]	−216.72	3.12	11.43
Mg II	2796.352[a]	−215.82	3.82	13.59:
	2796.352[b]	−215.45	4.35	13.28:
	2803.531[a]	−215.84	4.59	13.27
	2803.531[b]	−215.48	4.37	13.25
Mn II	2576.877	−216.71	1.50	11.28:
O I.....	1302.169	−216.34	4.90	14.44
O I**	1306.029	−215.47	4.45	12.57
S II.....	1253.811	−214.55	5.57	13.33
	1259.519	−216.43	3.71	13.44
Si II.....	1304.370	−215.80	4.82	13.55
	1526.707	−216.15	3.91	13.48
Si II*.....	1264.738	−216.70	3.62	12.54
	1265.002	−216.55	2.54	12.64
	1309.276	−216.85	2.92	12.18
		−185 km s^{-1} Component		
Al II.....	1670.787	−185.02	1.76	11.00
C II.....	1334.532[a]	−182.06	5.37	13.04
	1334.532[b]	−185.30	4.08	13.09
Fe II.....	1608.451	−187.12	1.69	12.34
	2382.765	−185.64	2.18	12.06
	2586.650	−185.33	4.05	12.20
	2600.173	−185.39	2.45	12.09
Mg I	2852.964[b]	−186.03	1.50	10.30:
Mg II	2796.352[a]	−183.18	3.26	11.54
	2796.352[b]	−185.11	3.40	11.88
	2803.531[a]	−182.43	3.44	11.66
	2803.531[b]	−184.51	3.05	11.81
O I.....	1302.169	−185.64	3.90	13.03
S II.....	1253.811	−181.30	1.50	13.24
Si II.....	1304.370	−185.05	4.61	12.51
	1526.707	−184.12	5.39	12.56
		−166 km s^{-1} Component		
Al II.....	1670.787	−165.54	4.47	12.33
C II.....	1334.532[a]	−165.27	5.59	14.32:
	1334.532[b]	−166.30	6.32	14.32:
Fe II.....	1608.451	−166.26	4.27	13.18
	2382.765	−166.74	4.35	13.07

TABLE 2—*Continued*

Ion	λ	v	b	log N
	2586.650	−165.87	3.57	13.07
	2600.173	−166.35	4.26	13.08
Mg I	2852.964[a]	−165.90	4.67	11.11
	2852.964[b]	−165.41	4.00	11.11
Mg II	2796.352[a]	−165.77	4.81	12.97
	2796.352[b]	−166.02	5.33	12.97
	2803.531[a]	−165.29	4.65	13.00
	2803.531[b]	−165.18	5.09	12.98
O I.....	1302.169	−165.84	4.70	13.81
S II.....	1250.584	−166.00	6.04	13.65
	1253.811	−166.00	7.00	13.54
	1259.519	−165.82	4.56	13.19
Si II.....	1304.370	−165.71	4.56	13.42
	1526.707	−165.74	4.93	13.42
Si II*.....	1264.738	−165.40	3.95	11.52
C IV	1548.195	−170.43	12.00	12.66
		−153 km s^{-1} Component		
Al II.....	1670.787	−153.10	5.15	11.80
C II.....	1334.532[a]	−153.55	7.43	13.99
	1334.532[b]	−153.27	6.87	13.92
Fe II.....	1608.451	−153.25	2.15	12.44
	2382.765	−154.11	3.43	12.38
	2586.650	−153.96	3.58	12.45
	2600.173	−153.92	3.49	12.43
Mg I	2852.964[a]	−151.33	1.50	10.30:
	2852.964[b]	−152.72	1.97	10.48:
Mg II	2796.352[a]	−153.76	4.62	12.41
	2796.352[b]	−153.12	4.41	12.37
	2803.531[a]	−153.54	4.74	12.42
	2803.531[b]	−152.55	3.67	12.37
O I.....	1302.169	−153.59	3.87	13.29
Si II.....	1304.370	−152.38	4.14	12.73
	1526.707	−152.91	3.94	12.80
C IV	1548.195	−149.19	12.00	12.94
	1550.770	−155.46	12.00	12.72
Si IV.....	1393.755[a]	−156.70	12.00	12.27
	1393.755[b]	−158.72	9.31	12.15
	1402.770[a]	−160.49	6.41	12.23
	1402.770[b]	−158.43	12.00	12.38
		−137 km s^{-1} Component		
Al II.....	1670.787	−136.44	7.34	11.51
C II.....	1334.532[a]	−134.49	9.00	13.81
	1334.532[b]	−135.92	8.50	13.78
Fe II.....	2382.765	−138.29	2.66	11.76
	2586.650	−136.79	2.92	11.83
	2600.173	−138.39	5.24	11.94
Mg II	2796.352[a]	−136.51	7.10	12.07
	2796.352[b]	−136.65	7.19	12.13
	2803.531[a]	−136.36	7.01	12.18
	2803.531[b]	−136.87	8.00	12.23
Si II.....	1304.370	−137.00	2.32	11.20:
	1526.707	−139.10	6.46	12.44
		−120 km s^{-1} Component		
Al II.....	1670.787	−119.85	4.81	11.68
C II.....	1334.532[a]	−117.65	6.93	13.99:
	1334.532[b]	−120.31	6.46	13.90:
C II*	1335.708[a]	−119.54	6.31	13.54
	1335.708[b]	−121.09	4.60	13.41
Fe II.....	2382.765	−120.86	3.67	12.40
	2586.650	−120.83	4.36	12.46
	2600.173	−120.53	4.08	12.48
Mg I	2852.964[a]	−119.47	1.87	10.48:
	2852.964[b]	−120.08	4.96	10.78
Mg II	2796.352[a]	−119.97	4.34	12.47

TABLE 2—*Continued*

Ion	λ	v	b	log N
	2796.352[b]	−120.17	4.07	12.52
	2803.531[a]	−119.50	4.70	12.52
	2803.531[b]	−119.57	4.56	12.58
O I.....	1302.169	−120.42	4.30	13.65
Si II.....	1304.370	−119.24	4.25	12.59
	1526.707	−120.05	4.66	12.80
Si II*.....	1264.738	−121.72	2.48	11.26
C IV	1548.195	−128.38	12.00	13.06
	1550.770	−125.89	12.00	13.03
Si IV.....	1402.770[a]	−127.31	12.00	12.52
	1402.770[b]	−127.79	12.00	12.66
	−101 km s^{-1} Component			
Al II.....	1670.787	−98.65	9.80	12.45
C II*	1335.708[a]	−99.96	9.41	13.83:
	1335.708[b]	−99.77	10.00	13.84:
Fe II.....	1608.451	−101.75	3.01	12.71
	1611.201	−102.62	2.37	13.89
	2382.765	−102.38	6.78	12.94
	2586.650	−101.98	6.91	12.96
	2600.173	−102.28	6.64	12.93
Mg I	2852.964[a]	−100.98	8.06	11.11
	2852.964[b]	−97.24	7.00	11.04
Mg II	2796.352[a]	−97.58	8.72	13.43:
	2796.352[b]	−97.96	9.34	13.35:
	2803.531[a]	−98.57	8.06	13.28
	2803.531[b]	−98.08	8.52	13.35
S II.....	1253.811	−101.00	8.00	13.37
	1259.519	−100.00	7.00	13.27
Si II.....	1304.370	−99.03	7.46	13.62
	1526.707	−99.50	7.33	13.60
C IV	1548.195	−113.00	11.32	13.02
	1548.195	−97.62	7.09	12.94
	1550.770	−96.39	12.00	13.15
Si IV.....	1402.770[a]	−99.03	9.36	12.61
	1402.770[b]	−101.78	9.00	12.73
	−77 km s^{-1} Component			
Al II.....	1670.787	−77.69	10.00	12.67
Fe II.....	1608.451	−76.10	8.79	12.93
	2382.765	−77.78	10.00	13.13
	2586.650	−80.48	10.00	13.02
	2600.173	−78.76	10.00	13.08
Mg I	2852.964[a]	−77.11	10.00	11.82
	2852.964[b]	−77.67	10.00	11.72
Mg II	2796.352[a]	−74.86	10.00	13.63:
	2796.352[b]	−77.54	10.00	13.41:
	2803.531[a]	−75.77	10.00	13.79:
	2803.531[b]	−75.88	8.38	13.97:
Mn II	2594.499	−77.00	6.00	11.62
P II	1532.533	−79.12	1.50	12.78:
S II.....	1250.584	−78.62	6.00	13.81
	1253.811	−77.00	9.00	14.03
	1259.519	−75.94	9.00	13.97
Si II.....	1304.370	−76.06	10.00	13.95
	1526.707	−76.21	10.00	13.97
C IV	1548.195	−83.56	12.00	13.12
Si IV.....	1402.770[a]	−85.67	7.64	12.60
	1402.770[b]	−88.34	7.46	12.71
	−63 km s^{-1} Component			
Al II.....	1670.787	−63.85	9.80	12.26
Fe II.....	1608.451	−64.20	3.05	12.56
	2382.765	−63.82	4.75	12.57
	2586.650	−65.85	8.50	12.91
	2600.173	−64.65	7.00	12.77
Mg I	2852.964[a]	−63.00	6.71	10.78
	2852.964[b]	−63.00	7.49	11.18

TABLE 2—*Continued*

Ion	λ	v	b	log N
Mg II	2796.352[a]	−63.00	9.00	12.81:
	2796.352[b]	−63.00	5.04	12.92:
	2803.531[a]	−60.06	2.01	12.31:
	2803.531[b]	−61.60	4.27	12.66:
Mn II	2594.499	−63.12	4.29	11.34:
O I].....	1355.598[a]	−63.90	5.16	17.28
S II.....	1250.584	−63.00	7.85	13.53
	1253.811	−63.00	7.00	13.68
	1259.519	−63.00	6.00	13.32
Si II.....	1304.370	−64.00	7.14	13.23
	1526.707	−63.92	7.06	13.28
C IV	1548.195	−65.00	12.00	12.85
	1550.770	−65.17	9.83	12.54
Si IV.....	1393.755[a]	−70.99	11.60	12.60
	1393.755[b]	−70.22	12.00	12.44
	1402.770[a]	−70.99	9.54	12.30
	1402.770[b]	−71.04	12.00	12.70
	−38 km s^{-1} Component			
Cl I.....	1347.240[a]	−36.24	2.77	12.00
Cu II	1358.773[a]	−38.21	3.86	11.89
	1358.773[b]	−35.92	4.47	11.88
Fe I.....	2484.021	−37.74	5.01	11.46
Fe II.....	1608.451	−38.80	3.60	15.64:
	1611.201	−38.65	5.67	14.90
	2586.650	−37.94	3.87	15.90:
Ga II.....	1414.402[a]	−36.33	2.72	10.60
	1414.402[b]	−40.08	1.98	10.78
Ge II	1237.059	−36.07	5.72	11.41
Mg I	1683.412	−41.39	1.50	13.54
	2852.964[a]	−37.41	5.61	12.89:
	2852.964[b]	−37.15	5.32	13.11:
Mg II	1239.925	−36.54	5.40	15.49
	1240.395	−37.13	4.98	15.46
Mn II	2576.877	−37.57	6.27	13.03
	2594.499	−37.74	6.26	13.02
	2606.462	−37.83	6.36	13.01
Ni II.....	1317.217[a]	−38.10	5.05	13.51
	1317.217[b]	−38.21	5.16	13.48
	1370.132[a]	−37.26	5.28	13.51
	1370.132[b]	−37.50	4.70	13.49
	1454.842[a]	−36.78	3.83	13.20
	1454.842[b]	−38.01	4.03	13.18
O I*	1304.858	−36.63	4.32	13.68
O I**	1306.029	−37.26	4.72	13.72
S II.....	1250.584	−36.75	5.68	15.63:
Si II*.....	1264.738	−33.00	6.80	14.71:
	1265.002	−33.94	6.89	14.34:
	1309.276	−33.96	6.57	14.12
	1533.431	−34.00	7.11	14.29:
C IV	1548.195	−43.38	5.88	14.05:
	1550.770	−43.92	5.06	14.08
Si IV.....	1393.755[a]	−43.85	4.77	14.64:
	1393.755[b]	−43.54	5.28	14.38:
	1402.770[a]	−46.24	4.05	14.37:
	1402.770[b]	−44.60	5.24	14.38:
	−28 km s^{-1} Component			
Cl I.....	1347.240[a]	−27.71	3.61	12.01
Cu II	1358.773[a]	−28.00	4.00	11.89
Fe II.....	1608.451	−28.00	2.46	14.10:
	1611.201	−28.26	1.50	14.05
	2586.650	−28.00	2.58	14.79:
Ga II.....	1414.402[a]	−27.84	1.50	10.70:
Mg I	2852.964[a]	−28.00	1.50	13.22:
	2852.964[b]	−28.00	2.50	11.99:
Mg II	1239.925	−28.01	2.37	14.90
	1240.395	−27.44	1.50	14.79

TABLE 2—*Continued*

Ion	λ	*v*	*b*	log *N*
Mn II.....	2576.877	−27.78	1.92	12.14
	2594.499	−28.09	2.19	12.21
	2606.462	−28.81	1.53	11.97
Ni II.....	1317.217[a]	−26.97	2.73	12.68
	1317.217[b]	−28.07	1.50	12.27
	1370.132[a]	−26.31	1.68	12.57
	1370.132[b]	−27.42	2.66	12.66
	1454.842[a]	−28.22	3.95	12.41
	1454.842[b]	−26.42	1.50	12.23:
O I*	1304.858	−27.96	2.95	13.24
O I**	1306.029	−28.96	2.33	13.10
S II.....	1250.584	−28.00	1.70	15.20:
C IV	1548.195	−29.67	5.74	13.82:
	1550.770	−30.92	6.45	14.01
Si IV.....	1393.755[a]	−28.62	3.90	14.26:
	1393.755[b]	−29.88	4.49	14.23:
	1402.770[a]	−32.70	6.46	14.26:
	1402.770[b]	−30.37	3.88	14.57:
	−19 km s^{-1} Component			
Cu II.....	1358.773[a]	−18.56	2.64	11.89
	1358.773[b]	−19.45	2.00	11.89
Fe II.....	1608.451	−19.00	4.11	14.19:
	1611.201	−18.85	3.55	14.81
Ga II.....	1414.402[a]	−19.34	2.09	11.08
	1414.402[b]	−19.08	1.50	11.04
Ge II.....	1237.059	−19.21	2.08	11.76
Mg I	2852.964[a]	−19.00	5.02	12.48:
	2852.964[b]	−19.00	6.87	12.58:
Mg II	1239.925	−18.25	4.27	15.61
	1240.395	−18.33	3.29	15.56
Mn II	2576.877	−17.82	4.19	13.52
	2594.499	−17.93	4.26	13.47
	2606.462	−18.91	4.53	13.43
Ni II.....	1317.217[a]	−16.56	4.97	13.09
	1317.217[b]	−17.02	5.94	13.07
	1370.132[a]	−16.37	4.86	13.07
	1370.132[b]	−16.82	4.06	13.00
	1454.842[a]	−16.70	4.12	12.75
	1454.842[b]	−16.72	3.47	12.57
O I].....	1355.598[a]	−19.34	2.11	17.58
	1355.598[b]	−19.03	2.58	17.50
O I**	1306.029	−15.61	8.80	13.71
P II	1532.533	−19.09	3.51	13.96
S II.....	1250.584	−19.00	5.70	15.46:
Si II*.....	1264.738	−18.83	7.31	13.50:
	1265.002	−17.32	6.48	13.24
	1309.276	−17.21	5.84	12.95
	1533.431	−17.00	6.14	13.28
C IV	1548.195	−19.00	8.00	13.18
	1550.770	−19.00	10.00	13.08
Si IV.....	1393.755[a]	−19.00	5.00	12.30
	1393.755[b]	−19.00	9.00	12.38
	1402.770[a]	−19.00	8.00	12.17
	1402.770[b]	−19.00	3.20	12.23
	−3 km s^{-1} Component			
Cl I	1347.240[a]	−5.03	4.61	12.67
	1347.240[b]	−4.85	4.76	12.72
Cu II.....	1358.773[a]	−4.84	4.43	11.99
	1358.773[b]	−3.13	7.00	12.14
Fe I.....	2484.021	−2.68	2.12	11.08
Fe II.....	1608.451	−2.00	7.00	15.48:
	1611.201	−3.51	5.92	15.02
Ga II.....	1414.402[b]	−2.32	8.09	11.26
Ge II.....	1237.059	−4.78	7.00	11.63
Mg I	2852.964[a]	−2.00	8.00	13.25:
	2852.964[b]	−2.00	8.00	13.08:

TABLE 2—*Continued*

Ion	λ	*v*	*b*	log *N*
Mg II	1239.925	−2.86	5.00	15.68
	1240.395	−2.88	5.06	15.64
Mn II	2576.877	−3.75	5.00	13.28
	2594.499	−3.73	5.00	13.28
	2606.462	−3.76	6.00	13.32
Ni II.....	1317.217[a]	−3.60	4.86	13.54
	1317.217[b]	−2.86	5.39	13.53
	1370.132[a]	−2.47	4.97	13.56
	1370.132[b]	−2.30	6.03	13.64
	1454.842[a]	−3.08	4.30	13.23
	1454.842[b]	−2.09	6.10	13.34
O I].....	1355.598[a]	−2.84	7.00	17.48
	1355.598[b]	−3.44	7.00	17.36
P II	1532.533	−2.75	7.00	14.00
S II.....	1250.584	−2.00	6.00	16.82:
Si II*.....	1264.738	−2.32	1.97	12.41
	1265.002	−1.33	2.69	12.44
	1309.276	−2.82	2.21	12.14
	1533.431	−2.55	2.27	12.51
C IV	1548.195	−5.72	8.00	12.98
	1550.770	−5.77	8.00	12.76
Si IV.....	1393.755[a]	−7.06	7.48	12.24
	1393.755[b]	−4.36	3.65	11.97
	1402.770[a]	−5.12	8.16	12.30
	1402.770[b]	−6.68	7.83	12.42
	8 km s^{-1} Component			
Cl I	1347.240[a]	6.91	3.56	13.89
	1347.240[b]	6.90	3.09	14.15
Cu II.....	1358.773[a]	7.43	4.57	12.44
	1358.773[b]	8.15	2.81	12.24
Fe I.....	2484.021	7.52	3.46	11.79
Fe II.....	1608.451	8.00	7.40	15.22:
	1611.201	7.63	3.59	15.00
Ga II.....	1414.402[a]	7.68	2.06	11.38
	1414.402[b]	8.31	2.03	11.51
Ge II.....	1237.059	8.09	3.07	12.23
Mg I	1683.412	8.02	1.96	14.18
	2852.964[a]	8.00	7.00	12.94:
	2852.964[b]	8.00	7.00	13.10:
Mg II	1239.925	8.14	3.82	15.99
	1240.395	8.15	3.68	16.03
Mn II	2576.877	6.98	4.00	13.82:
	2594.499	7.12	3.71	13.88
	2606.462	7.05	4.06	13.68
Ni II.....	1317.217[a]	7.58	4.67	13.68
	1317.217[b]	7.74	4.60	13.60
	1370.132[a]	8.26	4.87	13.67
	1370.132[b]	8.31	4.35	13.61
	1454.842[a]	8.12	4.94	13.42
	1454.842[b]	8.05	3.76	13.26
O I].....	1355.598[a]	7.50	2.93	17.72
	1355.598[b]	8.29	2.05	17.70
O I**	1306.029	8.73	4.50	12.62
P II	1532.533	7.68	2.73	14.30
S I.....	1401.514[a]	8.23	1.52	13.52
	1401.514[b]	7.87	1.95	13.34
	1425.030[a]	7.79	2.34	13.18
	1425.030[b]	7.16	2.20	13.24
	1425.188[a]	8.44	1.50	13.43
	1425.188[b]	7.88	1.57	13.31
S II.....	1250.584	8.00	8.88	15.66:
Si I.....	2515.073	7.85	1.79	12.27
Si II*.....	1264.738	7.23	1.50	11.20
	1533.431	7.99	1.50	11.85
C IV	1548.195	5.00	8.00	12.95
	1550.770	4.04	5.66	12.72
Si IV.....	1393.755[a]	5.70	7.39	12.45
	1393.755[b]	5.76	5.34	12.34

TABLE 2—*Continued*

Ion	λ	*v*	*b*	log *N*
	1402.770[a]	6.51	6.62	12.44
	1402.770[b]	5.26	6.30	12.38
	17 km s^{-1} Component			
Fe II.....	1611.201	15.67	1.50	13.88
Mn II	2576.877	16.69	2.50	11.96
	2594.499	17.27	2.50	11.97
	2606.462	17.53	2.66	11.94
Ni II.....	1317.217[a]	18.06	1.50	12.55
	1317.217[b]	16.95	1.50	12.41
	1370.132[a]	18.51	1.54	12.40
	1370.132[b]	18.12	2.55	12.58
	1454.842[a]	18.64	1.50	12.17:
C IV	1548.195	16.55	6.97	12.70
	1550.770	16.11	7.74	12.70
Si IV.....	1393.755[a]	16.56	7.33	12.16
	1393.755[b]	16.17	7.47	12.13
	1402.770[a]	19.07	6.92	12.18
	1402.770[b]	16.40	5.08	12.10
	26 km s^{-1} Component			
Cl I	1347.240[b]	27.81	1.50	11.68:
Fe I.....	2484.021	25.68	1.50	11.23
Fe II.....	1608.451	26.17	2.03	14.10
	1611.201	25.51	1.50	14.01
	2586.650	26.05	2.09	14.41
Mg I	2852.964[a]	24.83	4.69	12.01
	2852.964[b]	25.13	4.08	12.03
Mg II	1239.925	26.18	1.50	14.29
	1240.395	21.02	5.57	14.94
Mn II	2576.877	24.10	5.16	12.09
	2594.499	25.11	4.86	12.13
	2606.462	25.01	3.58	11.86
Ni II.....	1317.217[a]	25.49	2.97	12.52
	1317.217[b]	25.02	3.66	12.68
	1370.132[a]	26.07	3.69	12.66
	1370.132[b]	26.16	2.09	12.54
	1454.842[a]	27.50	1.50	12.20:
P II	1532.533	25.13	1.50	13.00:
S II.....	1250.584	26.00	4.45	14.05
	1253.811	26.00	6.21	14.20
	38 km s^{-1} Component			
Al II.....	1670.787	38.33	3.19	11.28
Fe II.....	2382.765	37.34	2.44	12.25
	2586.650	37.73	2.11	12.29
	2600.173	37.56	3.02	12.30
Mg I	2852.964[a]	37.66	1.50	10.48:
Mg II	1240.395	36.29	1.50	14.50:
	2796.352[a]	38.91	2.90	12.20
	2796.352[b]	37.69	3.59	12.38
	2803.531[a]	39.30	2.14	12.19
	2803.531[b]	37.41	4.14	12.40
S II.....	1253.811	43.93	3.69	13.23
Si II.....	1304.370	39.09	3.27	12.69
	1526.707	38.06	4.19	12.79
C IV	1548.195	33.20	12.00	12.52
	61 km s^{-1} Component			
Al II.....	1670.787	62.80	3.10	10.30:
C II*	1335.708[a]	62.76	2.74	13.00
	1335.708[b]	61.67	3.14	13.35
Fe II.....	2382.765	61.58	2.07	11.20
	2586.650	62.52	1.50	11.81:
	2600.173	60.48	2.72	11.45
Mg II	2796.352[a]	61.91	2.51	11.95

TABLE 2—*Continued*

Ion	λ	*v*	*b*	log *N*
	2796.352[b]	61.81	2.72	11.97
	2803.531[a]	62.49	2.51	12.03
	2803.531[b]	61.67	2.21	11.93
O I.....	1302.169	61.42	3.25	13.57
Si II.....	1526.707	59.75	5.54	12.31
	69/72 km s^{-1} Component			
C II*	1335.708[a]	67.24	7.17	13.31
	1335.708[b]	71.46	3.09	12.06
Fe II.....	2382.765	72.23	2.00	11.08
	2600.173	72.07	2.72	11.11:
Mg II	2796.352[a]	69.06	3.26	11.94
	2796.352[b]	71.62	3.41	11.32
	2803.531[a]	69.04	1.90	11.90
	2803.531[b]	73.09	2.45	11.20
C IV	1548.195	66.28	12.00	12.45
	98 km s^{-1} Component			
Al II.....	1670.787	98.16	3.39	12.21
C II*	1335.663[a]	99.45	3.45	14.23
	1335.663[b]	97.88	3.90	14.27
	1335.708[a]	99.45	3.45	14.23
	1335.708[b]	97.88	3.90	14.27
Fe II.....	1608.451	97.83	3.39	13.34
	2382.765	97.74	1.98	14.39:
	2586.650	98.10	3.51	13.34
	2600.173	98.14	1.90	14.57:
Mg I	2852.964[a]	99.71	3.13	11.20
	2852.964[b]	98.51	4.09	11.38
Mg II	2796.352[a]	98.77	2.36	13.53:
	2796.352[b]	98.30	2.54	14.13:
	2803.531[a]	98.44	2.79	13.29
	2803.531[b]	97.97	2.44	14.14
Mn II	2576.877	97.54	2.95	11.26
	2594.499	97.99	4.99	11.43
	2606.462	95.40	2.11	11.41
Ni II.....	1317.217[a]	93.96	7.62	12.93
	1317.217[b]	101.33	4.18	12.37
	1370.132[a]	97.65	1.56	12.10:
	1454.842[b]	94.71	5.07	12.45
O I.....	1302.169	97.94	3.21	14.80:
O I*	1304.858	96.32	1.86	12.21
O I**	1306.029	96.21	2.55	12.51
S II.....	1250.584	99.06	2.82	13.38
	1253.811	98.18	3.60	13.47
Si II.....	1526.707	97.86	3.32	13.46
Si II*	1264.738	98.10	3.75	12.33
	1265.002	97.75	4.09	12.33
	1309.276	97.76	2.37	12.02
	1533.431	97.65	2.05	12.18
	110 km s^{-1} Component			
Al II.....	1670.787	109.86	2.04	11.60
C II*	1335.708[a]	110.97	3.73	13.58
	1335.708[b]	109.13	3.16	13.82
Fe II.....	1608.451	109.43	1.62	12.71
	2382.765	108.83	1.50	13.02
	2586.650	109.51	1.64	12.81
	2600.173	109.33	1.54	13.00
Mg I	2852.964[a]	111.09	5.00	10.78
	2852.964[b]	110.26	2.47	10.70
Mg II	2796.352[a]	110.20	2.14	12.62
	2796.352[b]	109.52	2.00	13.14
	2803.531[a]	110.03	2.30	12.52
	2803.531[b]	109.34	2.23	12.82
O I.....	1302.169	109.29	3.06	14.11
S II.....	1253.811	108.76	5.00	13.39

TABLE 2—*Continued*

Ion	λ	v	b	log N
Si II.....	1526.707	109.44	1.92	12.97
Si II*.....	1264.738	109.76	2.59	11.78
120 km s^{-1} Component				
Al II.....	1670.787	119.98	1.50	10.70:
C II*	1335.708[a]	122.52	5.16	12.46
	1335.708[b]	120.38	1.50	12.14
Fe II.....	2382.765	119.74	1.50	11.45
	2586.650	121.24	1.93	11.75:
	2600.173	120.85	3.16	11.56
Mg II	2796.352[a]	118.28	3.57	11.15
	2796.352[b]	120.71	1.75	11.34
	2803.531[a]	120.13	3.87	11.30
	2803.531[b]	120.51	1.50	11.04:
O I.....	1302.169	120.46	2.34	12.42
S II.....	1253.811	120.00	6.00	13.39
127 km s^{-1} Component				
Fe II.....	2382.765	127.38	5.09	11.56
	2586.650	128.25	1.50	11.61:
	2600.173	128.77	1.50	11.36:
Mg II	2796.352[a]	125.58	2.81	11.30
	2796.352[b]	127.74	3.22	11.45
	2803.531[a]	125.55	1.50	11.30
	2803.531[b]	127.86	4.99	11.52

NOTES.—Units for velocity v, dispersion b, and column density N are, respectively, km s^{-1}, km s^{-1}, and cm^{-2}. Column densities that are more uncertain because of weak, blended, or saturated components are marked with colons. Error estimates are provided in the text. Table 2 is also available in machine-readable form in the electronic edition of the *Astrophysical Journal Supplement*.

[a] 1997.

[b] 1999.

The ground-based and *IUE* studies resolved 11 low-ionization velocity components toward HDE 303308, of which seven had very high velocities. The fact that so many high-velocity components are visible in the relatively weak Ca II lines is directly related to the heavy blending encountered in the strong UV lines. In the STIS data, 24 low-ionization components between -175 and $+98$ km s^{-1} are distinguished, although many of the measurements are relatively uncertain due to the blending.

The weak, low- to intermediate-velocity lines (Figs. 6*a*–6*b*) have essentially the same structure as in CPD $-59^{\circ}2603$ and HD 93205, although the principal components are more blended and hence less distinct. Also, the component at -19 to -18 km s^{-1} in the other two stars, that becomes relatively stronger in Mg II and Mn II, has shifted to -24 km s^{-1} in HDE 303308, thus becoming more blended with the next higher negative-velocity one. Also unlike the other two stars, HDE 303308 has significant absorption in Cl I at intermediate negative velocities. As in HD 93205, some very high-velocity features are already well defined in Mn II and S II (Fig. 6*b*). In the strongest lines, Mg II and C II, C II* (Figs. 6*d* and 7), there are no unblended components except for the weak new ones at the extreme velocities of -133 and -175 km s^{-1}.

Unlike in HD 93205, the high-ionization component at -60 km s^{-1} and another at -78 km s^{-1} toward HDE 303308 (Fig. 12) are strongest at the intermediate ionization of Si IV. On the other hand, the blended -3 and $+6$ km s^{-1} components are strongest in Al III, analogously to HD 93205.

4.4. *HD 93222*

HD 93222 is located in the southern part of the Carina Nebula, 20′–25′ from the other three stars, and it holds the interstellar speed record in this region, with a strong component in Mg II and C II at -350 km s^{-1} found in the *IUE* data (Walborn & Hesser 1982). Some apparent relationships to diffuse X-ray emission and near-UV nebulosity were pointed out in that paper. The STIS observations of the low-ionization interstellar lines are displayed in Figures 8*a*–8*d* and 9, the high-ionization lines in Figure 13, and some further excited-state lines in Figures 14 and 15. The measurements are listed in Table 5.

Five interstellar low-ionization velocity components were resolved in the ground-based and *IUE* work, including two with very high velocities. The high-ionization lines toward this star seemed to show more discrete velocity structure than those toward the other stars in the *IUE* data, although the S/N was modest (Walborn et al. 1984). The STIS data resolve 26 low-ionization velocity components between -388 and $+93$ km s^{-1}, and they amply confirm the interpretation of the high-ionization profiles in the *IUE* data. Remarkably, the -350 km s^{-1} feature breaks up into six subcomponents, with the strongest at -372 km s^{-1}; some of them are clearly present in C IV as well.

The profiles of the weak, low-velocity lines (Figs. 8*a*–8*b*) are qualitatively different from those toward the other three stars in the northern part of the nebula, showing that the global and Galactic line-of-sight structures are different toward the southern part. The strongest component is at -23 km s^{-1}, with two additional principal components at -6 and $+6$ km s^{-1}, the latter itself likely composite. Cl I has a well-resolved double structure corresponding to the last two velocities, but the $+6$ km s^{-1} component does not appear composite in this line. Intricate higher velocity structure first appears in Si II and S II (Fig. 8*b*) and develops progressively in the stronger lines (Figs. 8*c*–8*d*), including the multiple extreme negative-velocity feature. The latter is relatively weaker in O I, however; note also that this feature from C II* blends with the shortward edge of the black trough at lower velocities in C II (Fig. 9), as was already shown by the *IUE* data.

The high-ionization interstellar lines toward HD 93222 (Fig. 13) show stronger discrete velocity structure than those toward the other stars. There are five major components, at -20, -34, -48, -66, and -83 km s^{-1}. All of them have close counterparts in the low-ionization lines. Curiously, unlike in the other stars, none of them is completely black in C IV, in which the -66 km s^{-1} is the strongest. In contrast, the -20 km s^{-1} component is dominant (and black) in Si IV and Al III. There appears to be a correlation between absolute velocity and ionization among all of the high-ionization components. As in HD 93205 and HDE 303308, one at $+6$ km s^{-1}, presumably from the Galactic line of sight, is strongest in Al III; components at $+17$, -20, -34, and -48 km s^{-1} are strongest in Si IV; while those at -66 and -83 km s^{-1} are strongest in C IV. As already mentioned, some of the extreme negative-velocity subcomponents are also present in C IV. The principal components in the excited-state lines (Figs. 14 and 15) are at

TABLE 3
HD 93205

Ion	λ	v	b	log N
	−142 km s^{-1} Component			
Al II.....	1670.787[a]	−141.68	4.17	11.80
	1670.787[b]	−142.66	4.33	11.80
C II.....	1334.532	−142.00	5.43	13.84
Fe II.....	1608.451	−142.11	2.83	12.72
	2382.765	−143.44	3.35	12.82
	2586.650	−142.58	3.33	12.86
	2600.173	−143.00	3.41	12.82
Mg I	2852.964	−142.15	4.19	10.85
Mg II	2796.352	−142.36	3.36	12.73
	2803.531	−141.72	3.46	12.68
O I.....	1302.169	−142.06	3.42	12.97
O I**	1306.029	−141.67	2.13	12.09
S II.....	1259.519	−142.18	6.90	13.17
Si II.....	1304.370	−141.86	3.60	12.97
	1526.707	−142.06	3.42	12.97
Si II*.....	1264.738	−142.57	4.63	11.92
C IV	1548.195	−128.91	5.00	11.99
	1550.770	−133.50	3.96	11.81
	−98 km s^{-1} Component			
Al II.....	1670.787[a]	−98.89	5.04	12.44
	1670.787[b]	−98.34	6.81	12.60
Fe II.....	1608.451	−98.18	5.65	13.21
	2382.765	−100.41	4.76	13.19
	2586.650	−98.71	5.43	13.26
	2600.173	−99.63	4.87	13.23
Mg I	2852.964	−98.21	4.41	11.72
Mn II	2576.877	−98.00	5.37	11.34
	2594.499	−99.96	2.19	11.46
	2606.462	−99.51	4.76	11.65
O I**	1306.029	−99.63	1.50	12.09:
S II.....	1250.584	−97.93	5.74	14.03
	1253.811	−97.51	6.34	14.01
	1259.519	−98.93	5.28	13.93
Si II.....	1304.370	−98.56	5.19	14.00
	1526.707	−99.67	4.50	13.89
Si II*.....	1264.738	−98.31	3.69	12.11
	1309.276	−98.00	3.58	12.10
Al III.....	1854.716	−102.52	7.00	11.49
	1862.790	−97.39	9.98	11.89
C IV	1548.195	−100.26	8.85	12.72
	1550.770	−99.62	6.85	12.64
Si IV.....	1402.770	−99.40	3.44	11.89
	−89 km s^{-1} Component			
Al II.....	1670.787[a]	−89.00	1.59	14.50:
	1670.787[b]	−89.00	2.17	13.79:
Fe II.....	1608.451	−88.89	2.11	13.70:
	1611.201	−86.04	5.85	14.21
	2382.765	−90.16	1.77	14.11:
	2586.650	−90.19	1.50	13.60:
	2600.173	−89.00	3.24	13.71:
Mg I	1827.935	−86.04	8.48	12.76:
	2852.964	−89.23	2.54	11.94
Mn II	2576.877	−89.00	3.66	11.88
	2594.499	−90.44	1.63	11.63
Ni II.....	1370.132	−90.29	3.00	12.42
O I**	1306.029	−89.15	2.80	13.17
S II.....	1250.584	−88.59	3.12	14.07
	1253.811	−88.77	2.84	14.09
	1259.519	−89.12	3.32	14.13
Si II.....	1304.370	−89.00	3.72	14.14:
	1526.707	−89.00	4.66	14.09:

TABLE 3—*Continued*

Ion	λ	v	b	log N
	1808.013	−89.07	2.63	14.19
Si II*.....	1264.738	−88.00	3.45	12.87
	1309.276	−88.45	3.07	12.62
Al III.....	1854.716	−89.72	7.50	12.18
	1862.790	−87.55	5.73	11.95
C IV	1548.195	−89.97	6.86	12.57
	1550.770	−88.82	4.86	12.43
Si IV.....	1402.770	−91.54	4.21	12.07
	−83 km s^{-1} Component			
Al II.....	1670.787[a]	−83.00	4.06	12.66:
	1670.787[b]	−83.00	3.71	12.52:
Fe II.....	1608.451	−82.94	2.41	13.84
	2382.765	−86.33	6.76	13.66:
	2586.650	−84.66	4.21	13.90:
	2600.173	−83.00	4.67	13.39:
Mg I	2852.964	−83.17	1.97	12.19
Mn II	2576.877	−83.02	2.64	11.86
	2594.499	−84.15	3.80	12.10
	2606.462	−86.48	5.31	12.13:
Ni II.....	1317.217[c]	−85.07	5.13	12.71:
	1317.217[d]	−85.15	5.21	12.66:
	1370.132	−84.14	3.00	12.66
	1709.600	−85.39	4.10	12.58:
	1741.549	−84.56	5.59	12.90:
	1751.910	−85.39	4.61	12.67:
O I**	1306.029	−83.21	2.03	13.26
S I.....	1425.030	−84.14	2.13	12.00
S II.....	1250.584	−82.22	2.07	14.12
	1253.811	−82.61	2.55	14.13
	1259.519	−83.05	1.85	14.05
Si II.....	1304.370	−83.00	5.16	14.13:
	1526.707	−83.00	5.93	13.97:
	1808.013	−83.02	2.46	14.22
Si II*.....	1264.738	−83.00	3.54	12.73
	1309.276	−82.94	1.92	12.69
	−75 km s^{-1} Component			
Al II.....	1670.787[a]	−74.11	3.00	11.34
	1670.787[b]	−74.91	3.22	11.43
Mg I	2852.964	−75.00	5.07	11.08
Mg II	2803.531	−71.07	3.00	12.12:
S II.....	1259.519	−78.46	2.40	13.31
Si II.....	1304.370	−72.34	3.00	12.68
	1526.707	−71.31	3.00	12.34:
	−66 km s^{-1} Component			
Al II.....	1670.787[a]	−65.40	1.84	12.28
	1670.787[b]	−66.44	2.61	12.20
Fe II.....	1608.451	−65.37	1.57	13.47
	2382.765	−66.17	2.42	13.35
	2586.650	−65.66	1.76	13.51
	2600.173	−65.91	2.11	13.52
Mg I	2852.964	−65.56	1.76	11.11
Mg II	2803.531	−65.21	1.95	13.94:
Mn II	2576.877	−65.63	3.68	11.70
	2594.499	−65.08	4.50	11.72
	2606.462	−66.99	3.06	11.45
Ni II.....	1317.217[c]	−63.64	4.48	12.43
	1370.132	−64.57	3.15	12.53
	1741.549	−64.46	2.15	12.45
S II.....	1250.584	−64.45	1.55	13.30
	1253.811	−65.33	4.42	13.57
	1259.519	−65.66	2.36	13.43

TABLE 3—*Continued*

Ion	λ	*v*	*b*	log *N*
Si II.....	1304.370	−65.21	2.33	13.59
	1526.707	−65.36	2.00	13.74
	1808.013	−62.75	6.33	13.95:
Si II*.....	1264.738	−65.96	2.00	10.90
	−58 km s^{-1} Component			
Al II.....	1670.787[a]	−60.00	6.00	11.80
	1670.787[b]	−59.85	3.00	11.59
Fe II.....	2382.765	−58.86	3.04	12.78
	2586.650	−57.76	3.96	12.90
	2600.173	−58.55	3.00	12.76
Si II.....	1304.370	−59.00	5.00	13.14:
	1526.707	−59.00	5.00	13.08:
Al III.....	1854.716	−61.55	4.55	11.60
	1862.790	−62.12	4.56	11.65
C IV	1548.195	−60.47	6.74	13.19
	1550.770	−60.61	6.75	13.20
Si IV.....	1393.755	−60.60	6.15	12.63
	1402.770	−61.12	6.34	12.67
	−53 km s^{-1} Component			
Al II.....	1670.787[a]	−53.13	3.55	11.99
	1670.787[b]	−54.15	3.71	12.03
Fe II.....	1608.451	−54.34	6.29	13.21:
	2382.765	−53.78	1.70	13.19
	2586.650	−52.61	1.50	12.86
	2600.173	−53.21	2.05	12.97
Mg I	2852.964	−54.43	3.55	10.85
Mn II	2576.877	−55.00	3.52	11.36:
Ni II.....	1370.132	−52.27	3.07	12.41:
S II.....	1250.584	−54.26	1.91	13.34
	1253.811	−53.28	3.48	13.64
	1259.519	−54.81	3.78	13.72
Si II.....	1304.370	−54.14	2.60	13.50
	1526.707	−54.56	2.42	13.60
	1808.013	−52.95	1.50	13.58
	−35 km s^{-1} Component			
Cl I	1347.240	−36.05	5.58	12.03
Cu II	1358.773	−33.42	6.41	11.95
Fe II.....	1608.451	−34.09	7.47	14.58:
	1611.201	−34.69	6.17	14.76
Ga II.....	1414.402	−36.66	7.62	11.23
Ge II	1237.059	−33.93	8.21	11.79
Mg I	1747.794	−36.51	4.16	12.97
	1827.935	−35.82	8.50	13.18
	2852.964	−35.01	4.94	14.03:
Mg II	1239.925	−34.81	7.32	15.63
	1240.395	−35.16	7.28	15.65
Mn II	2576.877	−34.85	7.23	13.09
	2594.499	−34.71	7.07	13.10
	2606.462	−35.25	7.37	13.08
Ni II.....	1317.217[c]	−31.94	5.81	13.37
	1317.217[d]	−33.53	6.49	13.42
	1370.132	−32.59	4.58	13.33
	1454.842	−32.74	3.83	12.81
	1709.600	−32.39	5.27	13.44
	1741.549	−32.43	5.98	13.49
	1751.910	−31.74	5.55	13.45
O I**	1306.029	−36.22	5.41	14.28
S I.....	1425.030	−36.42	9.48	12.41
S II.....	1250.584	−33.76	6.96	15.82:
Si II.....	1808.013	−34.51	7.10	15.97:
Si II*.....	1265.002	−35.83	5.72	14.56:
	1309.276	−35.82	5.55	14.31:

TABLE 3—*Continued*

Ion	λ	*v*	*b*	log *N*
Al III.....	1854.716	−35.81	8.03	13.78:
	1862.790	−35.46	7.93	13.81:
C IV	1548.195	−34.85	7.83	14.31:
	1550.770	−34.83	7.87	14.32:
Si IV.....	1393.755	−33.39	7.60	14.81:
	1402.770	−34.69	7.18	14.91:
	−18 km s^{-1} Component			
Cu II	1358.773	−18.08	3.08	11.95
Fe II.....	1611.201	−18.36	3.03	14.72
Ga II.....	1414.402	−18.90	2.79	11.11
Ge II	1237.059	−18.68	2.31	11.78
Mg I	1747.794	−18.00	2.65	12.77:
	1827.935	−18.69	6.00	12.68
	2852.964	−18.00	3.22	12.32:
Mg II	1239.925	−18.09	3.11	15.50
	1240.395	−18.28	3.17	15.54
Mn II	2576.877	−18.75	2.55	13.92
	2594.499	−18.88	2.54	13.82
	2606.462	−19.33	3.45	13.40
Ni II.....	1317.217[c]	−14.55	5.66	13.17
	1317.217[d]	−15.88	4.76	13.07
	1370.132	−15.98	5.00	13.07
	1454.842	−14.85	4.97	12.54
	1709.600	−15.74	5.45	13.21
	1741.549	−14.93	5.80	13.22
	1751.910	−13.97	5.29	13.24
O I].....	1355.598	−18.31	2.62	17.44
O I**	1306.029	−18.31	3.82	13.00
S II.....	1250.584	−17.62	3.61	15.53
Si II.....	1808.013	−18.13	3.12	15.50
Si II*.....	1265.002	−15.09	2.24	12.79
	1309.276	−16.34	8.24	12.57
Al III.....	1854.716	−18.00	8.00	12.21
	1862.790	−18.00	4.73	11.99
C IV	1548.195	−18.00	9.40	13.14
	1550.770	−18.00	9.41	13.14
Si IV.....	1393.755	−18.00	8.22	12.49
	1402.770	−18.00	5.04	12.68
	−3 km s^{-1} Component			
Cl I	1347.240	−2.78	2.50	12.69
Cu II	1358.773	−3.15	6.17	12.07
Fe II.....	1611.201	−3.51	5.81	14.94
Ga II.....	1414.402	−3.95	7.87	11.36
Ge II	1237.059	−1.75	7.95	11.93
Mg I	1747.794	−2.84	7.53	13.41
	1827.935	−4.29	3.76	13.15
	2852.964	−3.40	6.29	13.55:
Mg II	1239.925	−2.68	6.32	15.79
	1240.395	−2.15	7.15	15.83
Mn II	2576.877	−3.80	6.18	13.34:
	2594.499	−3.93	6.42	13.32
	2606.462	−3.95	6.69	13.33
Ni II.....	1317.217[c]	−2.88	4.13	13.46
	1317.217[d]	−3.73	4.98	13.48
	1370.132	−2.90	5.56	13.61
	1454.842	−3.78	4.20	13.17
	1709.600	−2.67	4.97	13.64
	1741.549	−3.30	4.05	13.56
	1751.910	−2.02	4.88	13.65
O I].....	1355.598	−2.96	6.77	17.41
S I.....	1295.653	−3.03	1.50	11.92:
	1425.030	−4.57	5.24	12.20

TABLE 3—*Continued*

Ion	λ	v	b	log N
S II.....	1250.584	−3.40	5.58	15.96:
Si II.....	1808.013	−3.40	7.37	15.75:
Al III.....	1854.716	−4.28	5.61	12.45
	1862.790	−3.97	6.66	12.58
C IV	1548.195	−3.00	8.00	13.06
	1550.770	−3.00	7.50	13.03
Si IV.....	1393.755	−3.00	8.00	12.34
	1402.770	−3.00	8.00	12.47
8 km s^{-1} Component				
Cl I	1347.240	7.36	3.94	13.95
Cu II	1358.773	7.71	3.07	12.13
Fe II.....	1611.201	7.81	4.12	15.01
Ga II.....	1414.402	7.98	3.87	11.46
Ge II	1237.059	8.25	3.54	12.04
Mg I	1747.794	7.41	4.00	13.62
	1827.935	6.38	4.09	13.70
	2852.964	7.80	4.82	13.21:
Mg II	1239.925	8.77	4.00	15.88
	1240.395	8.78	3.71	15.88
Mn II	2576.877	7.20	4.51	13.64:
	2594.499	7.37	4.59	13.51
	2606.462	7.09	4.47	13.52
Ni II.....	1317.217[c]	8.31	6.25	13.69
	1317.217[d]	7.86	5.58	13.62
	1370.132	8.55	4.85	13.65
	1454.842	7.43	5.83	13.41
	1709.600	8.37	5.29	13.77
	1741.549	7.95	6.34	13.83
	1751.910	9.24	5.31	13.75
O I].....	1355.598	7.97	3.87	17.70
S I.....	1295.653	8.40	2.38	12.53
	1425.030	7.53	1.67	12.33
S II.....	1250.584	7.80	6.44	15.83:
Si II.....	1808.013	7.80	4.78	15.89:
Si II*.....	1264.738	8.22	2.00	11.30
Al III.....	1854.716	7.21	7.84	12.77
	1862.790	7.68	6.75	12.70
C IV	1548.195	8.00	7.37	13.01
	1550.770	8.00	7.81	13.04
Si IV.....	1393.755	8.00	7.79	12.41
	1402.770	8.00	7.18	12.38
18 km s^{-1} Component				
Fe II.....	2586.650	22.76	1.71	13.15:
Mg I	2852.964	18.00	5.00	11.90:
Mn II	2576.877	18.00	2.49	11.93
	2594.499	18.00	4.47	12.03
	2606.462	18.00	6.22	12.14
Ni II.....	1370.132	18.27	1.50	12.36
	1709.600	19.52	3.02	12.70
S II.....	1250.584	18.00	2.44	14.27:
Si II.....	1808.013	18.00	2.70	14.30
Al III.....	1854.716	18.00	2.97	11.20
	1862.790	18.00	5.84	11.82
C IV	1548.195	18.00	5.01	12.61
	1550.770	18.00	5.14	12.44
Si IV.....	1393.755	18.00	5.00	11.83
	1402.770	18.00	7.51	12.18
27 km s^{-1} Component				
Cu II	1358.773	27.21	2.36	11.34:
Fe II.....	1608.451	27.45	1.50	12.95
	2586.650	27.02	1.50	13.16
Mg I	2852.964	25.90	2.77	11.38

TABLE 3—*Continued*

Ion	λ	v	b	log N
Mn II	2576.877	24.48	3.50	11.57
	2594.499	27.00	7.55	11.73
Ni II.....	1370.132	24.81	7.00	12.60
	1751.910	24.09	4.10	12.63
S II.....	1250.584	23.21	4.07	13.94
Si II.....	1808.013	25.11	4.00	13.87
C IV	1548.195	26.12	3.64	12.18
	1550.770	27.00	8.84	12.62
Si IV.....	1393.755	27.80	7.00	11.43
35 km s^{-1} Component				
Al II.....	1670.787[a]	36.24	7.99	11.65
	1670.787[b]	35.08	4.92	11.43
C II*	1335.708	36.07	7.68	13.46:
Fe II.....	1608.451	35.68	1.50	12.18:
	2382.765	34.69	5.31	12.33
	2586.650	33.64	4.63	12.39
	2600.173	35.88	1.99	11.83
Mg I	2852.964	34.21	1.82	10.48
Mg II	2803.531	35.00	7.36	13.14:
Si II.....	1526.707	34.22	6.47	13.13
C IV	1548.195	35.00	7.00	12.25
	1550.770	35.00	1.85	11.58
47 km s^{-1} Component				
Al II.....	1670.787[a]	48.53	1.50	10.78
	1670.787[b]	45.92	3.94	11.26
C II*	1335.708	47.38	2.11	13.36
Fe II.....	1608.451	47.36	1.50	12.18
	2382.765	47.07	1.50	12.10
	2586.650	47.50	1.50	12.13
	2600.173	47.35	1.50	12.00
Mg I	2852.964	47.47	1.50	10.60
Mg II	2796.352	47.10	2.21	12.36
	2803.531	45.33	4.25	12.55
Si II.....	1526.707	44.11	5.33	12.77
69 km s^{-1} Component				
Al II.....	1670.787[a]	69.23	3.53	11.18
	1670.787[b]	69.24	6.58	11.53
C II	1334.532	68.96	8.06	13.87
C II*	1335.708	69.44	5.38	13.12
Fe II.....	1608.451	67.78	2.04	12.18
	2382.765	68.01	4.69	12.26
	2586.650	68.18	5.73	12.31
	2600.173	67.84	3.95	12.17
Mg II	2796.352	68.57	5.38	12.34
	2803.531	68.35	5.56	12.34
O I.....	1302.169	68.66	5.54	12.63
Si II.....	1526.707	68.66	5.54	12.63
80 km s^{-1} Component				
Al II.....	1670.787[a]	79.19	3.52	11.60
	1670.787[b]	78.96	2.80	11.53
C II	1334.532	80.00	5.80	13.88:
C II*	1335.708	78.76	3.36	13.28
Fe II.....	1608.451	79.94	2.81	12.58
	2382.765	79.26	3.49	12.71
	2586.650	79.86	3.45	12.70
	2600.173	79.46	3.35	12.71
Mg II	2796.352	79.92	3.53	12.63
	2803.531	79.84	3.56	12.62
O I.....	1302.169	79.79	3.85	12.88
Si II.....	1526.707	79.79	3.85	12.88

TABLE 3—*Continued*

Ion	λ	v	b	log N
C IV	1548.195	82.42	2.79	11.92
	1550.770	83.59	3.00	11.87
	88 km s^{-1} Component			
Al II.....	1670.787[a]	87.20	6.08	11.51
	1670.787[b]	86.46	4.45	11.53
C II	1334.532	88.00	4.36	13.97:
C II*	1335.708	86.18	4.56	13.53
Fe II.....	1608.451	87.72	1.74	12.26
	2382.765	87.57	2.65	12.30
	2586.650	88.31	2.68	12.18
	2600.173	87.64	2.43	12.26
Mg II	2796.352	88.26	3.72	12.36
	2803.531	87.86	3.71	12.38
O I.....	1302.169	88.29	3.02	12.69
Si II.....	1526.707	88.29	3.02	12.69
Si II*.....	1264.738	85.52	6.00	11.43
C IV	1548.195	91.94	4.04	12.05
	1550.770	95.43	6.00	12.49
Si IV.....	1393.755	91.31	7.51	11.90
	100 km s^{-1} Component			
Al II.....	1670.787[a]	100.23	3.49	12.18
	1670.787[b]	99.68	4.82	12.29
Fe II.....	1608.451	99.60	2.88	13.15
	2382.765	99.63	3.41	13.34
	2586.650	99.33	2.93	13.16
	2600.173	99.80	3.49	13.25
Mg I	2852.964	99.95	3.56	11.23
Mg II	2803.531	99.74	3.89	13.17
Mn II	2606.462	99.09	3.96	11.32:
S II.....	1250.584	100.00	5.97	13.47:
	1253.811	100.00	3.34	13.12
Si II.....	1526.707	99.69	3.53	13.44
Si II*.....	1264.738	100.02	3.31	12.01
	108 km s^{-1} Component			
Al II.....	1670.787[a]	108.64	3.39	12.05
	1670.787[b]	107.54	1.96	11.88
Fe II.....	1608.451	107.99	2.69	13.06
	2382.765	107.12	1.50	13.14
	2586.650	107.96	3.43	13.16
	2600.173	107.29	1.78	12.98
Mg I	2852.964	108.33	3.00	10.90
Mg II	2803.531	108.64	3.54	13.14
S II.....	1250.584	108.00	4.00	13.41
	1253.811	108.00	3.74	13.36
Si II.....	1526.707	108.54	3.41	13.46
Si II*.....	1264.738	107.82	4.00	11.69
C IV	1548.195	104.31	9.91	12.47
	1550.770	108.56	5.00	12.18
Si IV.....	1393.755	104.16	3.71	11.38
	113 km s^{-1} Component			
Al II.....	1670.787[a]	113.71	2.15	11.67
	1670.787[b]	111.54	1.68	11.72
Fe II.....	1608.451	113.58	1.93	12.78
	2382.765	112.64	4.89	13.24:
	2586.650	113.41	1.54	12.72
	2600.173	113.43	4.98	13.19
Mg I	2852.964	113.00	3.00	10.78
Mg II	2803.531	113.93	1.56	12.69
Si II.....	1526.707	114.12	1.95	13.03
Si II*.....	1264.738	113.00	3.00	11.38

TABLE 3—*Continued*

Ion	λ	v	b	log N
	118 km s^{-1} Component			
Al II.....	1670.787[a]	118.72	2.91	12.21
	1670.787[b]	117.28	3.55	12.22
Fe II.....	1608.451	118.58	2.13	13.20
	2382.765	117.86	1.50	14.11:
	2586.650	117.97	2.23	13.22
	2600.173	118.45	1.50	13.53
Mg I	2852.964	118.48	2.61	11.08
Mg II	2803.531	118.65	2.40	13.29
Mn II	2576.877	118.11	1.50	11.08:
	2594.499	116.83	1.71	11.28
	2606.462	117.62	3.01	11.20
Ni II.....	1370.132	120.05	5.00	12.48:
O I*	1304.858	117.65	4.81	12.57
O I**	1306.029	119.82	3.04	12.17
S II.....	1250.584	119.00	5.26	13.54
	1253.811	118.44	4.36	13.56
Si II.....	1526.707	118.56	2.40	13.54
Si II*.....	1264.738	118.80	2.94	11.89
	1265.002	118.64	2.84	12.03
C IV	1548.195	118.98	2.80	11.72
Si IV.....	1393.755	117.58	3.45	11.34

NOTES.—Units for velocity v, dispersion b, and column density N are, respectively, km s^{-1}, km s^{-1}, and cm^{-2}. Column densities that are more uncertain because of weak, blended, or saturated components are marked with colons. Error estimates are provided in the text. Table 3 is also available in machine-readable form in the electronic edition of the *Astrophysical Journal Supplement*.

[a] Exposure with central $\lambda = 1598$ Å.

[b] Exposure with central $\lambda = 1763$ Å.

[c] Exposure with central $\lambda = 1234$ Å.

[d] Exposure with central $\lambda = 1416$ Å.

−24–25 km s^{-1}, similarly to those in Si IV and Al III, and to the strongest component in the low-ionization lines.

4.5. *Collation of Velocity Components among Stars*

Table 6 compares the low- and high-ionization velocity components observed toward the four stars, with CPD −59° 2603 as the reference. The occurrence of identical velocities in low- and high-ionization components generally indicates that the latter were adopted from the former to resolve ambiguous, blended profiles. While many velocity components are unique to each star, several similar velocities are seen to occur in some or all of them. The most notable of the latter are at approximately −100, −90, −65, −35, −20, −5, +5, +20, +35, +65, +90, and +100 km s^{-1}. The apparent symmetry between negative and positive velocities is illusory, however, because these are heliocentric values; they must be corrected by +14 km s^{-1} to the Carina Nebula rest frame as defined by the double nebular emission lines (Walborn & Hesser 1975). The two lowest (absolute) velocities likely correspond primarily to the full ∼2500 pc line of sight to the Carina Nebula, and the black troughs from about −50 to +30 km s^{-1} in the intermediate-strength, low-ionization lines are very similar in all the stars. The components near −35 km s^{-1} likely correspond to the near side of the globally expanding H II region, because they coincide with the blueward component of the double nebular emission lines and dominate the high-ionization absorp-

TABLE 4
HDE 303308

Ion	λ	v	b	log N
	−175 km s^{-1} Component			
C II.....	1334.532	−175.19	2.28	12.31
Si II.....	1526.707	−177.92	2.81	11.89
	−133 km s^{-1} Component			
Al II.....	1670.787[b]	−134.00	1.50	10.30
C II.....	1334.532	−134.08	4.35	12.40
C II*	1335.708	−133.00	1.80	11.71
Fe II.....	2382.765	−131.37	3.71	11.15
	2600.173	−130.91	2.58	11.18
Mg II	2796.352	−133.01	1.50	10.90
	2803.531	−134.76	5.91	10.90:
C IV	1548.195	−129.12	12.00	12.23
Si IV.....	1402.770	−136.43	7.55	11.71
	−111 km s^{-1} Component			
Al II.....	1670.787[a]	−111.68	3.19	12.51
	1670.787[b]	−112.12	3.93	12.47
C II*	1335.708	−111.00	8.44	14.54:
Fe II.....	1608.451	−111.48	2.90	13.52
	2382.765	−110.31	4.32	13.73:
	2586.650	−111.54	2.92	13.53
	2600.173	−111.62	3.58	13.51:
Mg I	2852.964	−110.89	3.99	11.59
Mg II	2796.352	−111.00	4.13	13.55:
	2803.531	−111.00	3.75	13.42:
Mn II	2576.877	−112.56	3.07	11.46
	2594.499	−113.17	3.17	11.43
	2606.462	−107.43	6.63	11.57:
Ni II.....	1709.600	−111.16	2.30	12.35
	1751.910	−111.00	5.00	12.79
O I**	1306.029	−108.97	7.76	12.73
S II.....	1250.584	−108.54	4.05	13.93
	1253.811	−110.50	3.64	13.66
	1259.519	−111.46	3.74	13.76
Si II.....	1304.370	−111.04	3.59	13.86
	1526.707	−111.31	3.85	13.82
Si II*.....	1264.738	−110.66	3.49	12.37
	1309.276	−110.86	3.00	11.86
Al III.....	1854.716	−106.76	7.78	11.64
C IV	1548.195	−110.69	8.10	12.52
	1550.770	−111.00	7.35	12.02
Si IV.....	1402.770	−109.55	6.67	11.92
	−104 km s^{-1} Component			
Al II.....	1670.787[a]	−103.89	3.68	12.45
	1670.787[b]	−104.67	3.77	12.41
C II*	1335.708	−104.00	4.51	14.44:
Fe II.....	1608.451	−103.70	2.74	13.35
	2382.765	−103.67	2.89	13.31:
	2586.650	−103.86	3.04	13.40
	2600.173	−103.89	3.16	13.35:
Mg I	2852.964	−103.32	3.08	11.38
Mg II	2796.352	−104.00	3.85	13.66:
	2803.531	−104.00	4.02	13.69:
Mn II	2576.877	−104.98	4.70	11.54
S II.....	1250.584	−101.87	1.50	13.32:
	1253.811	−103.22	2.65	13.60
	1259.519	−104.32	2.65	13.51
Si II.....	1304.370	−103.40	3.06	13.72
	1526.707	−103.56	3.07	13.68

TABLE 4—*Continued*

Ion	λ	v	b	log N
Si II*.....	1264.738	−103.73	2.84	12.19
	1309.276	−103.04	4.17	11.96
	−91 km s^{-1} Component			
Al II.....	1670.787[a]	−90.44	5.00	11.64
	1670.787[b]	−92.03	5.00	11.65
Fe II.....	1608.451	−90.74	1.50	12.00:
	2382.765	−91.40	2.91	12.12
	2586.650	−90.99	1.72	12.02
	2600.173	−90.68	3.41	12.09
Mg II	2796.352	−90.00	3.85	12.50
	2803.531	−89.13	4.50	12.54
Si II.....	1304.370	−90.17	4.17	12.73
	1526.707	−90.28	3.51	12.68
C IV	1548.195	−92.47	12.00	13.15
	1550.770	−95.05	12.00	13.04
Si IV.....	1402.770	−92.00	8.83	12.74
	−82 km s^{-1} Component			
Al II.....	1670.787[a]	−82.19	1.97	12.22
	1670.787[b]	−83.25	2.68	12.16
Fe II.....	1608.451	−82.34	1.75	13.18
	2382.765	−82.99	2.14	13.34
	2586.650	−82.34	1.90	13.17
	2600.173	−82.70	1.91	13.40
Mg I	2852.964	−82.23	2.13	11.15
Mg II	1239.925	−84.05	6.07	14.60
Mn II	2576.877	−82.00	4.00	11.38
Ni II.....	1751.910	−81.36	3.70	12.76
S II.....	1253.811	−81.97	1.97	13.21
	1259.519	−81.92	2.28	13.22
Si II.....	1304.370	−82.38	2.44	13.29
	1526.707	−82.26	2.45	13.42
Si II*.....	1264.738	−82.27	2.22	12.01
	−76 km s^{-1} Component			
Al II.....	1670.787[a]	−76.15	2.56	12.10:
	1670.787[b]	−76.20	2.99	12.57:
Fe II.....	1608.451	−75.99	2.14	13.17
	2382.765	−75.92	1.86	13.89:
	2586.650	−76.04	2.02	13.18
	2600.173	−75.58	2.11	13.62
Mg I	2852.964	−76.00	2.54	11.15
Mn II	2576.877	−76.00	6.00	11.20
	2594.499	−75.25	6.39	11.64:
	2606.462	−73.69	2.60	11.18:
Ni II.....	1317.217[c]	−77.33	5.36	12.31:
	1317.217[d]	−75.34	5.81	12.37:
S II.....	1250.584	−78.33	9.10	14.00:
	1253.811	−76.00	2.82	13.38
	1259.519	−76.05	2.55	13.40
Si II.....	1304.370	−75.46	2.15	13.24:
	1526.707	−76.23	1.52	13.32:
Si II*.....	1264.738	−75.41	2.24	11.76:
Al III.....	1854.716	−78.97	12.00	12.33
	1862.790	−79.93	9.00	11.77
C IV	1548.195	−76.37	7.47	13.19
	1550.770	−77.13	8.15	13.15
Si IV.....	1393.755	−77.36	6.78	13.30
	1402.770	−77.44	5.87	13.28
	−71 km s^{-1} Component			
Al II.....	1670.787[a]	−71.54	5.08	12.46:
	1670.787[b]	−70.26	3.22	12.18:

TABLE 4—*Continued*

Ion	λ	*v*	*b*	log *N*
Fe II.....	1608.451	−71.06	5.02	13.30
	2382.765	−70.80	3.59	13.35:
	2586.650	−71.06	5.00	13.33
	2600.173	−70.25	2.79	13.03
Mg I	2852.964	−71.00	5.32	11.51
Mg II	1239.925	−72.65	4.04	14.24:
Mn II	2576.877	−71.00	6.00	11.30
Ni II.....	1751.910	−73.13	1.71	12.63:
S II.....	1250.584	−68.88	6.25	13.47:
	1253.811	−71.00	3.28	13.49
	1259.519	−70.00	3.63	13.51
Si II.....	1304.370	−72.46	6.96	13.93:
	1526.707	−72.41	5.48	13.79:
Si II*.....	1264.738	−71.00	8.07	12.31:
	−61 km s^{-1} Component			
Al II.....	1670.787[a]	−63.03	4.00	12.08:
	1670.787[b]	−61.00	6.21	12.60:
Fe II.....	1608.451	−59.32	4.68	13.37:
	2586.650	−61.00	3.66	12.96:
Mg I	2852.964	−60.62	4.20	11.23
S II.....	1253.811	−61.47	2.43	13.48
	1259.519	−58.50	3.50	13.51
Si II.....	1304.370	−59.32	5.25	13.84
	1526.707	−60.53	5.68	13.74:
Si II*.....	1264.738	−58.98	3.62	12.09
Al III.....	1854.716	−59.82	9.39	12.94
	1862.790	−58.87	11.31	12.98
C IV	1548.195	−61.72	9.20	13.41
	1550.770	−59.00	12.00	13.57
Si IV.....	1393.755	−61.22	5.57	13.31
	1402.770	−61.28	6.62	13.31
	−54 km s^{-1} Component			
Al II.....	1670.787[a]	−56.40	5.65	12.53:
Fe II.....	1611.201	−50.57	2.72	13.87:
	2586.650	−54.00	7.36	13.45:
Mg I	2852.964	−54.50	5.06	11.28:
Mn II	2576.877	−55.65	5.78	11.78
	2594.499	−53.00	3.88	11.72
	2606.462	−54.00	3.21	11.41
Ni II.....	1317.217[c]	−54.25	6.00	12.65
	1454.842	−54.00	6.00	13.04
	1709.600	−54.50	1.50	12.18:
	1741.549	−52.37	5.50	12.66
	1751.910	−54.54	5.00	12.94
S II.....	1250.584	−55.00	7.49	14.05:
	1253.811	−54.28	2.50	13.37
	−41 km s^{-1} Component			
Cl I	1347.240	−37.58	5.63	12.67
Fe II.....	1611.201	−41.58	4.17	14.48
Mg II	1239.925	−41.60	6.01	14.88
Mn II	2576.877	−41.68	6.53	12.78
	2594.499	−42.86	5.39	12.68
	2606.462	−42.47	6.04	12.71
Ni II.....	1317.217[c]	−41.47	5.04	13.35
	1317.217[d]	−42.25	4.95	13.20
	1370.132	−42.37	3.52	13.07
	1454.842	−42.15	4.64	13.40
	1709.600	−41.66	4.76	13.38
	1741.549	−42.03	4.47	13.34
	1751.910	−41.24	5.72	13.53

TABLE 4—*Continued*

Ion	λ	*v*	*b*	log *N*
S II.....	1250.584	−41.00	6.53	15.02:
Si II.....	1808.013	−40.30	7.51	15.19:
	−33 km s^{-1} Component			
Cl I	1347.240	−29.40	5.42	12.62
Fe II.....	1611.201	−33.53	3.12	14.42
Mg II	1239.925	−32.19	4.91	15.21
Mn II	2576.877	−32.74	4.55	12.85
	2594.499	−33.34	4.84	12.89
	2606.462	−33.35	4.97	12.84
Ni II.....	1317.217[c]	−32.76	3.36	13.12
	1317.217[d]	−32.18	5.13	13.32
	1370.132	−33.40	5.42	13.38
	1454.842	−32.34	4.51	13.45
	1709.600	−32.63	3.92	13.32
	1741.549	−32.09	5.24	13.51
	1751.910	−32.12	3.64	13.37
O I].....	1355.598	−32.25	4.34	16.88
O I**	1306.029	−28.44	12.00	14.23
S II.....	1250.584	−33.00	4.04	15.39:
Si II.....	1808.013	−32.89	4.15	15.33
Si II*.....	1309.276	−36.42	5.18	13.45
Al III.....	1854.716	−31.60	11.84	13.81:
	1862.790	−30.91	10.06	13.93:
C IV	1548.195	−36.88	11.61	14.46:
	1550.770	−35.85	9.57	14.62:
Si IV.....	1393.755	−37.64	10.09	14.65:
	1402.770	−38.52	11.93	14.32:
	−24 km s^{-1} Component			
Cl I	1347.240	−24.34	4.65	12.49
Cu II	1358.773	−23.85	1.50	11.46
Fe II.....	1611.201	−24.85	3.31	14.67
Ga II.....	1414.402	−23.07	2.03	10.90
Ge II	1237.059	−22.58	5.38	11.70
Mg II	1239.925	−23.78	3.54	15.31
Mn II	2576.877	−23.73	3.73	13.18
	2594.499	−23.84	4.01	13.14
	2606.462	−24.22	4.07	13.15
Ni II.....	1317.217[c]	−24.66	5.26	13.40
	1317.217[d]	−23.65	3.39	13.13
	1370.132	−22.30	6.00	13.39
	1454.842	−22.89	6.50	13.49
	1709.600	−23.11	5.66	13.50
	1741.549	−23.09	3.73	13.32
	1751.910	−23.29	6.00	13.58
O I].....	1355.598	−23.94	3.00	17.23
S II.....	1250.584	−24.00	3.89	16.19:
Si II.....	1808.013	−23.57	5.32	15.61
Si II*.....	1309.276	−23.84	7.91	13.39
	−16 km s^{-1} Component			
Cl I	1347.240	−16.59	1.50	11.62
Fe II.....	1611.201	−17.68	3.64	14.31
Ga II.....	1414.402	−14.32	2.63	10.70
Mg II	1239.925	−17.03	2.34	14.69
Mn II	2576.877	−16.00	4.50	12.50
	2594.499	−16.00	5.00	12.42
	2606.462	−16.00	4.50	12.38
Ni II.....	1317.217[c]	−14.56	5.20	13.13
	1317.217[d]	−16.00	5.27	13.00
	1370.132	−12.88	3.39	12.88
	1454.842	−12.34	3.41	13.14
	1709.600	−13.20	3.83	13.05
	1741.549	−13.64	6.70	13.37

TABLE 4—*Continued*

Ion	λ	v	b	log N
	1751.910	−12.87	5.62	13.27
S II.....	1250.584	−16.00	3.11	14.78:
Si II.....	1808.013	−16.00	1.50	14.13:
C IV	1548.195	−15.00	11.02	13.34
	1550.770	−14.87	10.36	13.33
Si IV.....	1393.755	−15.00	12.00	12.52
	1402.770	−15.00	12.00	12.50
	−3 km s^{-1} Component			
Cl I	1347.240	−2.56	8.11	12.86
Cu II	1358.773	−1.31	6.30	12.10
Fe II.....	1611.201	−2.17	7.00	15.03
Ga II.....	1414.402	−3.52	3.02	10.90
Ge II	1237.059	−4.69	6.51	11.92
Mg II	1239.925	−3.42	7.47	15.83
	1240.395	−3.85	7.25	15.81
Mn II	2576.877	−3.00	6.77	13.48
	2594.499	−4.54	6.43	13.35
	2606.462	−4.11	7.00	13.38
Ni II.....	1317.217[c]	−1.97	6.20	13.65
	1317.217[d]	−2.40	5.82	13.58
	1370.132	−1.71	5.53	13.63
	1454.842	−1.52	6.50	13.71
	1709.600	−2.17	5.24	13.68
	1741.549	−1.85	4.68	13.67
	1751.910	−0.98	5.20	13.73
O I].....	1355.598	−3.94	4.69	17.32
O I**	1306.029	−4.91	5.18	13.20
S II.....	1250.584	−3.00	6.89	15.93:
Si II.....	1808.013	−3.00	7.49	15.91:
Si II*	1309.276	−5.38	3.19	12.42
Al III.....	1854.716	−3.00	7.30	12.49
	1862.790	−3.00	6.72	12.45
	7 km s^{-1} Component			
Cl I	1347.240	6.58	2.56	14.74
	1379.528	6.48	3.17	14.32
Cu II	1358.773	7.78	3.87	12.35
Fe II.....	1611.201	8.08	3.56	14.94
Ga II.....	1414.402	7.27	3.81	11.56
Ge II	1237.059	7.05	4.01	12.32
Mg I	1747.794	7.02	2.26	13.55
Mg II	1239.925	7.38	3.84	16.05
	1240.395	7.27	4.13	16.07
Mn II	2576.877	7.00	3.73	13.94
	2594.499	6.49	4.39	13.77
	2606.462	6.49	3.95	13.81
Ni II.....	1317.217[c]	9.06	3.97	13.63
	1317.217[d]	8.69	4.27	13.63
	1370.132	9.33	4.43	13.66
	1454.842	9.18	3.66	13.67
	1709.600	8.64	4.95	13.82
	1741.549	8.87	4.90	13.82
	1751.910	9.81	4.38	13.80
O I].....	1355.598	6.88	4.15	17.90
S I.....	1295.653	7.63	4.30	13.11
	1425.030	7.89	4.18	12.94
	1473.994	8.06	4.45	13.04
S II.....	1250.584	7.00	7.47	15.80:
Si II.....	1808.013	7.00	5.00	15.90:
Si II*	1309.276	5.96	3.16	11.88
Al III.....	1854.716	7.00	7.82	12.76
	1862.790	7.00	7.42	12.70
C IV	1548.195	5.24	12.00	13.29
	1550.770	6.00	12.00	13.24

TABLE 4—*Continued*

Ion	λ	v	b	log N
Si IV.....	1393.755	5.78	12.00	12.63
	1402.770	5.99	12.00	12.68
	19 km s^{-1} Component			
Fe II.....	1608.451	22.57	2.18	13.52
Ge II	1237.059	19.23	2.94	11.26
Mg I	2852.964	23.55	2.46	11.54
Mg II	1239.925	17.88	6.50	14.78
	1240.395	17.14	1.71	14.55
Mn II	2576.877	17.17	6.00	12.29
	2594.499	18.38	5.04	12.12
	2606.462	16.71	5.00	12.20
Ni II.....	1317.217[c]	18.58	6.57	12.91
	1317.217[d]	18.24	4.74	12.48
	1370.132	18.19	2.23	12.47
	1454.842	19.42	4.76	12.93
	1709.600	21.14	5.50	12.79
	1741.549	21.25	5.41	12.77
	1751.910	21.35	5.17	12.94
S II.....	1250.584	21.28	5.50	14.39:
	1253.811	22.24	3.38	14.17
Si II.....	1808.013	18.91	5.04	14.52
Al III.....	1854.716	20.00	7.00	11.79
	1862.790	19.00	7.66	11.72
C IV	1548.195	27.88	12.00	12.73
	1550.770	27.42	10.61	12.56
	35 km s^{-1} Component			
Al II.....	1670.787[b]	31.12	3.80	11.28
	1670.787[a]	29.51	2.19	11.08
Fe II.....	2382.765	36.00	1.50	11.40
	2600.173	37.11	1.61	11.51
Mg II	2796.352	37.81	5.00	12.04
	2803.531	37.23	5.00	12.09
O I.....	1302.169	38.09	4.44	13.40
Si II.....	1526.707	38.49	3.70	12.28
Al III.....	1854.716	35.55	8.47	11.61
	50 km s^{-1} Component			
Al II.....	1670.787[a]	49.61	1.73	10.90
	1670.787[b]	50.00	2.00	10.95
Fe II.....	2382.765	49.42	1.74	12.18
	2586.650	49.98	1.50	11.87:
	2600.173	49.53	2.50	12.16
Mg II	2796.352	50.23	4.09	12.20
	2803.531	50.08	4.73	12.23
O I.....	1302.169	48.75	3.61	13.45
Si II.....	1526.707	48.96	3.02	12.33
	61 km s^{-1} Component			
Al II.....	1670.787[a]	60.98	4.00	12.17:
	1670.787[b]	60.42	4.95	12.21:
Fe II.....	1608.451	60.08	3.00	12.87
	2586.650	59.94	3.50	13.06
Mg I	2852.964	65.00	4.31	11.30
Mn II	2576.877	61.15	4.00	11.36
S II.....	1250.584	63.23	3.50	13.74
	1253.811	62.74	3.50	13.59
Si II.....	1526.707	60.16	3.50	13.23:
Al III.....	1854.716	56.96	5.97	11.45
C IV	1548.195	55.19	12.00	12.64
	1550.770	57.60	12.00	12.64
Si IV.....	1393.755	58.50	12.00	11.65:
	1402.770	61.33	7.22	11.79

TABLE 4—*Continued*

Ion	λ	v	b	log N
71 km s^{-1} Component				
Al II.....	1670.787[a]	71.00	4.07	13.68:
	1670.787[b]	71.00	5.73	13.30:
Fe II.....	1608.451	71.10	6.02	14.24:
	1611.201	71.66	3.90	14.09
	2586.650	70.92	5.20	14.35:
Mg I	2852.964	72.55	2.68	11.90
Mn II	2576.877	71.75	6.36	12.31
	2594.499	71.00	6.44	12.28
	2606.462	70.59	6.03	12.28
Ni II.....	1317.217[c]	72.00	5.95	12.92
	1317.217[d]	72.33	5.54	12.98
	1370.132	72.34	7.66	13.06
	1709.600	70.72	9.06	13.19
	1741.549	71.60	6.15	13.11
	1751.910	73.16	4.40	12.85
O I*.....	1304.858	70.89	5.20	12.76
O I**.....	1306.029	70.87	5.55	12.83
S II.....	1250.584	72.29	5.22	14.50
	1253.811	72.14	5.36	14.46
Si II.....	1526.707	71.00	7.37	14.36:
	1808.013	71.13	5.61	14.56
Si II*.....	1264.738	72.22	4.02	12.50:
	1265.002	72.00	3.05	12.36
	1309.276	71.40	3.66	12.06
Al III.....	1854.716	70.71	6.56	11.93
	1862.790	71.07	9.24	11.94
83 km s^{-1} Component				
Al II.....	1670.787[b]	80.61	3.00	11.86:
	1670.787[a]	80.77	3.00	12.13:
Fe II.....	1608.451	82.81	3.00	13.14:
	2586.650	81.02	3.00	13.23:
Mg I	2852.964	78.50	4.00	11.20
S II.....	1250.584	83.08	2.17	13.55
	1253.811	83.67	2.53	13.58
Si II.....	1526.707	82.54	2.50	13.22:
C IV	1548.195	78.33	12.00	12.63
	1550.770	75.54	12.00	12.59
Si IV.....	1393.755	81.68	11.64	11.97
	1402.770	82.36	9.41	12.03
90 km s^{-1} Component				
Al II.....	1670.787[a]	90.00	5.59	12.81:
	1670.787[b]	90.00	5.93	13.03:
Fe II.....	1608.451	90.03	4.22	13.84
	2586.650	90.29	5.03	13.93
Mg I	2852.964	90.09	5.20	11.62
Mg II	1240.395	92.30	1.50	14.37:
Mn II	2576.877	89.75	5.32	11.99
	2594.499	90.36	5.50	11.90
	2606.462	89.00	5.55	11.99
Ni II.....	1317.217[d]	91.67	8.67	12.82
	1370.132	91.52	4.61	12.53
	1709.600	92.43	8.51	12.91
	1741.549	91.78	8.20	12.90
	1751.910	90.62	5.28	12.66
O I*.....	1304.858	90.54	4.65	12.65
O I**.....	1306.029	93.01	7.56	12.70
S II.....	1250.584	91.01	4.72	14.29
	1253.811	90.64	3.59	14.24
Si II.....	1526.707	90.00	6.89	14.08:
	1808.013	91.02	4.81	14.35
Si II*.....	1264.738	90.73	4.21	12.14
	1265.002	92.51	1.95	11.87:
Al III.....	1854.716	89.28	9.97	11.93
	1862.790	92.83	10.99	11.82
98 km s^{-1} Component				
Al II.....	1670.787[a]	98.00	4.00	12.30:
	1670.787[b]	98.00	4.19	12.01:
Fe II.....	1608.451	97.16	4.00	13.40
	2586.650	98.27	3.60	13.29
Mg I	2852.964	98.60	3.40	11.11
Mn II	2576.877	98.50	4.71	11.53
	2606.462	98.77	1.54	11.26:
S II.....	1250.584	98.88	3.50	13.81
	1253.811	98.26	3.49	13.89
Si II.....	1526.707	98.00	3.60	14.04:
	1808.013	99.53	1.50	13.76:

NOTES.—Units for velocity v, dispersion b, and column density N are, respectively, km s^{-1}, km s^{-1}, and cm^{-2}. Column densities that are more uncertain because of weak, blended, or saturated components are marked with colons. Error estimates are provided in the text. Table 4 is also available in machine-readable form in the electronic edition of the *Astrophysical Journal Supplement*.

[a] Exposure with central $\lambda = 1598$ Å.

[b] Exposure with central $\lambda = 1763$ Å.

[c] Exposure with central $\lambda = 1234$ Å.

[d] Exposure with central $\lambda = 1416$ Å.

tion profiles (except in HD 93222 in the southern part of the nebula). There is the interesting possibility that the +69 km s^{-1} component that disappeared between 1997 and 1999 in CPD −59°2603 may be present in HD 93205, although it is not possible to rule out a chance velocity coincidence between the two stars. It will be difficult to establish coherent high-velocity physical structures among the stars because of the rapid spatial variations in the profiles, the sparse angular sampling, the unknown (small) distribution in depth of the stars, and the possibility that the radial velocities of any such structures would vary from star to star due to acceleration and projection effects.

5. DISCUSSION

This paper presents an atlas of profiles, measurements of individual velocity components, and some morphological inferences from the complex interstellar absorption lines toward four O stars in the Carina Nebula, as observed with *HST*/STIS. The principal results are the much larger numbers of velocity components, somewhat higher velocities, and especially the substructure found in most of the high-velocity components, in comparison with previous ground-based and *IUE* investigations. In addition, temporal variations were discovered in a number of velocity components toward one star observed at two epochs. These results provide vital new information about the physical origins of the phenomena and demonstrate the futility of quantitative analyses of the earlier data.

These new data provide the basis for further astrophysical studies directed toward improved understanding of the various velocity regimes in the interstellar profiles. Specifically, the hypotheses that the highest velocity fea-

TABLE 5
HD 93222

Ion	λ	v	b	log N
	−388 km s^{-1} Component			
C II.....	1334.532	−388.00	5.86	12.99
Mg II	2796.352	−388.21	6.46	11.54
	2803.531	−388.43	2.75	11.26
	−379 km s^{-1} Component			
Al II.....	1670.787[a]	−381.69	1.95	10.85
	1670.787[b]	−378.17	6.00	11.08
C II.....	1334.532	−379.00	3.68	13.19
Fe II.....	2382.765	−379.62	1.50	11.28
	2586.650	−379.58	5.00	12.14
	2600.173	−378.83	2.31	11.58
Mg II	2796.352	−379.00	3.43	11.77
	2803.531	−379.00	3.03	11.75
Si II.....	1304.370	−379.00	5.53	12.23
	1526.707	−379.28	2.06	11.85
	−372 km s^{-1} Component			
Al II.....	1670.787[a]	−371.18	3.55	11.82
	1670.787[b]	−372.40	2.98	11.67
C II.....	1334.532	−372.00	3.54	13.86:
Fe II.....	1608.451	−371.42	2.46	12.65
	2382.765	−372.28	1.65	12.47
	2586.650	−371.61	2.31	12.69
	2600.173	−371.90	1.76	12.53
Mg I	2852.964	−370.21	3.36	10.70
Mg II	2796.352	−371.08	3.04	12.74
	2803.531	−371.19	3.02	12.80
O I.....	1302.169	−370.73	3.65	13.31
S II.....	1253.811	−372.00	1.50	12.86:
Si II.....	1304.370	−370.88	3.18	13.02
	1526.707	−371.10	3.00	13.00
Si II*.....	1264.738	−373.35	1.54	11.18
C IV	1548.195	−369.45	6.23	12.01
	−365 km s^{-1} Component			
Al II.....	1670.787[a]	−363.99	4.55	11.51
	1670.787[b]	−365.84	3.91	11.57
C II.....	1334.532	−365.00	6.64	14.09:
Fe II.....	1608.451	−364.13	1.50	12.16:
	2382.765	−367.37	7.64	12.66
	2586.650	−365.01	2.66	12.34
	2600.173	−366.11	7.28	12.60
Mg I	2852.964	−363.24	4.00	10.48
Mg II	2796.352	−364.77	3.51	12.43
	2803.531	−365.55	2.38	12.12
O I.....	1302.169	−363.91	4.67	13.09
S II.....	1253.811	−365.00	4.74	13.14:
Si II.....	1304.370	−365.00	2.81	12.49
	1526.707	−364.80	1.84	12.42
	−359 km s^{-1} Component			
Al II.....	1670.787[a]	−358.60	2.93	11.41
	1670.787[b]	−359.84	2.40	11.38
C II.....	1334.532	−359.00	5.05	13.67:
Fe II.....	1608.451	−358.37	1.50	12.14:
	2382.765	−358.42	1.66	11.99
	2586.650	−359.00	3.71	12.27
	2600.173	−358.40	1.50	11.92
Mg I	2852.964	−357.14	1.50	10.48
Mg II	2796.352	−358.15	3.23	12.33
	2803.531	−359.82	5.71	12.59
O I.....	1302.169	−357.36	3.32	12.99
Si II.....	1304.370	−359.00	5.01	12.81
	1526.707	−358.94	3.37	12.59
C IV	1548.195	−359.07	3.10	12.01

TABLE 5—*Continued*

Ion	λ	v	b	log N
	1550.770	−362.02	4.00	11.91
Si IV.....	1393.755	−360.38	5.00	11.23:
	1402.770	−356.11	5.96	11.59:
	−350 km s^{-1} Component			
Al II.....	1670.787[a]	−350.65	4.45	10.70
	1670.787[b]	−352.42	6.07	11.20
C II.....	1334.532	−350.00	6.95	13.20
Mg II	2796.352	−349.99	5.97	11.79
	2803.531	−346.19	4.00	11.56
C IV	1548.195	−350.00	8.00	12.32
	−115 km s^{-1} Component			
Al II.....	1670.787[a]	−115.18	1.50	10.70
	1670.787[b]	−114.71	2.86	11.11
C II*.....	1335.708	−115.00	3.89	12.82
Fe II.....	2382.765	−115.50	1.50	11.40
	2600.173	−115.99	2.37	11.72
Mg II	2796.352	−115.09	2.92	11.74
	2803.531	−115.04	1.95	11.49
O I.....	1302.169	−114.20	4.24	12.76:
Si II.....	1304.370	−113.69	4.17	12.24:
	1526.707	−113.31	4.47	12.18
C IV	1548.195	−124.00	3.25	11.69
	−110 km s^{-1} Component			
Al II.....	1670.787[a]	−109.61	2.86	11.32
	1670.787[b]	−109.62	1.88	11.04
C II*.....	1335.708	−110.00	3.56	12.23
Fe II.....	2382.765	−109.25	4.57	11.75
	2600.173	−110.01	1.50	11.51
Mg II	2796.352	−109.88	3.24	11.95
	2803.531	−110.17	4.12	11.98
Si II.....	1526.707	−107.85	1.50	11.73
Al III.....	1854.716	−108.34	2.58	10.95
C IV	1548.195	−106.00	11.11	12.76
	1550.770	−105.58	8.48	12.48
Si IV.....	1402.770	−106.00	7.91	11.80
	−98 km s^{-1} Component			
Al II.....	1670.787[a]	−98.91	1.50	10.78:
C II*.....	1335.708	−97.00	4.03	12.67
Mg II	2796.352	−98.20	4.14	11.89
	2803.531	−97.74	4.21	11.92
Si II.....	1526.707	−98.15	2.36	11.97
	−87 km s^{-1} Component			
Al II.....	1670.787[a]	−86.09	5.13	11.82
	1670.787[b]	−87.80	3.86	11.64
C II*.....	1335.708	−87.00	4.03	13.23
Fe II.....	2382.765	−88.13	3.60	12.05
	2600.173	−87.80	3.05	12.05
Mg I	2852.964	−87.00	3.39	10.60
Mg II	2796.352	−87.24	3.89	12.61
	2803.531	−86.82	3.87	12.62
S II.....	1250.584	−87.44	7.00	13.72:
Si II.....	1304.370	−87.00	3.33	12.48
	1526.707	−87.54	3.03	12.64
	−81 km s^{-1} Component			
Al II.....	1670.787[a]	−80.27	2.34	11.20
	1670.787[b]	−81.75	4.05	11.63
C II*.....	1335.708	−81.00	4.50	12.91:
Fe II.....	2382.765	−82.15	2.85	11.93
	2600.173	−81.75	2.28	11.89

TABLE 5—*Continued*

Ion	λ	v	b	log N
Mg I	2852.964	−81.00	3.50	10.60
Mg II	2796.352	−81.41	3.18	12.22:
	2803.531	−80.71	3.73	12.47
Si II.....	1304.370	−81.00	4.94	12.61
	1526.707	−81.14	4.66	12.74
	1808.013	−82.82	1.79	13.37:
Al III.....	1854.716	−83.00	6.09	11.28
C IV	1548.195	−83.09	9.27	13.59
	1550.770	−83.29	7.87	13.54
Si IV.....	1402.770	−82.73	9.88	13.00
	−68 km s^{-1} Component			
Al II.....	1670.787[a]	−66.82	7.77	12.54
	1670.787[b]	−67.14	7.71	12.55
Fe II.....	1608.451	−67.48	3.39	13.02
	2382.765	−68.84	4.88	13.18
	2586.650	−69.32	3.89	13.03
	2600.173	−67.06	5.85	13.31
Mg I	2852.964	−68.00	4.00	10.60
S II.....	1253.811	−70.56	4.00	13.37
	1259.519	−68.18	5.42	13.12
Si II.....	1304.370	−68.69	4.86	13.38
	1526.707	−70.81	3.84	13.17
Al III.....	1854.716	−67.83	5.54	11.96
	1862.790	−67.82	5.84	11.69
C IV	1548.195	−65.62	7.65	13.82
	1550.770	−65.79	7.61	13.83
Si IV.....	1393.755	−66.10	7.69	13.34
	1402.770	−65.99	6.22	13.31
	−64 km s^{-1} Component			
Al II.....	1670.787[a]	−63.54	2.38	11.83
	1670.787[b]	−64.41	1.50	11.79
Fe II.....	1608.451	−63.13	1.50	12.73
	2382.765	−64.11	2.43	12.83
	2586.650	−64.00	3.03	13.07
	2600.173	−64.00	1.50	12.59
Mg I	2852.964	−64.66	4.11	11.53
Mn II.....	2576.877	−64.38	6.06	11.53:
	2594.499	−64.85	7.25	11.63:
	2606.462	−63.47	4.00	11.51:
S II.....	1250.584	−62.27	7.20	13.96:
	1253.811	−62.89	2.96	13.74
	1259.519	−63.56	2.55	13.49
Si II.....	1304.370	−63.60	3.01	13.69
	1526.707	−63.98	3.80	13.80
	1808.013	−65.49	4.56	13.87:
Si II*.....	1264.738	−64.30	3.18	11.92
	−50 km s^{-1} Component			
Fe II.....	1608.451	−50.07	3.22	13.28
	2586.650	−48.50	6.22	13.63
	2600.173	−47.87	6.51	13.63:
Mg I	2852.964	−52.44	3.49	11.53
Mn II.....	2576.877	−50.00	3.81	11.30
	2594.499	−50.00	4.03	11.72
	2606.462	−50.00	4.00	11.28:
Ni II.....	1317.217[c]	−47.51	6.00	12.39:
S II.....	1250.584	−49.41	5.03	14.41
	1253.811	−50.61	5.37	14.40
	1259.519	−51.07	4.63	14.26
Si II.....	1808.013	−48.78	5.70	14.54
Al III.....	1854.716	−48.99	5.07	12.46
	1862.790	−48.70	4.86	12.38
C IV	1548.195	−46.71	8.00	13.50
	1550.770	−46.90	7.76	13.44
Si IV.....	1393.755	−48.55	5.18	12.83
	1402.770	−46.78	7.79	13.21

TABLE 5—*Continued*

Ion	λ	v	b	log N
	−44 km s^{-1} Component			
Fe II.....	1608.451	−43.93	2.38	13.40
	2586.650	−43.88	1.50	13.17
	2600.173	−44.00	5.71	13.65:
Mg I	2852.964	−43.10	8.00	12.08:
Mn II.....	2576.877	−44.00	4.00	11.54:
	2594.499	−44.00	3.52	11.54
	2606.462	−44.00	5.00	11.67:
S II.....	1250.584	−43.36	1.62	13.77
	1253.811	−44.35	1.50	13.48
	1259.519	−44.42	2.41	13.75
Si II.....	1808.013	−42.07	2.33	13.72
Si II*.....	1264.738	−44.20	6.67	11.99:
	−38 km s^{-1} Component			
Fe II.....	1608.451	−38.14	2.92	13.12
	2586.650	−38.36	3.74	13.29
	2600.173	−38.00	4.50	12.85:
Mn II.....	2594.499	−38.00	4.00	11.64
Ni II.....	1317.217[c]	−36.36	5.00	12.15:
S II.....	1250.584	−38.39	3.87	14.19
	1253.811	−37.73	7.57	14.52
	1259.519	−39.27	6.50	14.29
Si II.....	1808.013	−37.90	2.88	13.91
Al III.....	1854.716	−34.00	8.68	12.72
	1862.790	−34.00	8.11	12.68
C IV	1548.195	−33.79	5.45	13.55
	1550.770	−33.97	5.57	13.54
Si IV.....	1393.755	−33.60	10.69	13.64:
	1402.770	−34.50	6.43	13.45
	−23 km s^{-1} Component			
B II	1362.461	−23.48	4.99	11.62
Cl I	1347.240	−22.57	2.12	11.53
Cu II	1358.773	−22.40	3.42	12.42
Fe II.....	1608.451	−23.55	4.22	15.26:
	1611.201	−23.07	3.04	15.00
	2586.650	−24.11	4.09	15.42:
Ga II.....	1414.402	−22.39	4.79	11.64
Ge II	1237.059	−23.09	4.45	12.21
Mg I	2852.964	−24.60	3.91	13.80:
Mg II	1239.925	−23.29	4.93	16.00
	1240.395	−23.31	5.07	16.07
Mn II.....	2576.877	−23.54	5.11	13.77:
	2594.499	−23.67	4.90	13.83:
	2606.462	−23.72	5.10	13.78:
Ni II.....	1317.217[c]	−21.40	3.13	13.37
	1317.217[d]	−22.03	3.14	13.37
	1370.132	−21.42	3.28	13.40
	1709.600	−21.29	2.76	13.50
	1741.549	−21.34	3.30	13.50
	1751.910	−20.59	2.33	13.42
O I].....	1355.598	−22.30	3.62	17.80
O I*	1304.858	−23.69	4.35	14.32:
O I**	1306.029	−24.87	4.52	14.13
P II	1532.533	−23.48	4.33	14.23
S I.....	1425.030	−23.10	2.32	11.72
S II.....	1250.584	−23.56	4.83	16.17:
	1253.811	−23.97	3.86	16.70:
Si II.....	1808.013	−23.89	4.67	16.36:
Si II*.....	1264.738	−24.94	5.31	14.19:
	1265.002	−24.87	5.06	14.28
	1309.276	−24.92	5.26	13.99
Al III.....	1854.716	−21.81	5.41	13.51:
	1862.790	−21.28	5.25	13.55
C IV	1548.195	−19.80	6.91	13.72
	1550.770	−19.76	6.65	13.68

TABLE 5—*Continued*

Ion	λ	v	b	log N
Si IV.....	1393.755	−17.76	3.56	14.95:
	1402.770	−19.21	4.55	14.38
	−6 km s^{-1} Component			
B II	1362.461	−6.70	1.65	11.08
Cl I	1347.240	−7.12	1.91	13.23
Cu II	1358.773	−5.80	2.53	12.05
Fe II.....	1608.451	−6.00	4.74	14.74:
	1611.201	−5.85	3.20	14.84
Ga II.....	1414.402	−6.34	3.77	11.30
Ge II	1237.059	−6.35	3.35	11.96
Mg I	2852.964	−6.00	6.37	12.81:
Mg II	1239.925	−5.91	3.16	15.85
	1240.395	−5.86	3.19	15.90
Mn II	2576.877	−6.45	3.24	13.69:
	2594.499	−6.54	3.58	13.55
	2606.462	−6.76	3.85	13.43
Ni II.....	1317.217[c]	−4.44	4.36	13.53
	1317.217[d]	−5.04	3.97	13.53
	1370.132	−4.55	4.21	13.51
	1709.600	−3.84	4.05	13.61
	1741.549	−4.34	4.58	13.67
	1751.910	−3.64	3.61	13.56
O I].....	1355.598	−6.88	2.85	17.50
P II	1532.533	−6.49	3.45	14.03
S I.....	1425.030	−7.18	2.84	12.18
S II.....	1250.584	−6.00	4.88	15.64:
	1253.811	−6.00	5.04	15.89:
Si II.....	1808.013	−5.21	4.86	15.73:
Al III.....	1854.716	−5.82	4.10	12.03
	1862.790	−4.89	4.07	12.08
C IV	1548.195	−7.00	8.00	13.22
	1550.770	−7.00	9.00	13.20
Si IV.....	1393.755	−5.72	5.40	12.76
	1402.770	−7.27	8.00	12.99
	6 km s^{-1} Component			
B II	1362.461	6.16	7.24	11.36
Cl I	1347.240	4.61	1.97	13.68
Cu II	1358.773	6.26	4.27	12.07
Fe II.....	1608.451	6.00	6.20	14.86:
	1611.201	5.80	6.19	14.99
Ga II.....	1414.402	6.24	3.74	11.28
Ge II	1237.059	6.46	3.92	12.08
Mg I	2852.964	6.00	7.00	12.88:
Mg II	1239.925	6.78	5.42	15.86
	1240.395	6.78	4.75	15.88
Mn II	2576.877	6.00	4.76	13.63:
	2594.499	5.89	5.00	13.57:
	2606.462	5.49	5.73	13.51
Ni II.....	1317.217[c]	7.34	6.20	13.63
	1317.217[d]	6.73	6.26	13.63
	1370.132	7.44	6.73	13.67
	1709.600	7.91	6.12	13.74
	1741.549	7.48	6.17	13.76
	1751.910	7.95	6.46	13.75
O I].....	1355.598	6.25	6.28	17.71
P II	1532.533	5.99	4.91	14.14
S I.....	1425.030	5.59	1.94	12.45
S II.....	1250.584	6.00	8.67	15.91:
	1253.811	6.00	7.07	16.18:
Si II.....	1808.013	7.32	4.27	15.98:
Si II*.....	1264.738	10.02	3.12	11.08
Al III.....	1854.716	5.63	8.67	12.79
	1862.790	6.24	8.58	12.80
C IV	1548.195	5.15	8.00	13.18
	1550.770	6.00	9.44	13.19

TABLE 5—*Continued*

Ion	λ	v	b	log N
Si IV.....	1393.755	4.72	5.58	12.82
	1402.770	5.00	7.00	12.87
	17 km s^{-1} Component			
Fe II.....	1608.451	17.00	3.50	13.85:
Mg I	2852.964	17.00	2.25	11.74
Mg II	1240.395	16.97	1.50	14.35:
Mn II	2576.877	17.00	4.00	12.04
	2594.499	17.00	4.00	12.10
	2606.462	17.00	4.00	11.86
Si II.....	1808.013	17.00	2.71	14.48
Al III.....	1854.716	17.00	3.23	11.11
	1862.790	17.00	1.50	11.11
C IV	1548.195	17.00	9.00	12.82
	1550.770	17.00	7.00	12.74
Si IV.....	1393.755	16.74	5.48	12.88
	1402.770	16.62	6.42	12.92
	23 km s^{-1} Component			
Cl I	1347.240	22.45	6.28	11.95
Fe II.....	1608.451	23.37	2.91	13.79
	1611.201	22.97	1.50	13.74
Mg I	2852.964	22.85	2.02	12.01
Mn II	2576.877	23.00	4.22	11.92
	2594.499	23.00	4.12	12.00
	2606.462	23.00	3.72	11.90
Ni II.....	1317.217[c]	21.98	4.34	12.74
	1317.217[d]	21.81	4.03	12.51
	1370.132	22.78	5.00	12.89
	1741.549	22.39	7.25	13.08
	1751.910	22.54	3.29	12.51
S II.....	1250.584	24.14	2.16	14.07
	1253.811	23.00	3.50	14.38
	1259.519	23.41	2.04	14.07
Si II.....	1808.013	23.00	2.69	14.29
C IV	1548.195	25.00	12.00	12.97
	1550.770	25.00	6.00	12.58
Si IV.....	1393.755	25.00	5.50	12.31
	1402.770	27.64	7.00	12.31
	43 km s^{-1} Component			
Al II.....	1670.787[b]	42.62	2.89	10.70
Mg II	2796.352	41.77	6.88	11.34
	2803.531	43.06	1.50	11.18:
O I.....	1302.169	40.63	6.75	12.80
S II.....	1253.811	43.00	7.13	13.75:
C IV	1548.195	46.78	12.00	12.46
Si IV.....	1393.755	52.19	6.12	11.94
	1402.770	49.52	6.97	12.16
	65 km s^{-1} Component			
Al II.....	1670.787[a]	64.12	7.38	11.15
	1670.787[b]	66.31	2.33	10.70
C II.....	1334.532	65.00	3.19	13.00:
C II*	1335.708	65.00	4.06	13.01
Fe II.....	2382.765	64.30	1.85	11.96
	2600.173	64.49	2.34	11.94
Mg II	2796.352	64.50	2.17	11.83
	2803.531	64.50	2.65	11.92
O I.....	1302.169	64.50	4.39	13.12
S II.....	1253.811	65.00	8.46	13.74:
Si II.....	1304.370	65.00	1.50	12.07
	1526.707	65.16	2.81	12.27
C IV	1548.195	65.00	7.94	11.92
Si IV.....	1393.755	65.96	3.11	11.85
	1402.770	64.67	2.14	11.79

TABLE 5—*Continued*

Ion	λ	v	b	log N
		72 km s^{-1} Component		
Al II.....	1670.787[a]	72.29	2.51	11.62
	1670.787[b]	72.56	4.00	11.85
C II.....	1334.532	72.00	6.51	14.12:
C II*	1335.708	71.50	3.61	13.37:
Fe II.....	1608.451	72.79	3.63	12.92
	2382.765	71.37	2.53	12.83
	2586.650	72.03	2.41	12.85
	2600.173	71.74	2.55	12.83
Mg II	2796.352	71.50	3.20	12.77
	2803.531	71.50	3.09	12.83
Mn II	2576.877	72.00	8.15	11.51:
O I.....	1302.169	71.50	4.59	14.20
S II.....	1253.811	72.00	4.47	13.18:
	1259.519	73.27	7.25	13.20:
Si II.....	1526.707	72.73	3.11	13.18
Si II*.....	1264.738	75.25	6.41	11.52
		78 km s^{-1} Component		
Al II.....	1670.787[a]	77.71	4.02	11.68
	1670.787[b]	79.16	4.29	11.40
C II.....	1334.532	78.00	4.34	14.02:
C II*	1335.708	77.50	5.15	13.73:
Fe II.....	1608.451	78.00	6.08	12.79
	2382.765	76.86	4.19	12.77
	2586.650	78.00	3.56	12.67
	2600.173	77.47	3.79	12.74
Mg II	2796.352	77.50	4.22	12.79
	2803.531	77.50	4.40	12.78
O I.....	1302.169	77.50	4.57	14.28
S II.....	1253.811	78.00	8.06	13.60:
Si II.....	1526.707	78.56	3.73	12.94
		93 km s^{-1} Component		
Al II.....	1670.787[b]	93.06	2.38	10.48:
Fe II.....	2382.765	92.21	1.93	11.40

NOTES.—Units for velocity v, dispersion b, and column density N are, respectively, km s^{-1}, km s^{-1}, and cm^{-2}. Column densities that are more uncertain because of weak, blended, or saturated components are marked with colons. Error estimates are provided in the text. Table 5 is also available in machine-readable form in the electronic edition of the *Astrophysical Journal Supplement*.

[a] Exposure with central $\lambda = 1598$ Å.

[b] Exposure with central $\lambda = 1763$ Å.

[c] Exposure with central $\lambda = 1234$ Å.

[d] Exposure with central $\lambda = 1416$ Å.

tures in the low-ionization lines arise from an interaction of the stellar winds with surrounding interstellar material, and that the dominant components in the high-ionization and excited-state lines correspond to the global expansion of the H II region, will be addressed by these studies. Additionally, Danks et al. (2001) pointed out the morphological similarity between the interstellar profiles toward CPD $-59^\circ 2603$ and a QSO narrow-line system (see also Bond et al. 2001). Quantitative comparisons between the Carina Nebula interstellar profiles and an array of QSO systems observed with comparable resolution, as well as a search for rapid temporal variations in the latter, will probe whether some of the QSO systems might arise in intervening starburst regions.

As a first astrophysical interpellation of the data, Figures 16*a*–16*b* show plots of column-density ratios as a function of local radial velocity (corrected by +14 km s^{-1} from heliocentric; Walborn & Hesser 1975) for Mg II/Fe II and Si II/Fe II, following Welty et al. (1997). All of these ions have similar ionization potentials and are dominant. Only the best quality column densities have been used for these calculations, i.e., very weak or badly saturated components have been omitted, and means of the same velocity component in different lines from the same species in a given star have been taken when possible. The uncertainties of the points in Figures 16*a*–16*b* range from 0.05 to 0.1 dex, as estimated from propagation of the column-density errors to the ratios, with the smaller uncertainties corresponding to means of components. Since Fe is more heavily depleted than Mg or Si, these plots show the Routly-Spitzer (1952) effect, with less depletion and hence smaller ratios at the higher velocities. For comparison, standard ratios from Savage & Sembach (1996) are indicated at the right for conditions ranging from the cool Galactic disk (highest depletions) to solar abundances (undepleted gas phase). The ranges of depletions in the Carina Nebula are in reasonable agreement with the standard values; the somewhat more extreme values in Mg II/Fe II may be due to measurement uncertainties in these strong lines. Because of the large number of components, the velocity range over which the lifting of the depletion occurs is exceptionally well defined, i.e. within ± 100 km s^{-1}. An analogous effect was shown in Na I/Ca II by Walborn (1982, Fig. 25). It is interesting that this effect occurs in the Carina Nebula high-velocity material, despite the quite different environment from those in which it is generally observed.

Figure 17 shows the C IV/Si IV column-density ratios, which diagnose ionization mechanisms (e.g., Franco & Savage 1982), as a function of local radial velocity. All available ratios have been plotted here; the uncertainty of most points in Figure 17, estimated from propagation of errors and comparison between doublet members, is $\sim$0.1 dex, but the three lowest points and one for HDE 303308 at -23 km s^{-1}, log ratio 0.03 correspond to saturated components and have errors of at least 0.2 dex. Walborn et al. (1984) found low values of the ratio in Carina Nebula intermediate-velocity components, indicative of photoionization and consistent with their interpretation as the near side of the globally expanding H II region; and higher values in high-velocity components, implying the presence of X-ray and/or collisional ionization. The present results in Figure 17 are in good agreement with the earlier ones. The observed ratios nicely span the typical range of the three ionization mechanisms, with the lowest values corresponding to photoionization at intermediate velocities. The envelope curve of the distribution suggests a gradual appearance of the other mechanisms as a function of increasing absolute velocity, but the curve is "filled in," implying an overlap of mechanisms at intermediate radial velocities. Perhaps some components with high ionization ratios and moderate radial velocities have large transverse, hence total, velocities. These results will be further discussed in future papers, including the possibility of velocity dispersions larger than the upper limit of 12 km s^{-1} adopted in the present fits, for lines in the collisional regime.

Despite the extensive presentation here, it does not exhaust the information content of the data. In particular, they contain rich sets of (overlapping) C I, C I*, C I**

TABLE 6

Comparative List of Low- and High-Ionization Interstellar Velocity Components toward Four Stars in the Carina Nebula (km s^{-1})

CPD −59°2603		HD 93205		HDE 303308		HD 93222	
Low	High	Low	High	Low	High	Low	High
−233	...	...	...	...	...	...	...
−216	...	...	...	...	...	...	...
−185	...	...	...	...	...	...	...
−166	−170	...	...	−175	...	...	...
−153	−158	...	...	...	...	...	...
−137	−128	−142	−130	−133	−133	...	...
−120	−113	...	...	...	...	−115	−124
...	...	...	...	−111	−110	−110	−106
−101	−98	−98	−100	−104	...	−98	...
...	−86	−89/−83	−90	−91/−82	−93	−87/−81	−83
−77	...	−75	...	−76/−71	−78	...	...
−63	−69	−66	−61	−61	−60	−68/−64	−66
...	...	−58/−53	...	−54	...	−50	−48
−38	−44	−35	−35	−41/−33	−33	−44/−38	−34
−28	−30	...	...	−24	...	−23	−20
−19	−19	−18	−18	−16	−15	...	...
−3	−6	−3	−3	−3	−3	−6	−6
8	6	8	8	7	6	6	6
17	16	18	18	19	...	17	17
26	...	27	27	...	23	23	25
38	33	35	35	35	35	...	...
61	66	...	...	61	58	65	65
69/72	...	69	...	71	71	72	...
...	...	80	82	83	79	78	...
...	...	88	92	90	91	93	...
98	...	100	104	98	...	...	...
110	...	108/113	...	...	...	...	...
120	...	118	118	...	...	...	...
127	...	...	...	...	...	...	...

profiles and absorption lines from numerous transitions of CO, which remain to be measured and analyzed.

Further STIS observations of these and other stars in the Carina Nebula will also be essential to fully characterize the phenomena. The one case observed at two epochs revealed large temporal variations. Additional epochs for this star and the other three observed here will support statistical inferences about the incidence and timescales of the variations, as well as the sizes, transverse velocities, and distances from the stars of the discrete absorbing structures. Furthermore, the ground-based and *IUE* work demonstrated rapid spatial variations of the interstellar profiles, with some velocity components possibly in common but many completely different between pairs of stars separated by small angular distances. In view of the far greater complexity of the profiles revealed by STIS, other stars near those discussed here must be similarly observed to constrain the spatial extents of the absorbing structures, in depth as well as across the line of sight. Excellent candidates near the present targets exist, namely HD 93204 (only 20″ or 0.24 pc in projection from HD 93205), CPD −59°2600, HD 93130, and HD 93146 (the last two in the southern part of the nebula). These additional observations need not cover the full range of wavelengths observed here, but just a few lines of intermediate and large intensities to define the variations.

Support for this work was provided by NASA through grants GO-7301-96A from the Space Telescope Science Institute, which is operated by AURA, Inc., under contract NAS 5-26555; and a grant to the STIS Instrument Definition Team (ACD). We thank the anonymous referee for several useful and courteous suggestions.

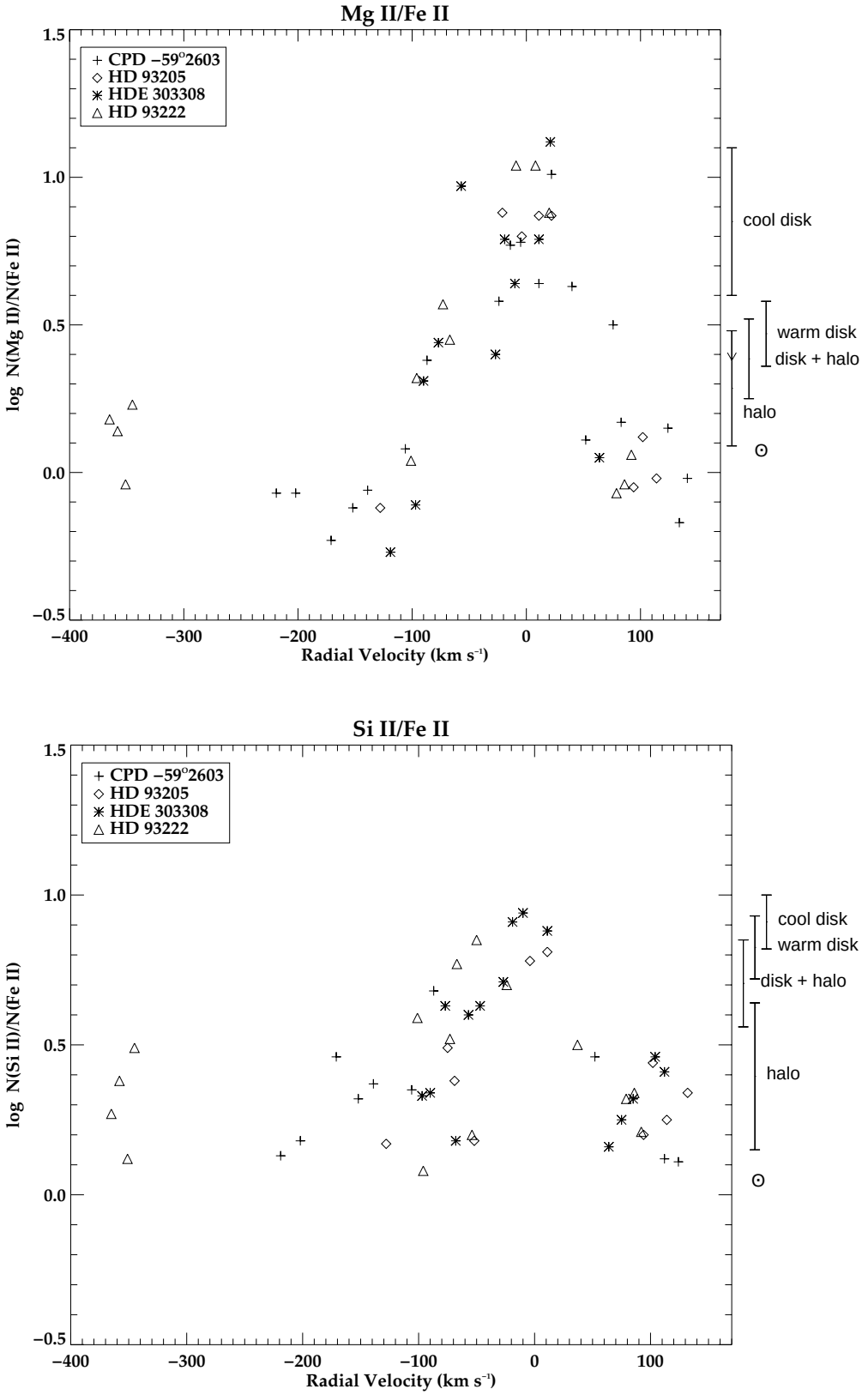

FIG. 16.—(*a*) Logarithmic column-density ratios of Mg II/Fe II vs. local radial velocity for discrete interstellar components toward all four stars, which are distinguished by the different symbols given in the key. Standard values of the ratio from Savage & Sembach (1996) are marked at the right, ranging from solar abundances (undepleted) to cool-disk depletions. (*b*) Same for Si II/Fe II.

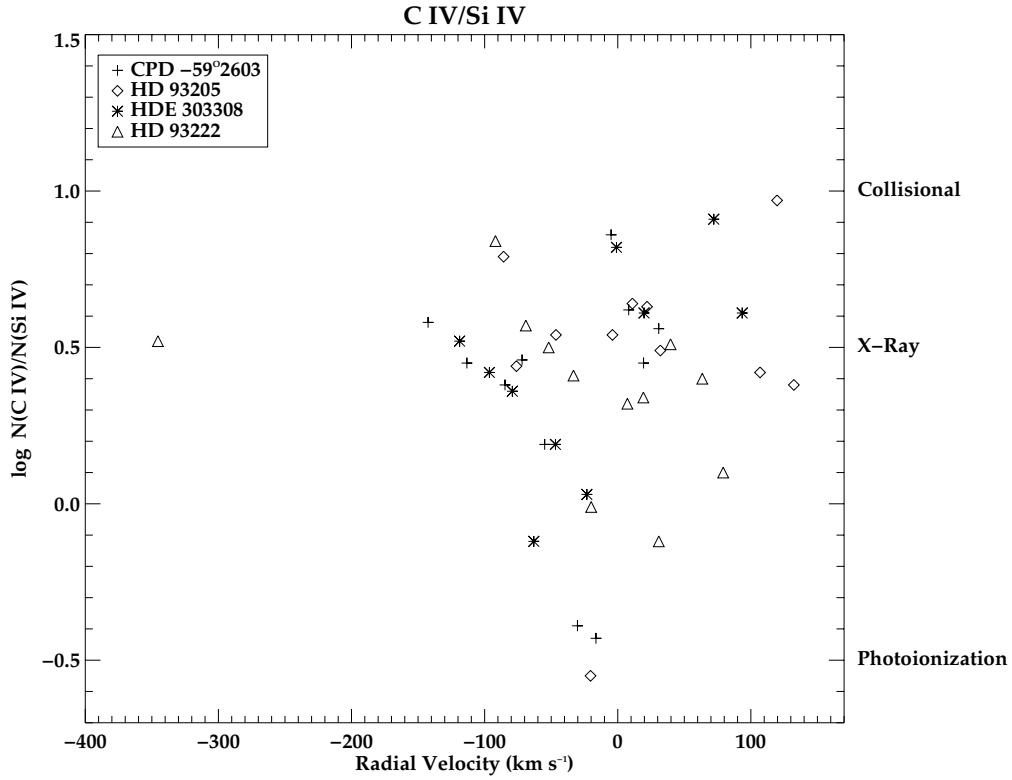

FIG. 17.—Logarithmic column-density ratios of C IV/Si IV vs. local radial velocity for discrete interstellar components toward the four stars, which are distinguished by the symbols given in the key. Typical values of the ratio for different ionization mechanisms (Franco & Savage 1982) are indicated at the right.

REFERENCES

Bond, N. A., Churchill, C. W., Charlton, J. C., & Vogt, S. S. 2001, ApJ, 562, 641
Danks, A. C., Walborn, N. R., Vieira, G., Landsman, W. B., Gales, J., & García, B. 2001, ApJ, 547, L155
Franco, J., & Savage, B. D. 1982, ApJ, 255, 541
Jenkins, E. B., & Tripp, T. M. 2001, ApJS, 137, 297
Rickard, J. J. 1974, A&A, 31, 47
Routly, P. M., & Spitzer, L., Jr. 1952, ApJ, 115, 227
Savage, B. D., & Sembach, K. R. 1996, ARA&A, 34, 279
Spitzer, L., Jr., & Fitzpatrick, E. L. 1993, ApJ, 409, 299
Walborn, N. R. 1982, ApJS, 48, 145
———. 1995, Rev. Mexicana Astron. Astrofis. Ser. Conf., 2, 51
Walborn, N. R., et al. 1998, ApJ, 492, L169
Walborn, N. R., Heckathorn, J. N., & Hesser, J. E. 1984, ApJ, 276, 524
Walborn, N. R., & Hesser, J. E. 1975, ApJ, 199, 535
———. 1982, ApJ, 252, 156
Welty, D. E., Lauroesch, J. T., Blades, J. C., Hobbs, L. M., & York, D. G. 1997, ApJ, 489, 672
Woodgate, B. E., et al. 1998, PASP, 110, 1183